U.PORTO

MESTRADO EM ONCOLOGIA
ESPECIALIZAÇÃO EM ONCOLOGIA LABORATORIAL

Targeting EGFR to modulate primary cilia in prostate cell lines harbouring ETS rearrangements

Sofia de Oliveira Costa

M

2024

U.PORTO

Sofia de Oliveira Costa. **Targeting EGFR to modulate primary cilia in prostate derived cell lines harbouring ETS rearrangements**

M.ICBAS 2024

INSTITUTO DE **CIÊNCIAS BIOMÉDICAS ABEL SALAZAR**

S O F I A D E O L I V E I R A C O S T A

TARGETING EGFR TO MODULATE PRIMARY CILIA IN PROSTATE CELL LINES HARBOURING ETS REARRANGEMENTS

Dissertação de Candidatura ao Grau de Mestre em Oncologia – Especialização em Oncologia Laboratorial – submetida ao Instituto de Ciências Biomédicas de Abel Salazar da Universidade do Porto

Orientador:
Doutora Paula Cristina Martins dos Santos Paulo
Investigadora Auxiliar no Grupo de Oncogenética do Centro de Investigação do Instituto Português de Oncologia do Porto

Co-orientadores:
Doutor Bernard Nunes de Almeida Orr
Investigador Júnior no Grupo de Oncogenética do Centro de Investigação do Instituto Português de Oncologia do Porto

Professor Doutor Manuel Rodrigues Teixeira
Professor Catedrático Convidado
Departamento de Patologia e Imunologia Molecular
Instituto de Ciências Biomédicas de Abel Salazar da Universidade do Porto
Diretor do Serviço de Genética Laboratorial
Coordenador do Grupo de Oncogenética do Centro de Investigação do Instituto Português de Oncologia do Porto

ACKNOWLEDGMENTS

Em primeiro lugar, gostaria de expressar a minha profunda gratidão ao Professor Manuel Teixeira, pela oportunidade de integrar o grupo de Oncogenética, e por me ter co-orientado durante esta tese de mestrado.

Quero dirigir um agradecimento muito especial à minha orientadora, Doutora Paula Paulo. A sua incansável dedicação e paciência, as incontáveis horas de trabalho e a confiança que sempre me transmitiu marcaram-me profundamente. Desde o primeiro dia desafiou-me a ir mais além e a acreditar nas minhas capacidades. Obrigada por partilhar comigo não só o conhecimento, mas também a paixão pela ciência. Levarei sempre no meu coração esta jornada que partilhámos.

Ao meu co-orientador, Doutor Bernard Orr, que me recebeu de braços abertos, quero agradecer por todos os conselhos e experiências de vida partilhadas. O trabalho no laboratório é muito mais leve de se levar com a tua presença. Obrigado por nos iluminares com a tua personalidade única.

A todo o grupo de Oncogenética, em especial à Doutora Andreia Brandão, pelo caloroso acolhimento e pelo apoio constante. Criaram um ambiente de trabalho único que me fez sentir em casa desde o primeiro dia.

Gostaria de expressar a minha gratidão à Doutora Margareta Correia, por todo o conhecimento e ajuda prestados na citometria de fluxo e no sorting das células; ao Professor Claudio Sunkel, por gentilmente disponibilizar o anticorpo para o GFP; e ao Doutor Tiago Dantas, por fornecer o vetor lentiviral GFP-Arl13B e compartilhar o seu extenso conhecimento sobre o cílio primário. A colaboração e orientação de todos vocês foram fundamentais para a concretização deste projeto.

Aos meus meninos de investigação, Madalena, Elsa, Luca e Inês, agradeço todos os momentos de cumplicidade, felicidade e companheirismo, assim como todos os de desespero e frustração. Este caminho só foi mais fácil com vocês ao meu lado. Sou uma sortuda por ter encontrado pessoas tão genuínas e por ter criado amizades que pretendo levar para a vida.

Ao meu pai, o meu maior pilar, quero agradecer por todo o apoio e amor que me deste ao longo da minha vida. Obrigada por acreditares sempre em mim e por seres a minha força nos momentos mais desafiantes. A tua presença constante e o teu exemplo de resiliência ensinaram-me a nunca desistir, a procurar sempre ser melhor e a lutar pelos meus sonhos. Espero, todos os dias, ser digna do teu amor incondicional e continuar a

encher-te de orgulho. Dedico-te esta conquista de coração cheio, com a promessa de continuar a honrar o caminho que traçaste para mim.

À minha mãe, que mesmo distante fisicamente, está sempre perto do meu coração. Obrigada por todo o amor, sabedoria e inspiração que me transmitiste ao longo da vida. A tua força e exemplo guiaram-me sempre, encorajando-me a crescer todos os dias. És e sempre serás uma parte essencial de todas as minhas vitórias.

Ao resto da minha família, em especial à minha madrinha, ao meu afilhado, aos meus avós e aos meus primos, agradeço por me terem acompanhado nesta jornada. Obrigada por nunca me deixarem cair e por serem um porto seguro nos momentos mais difíceis.

Às minhas amigas de longa data, Gisela, Sara, Mafalda e Matilde, obrigada por estarem comigo em cada passo desta caminhada, desde os tempos em que a paixão pela ciência começava a desabrochar. Obrigada pelos sorrisos partilhados nos dias felizes e pelos ombros que me deram nos momentos mais tristes. A vossa amizade é inestimável.

INDEX

FIGURE INDEX

TABLE INDEX

RELEVANT ABBREVIATIONS

ADT – Androgen Deprivation Therapy

Arl13B – ADP-Ribosylation Factor-like Protein 13B

AR – Androgen Receptor

BPH – Benign Prostatic Hyperplasia

BT – Brachytherapy

CNV – Copy Number Variation

CT – Computed Tomography

DMSO – Dimethyl Sulfoxide

DMEM – Dulbecco's Modified Eagle Medium

DRE – Digital Rectal Examination

EGF – Epidermal Growth Factor

EGFR – Epidermal Growth Factor Receptor

EMA – European Medicines Agency

ERG – V-ets Avian Erythroblastosis Virus E26 Oncogene Homolog

ESMO – European Society of Medical Oncology

ETS – E26 Transformation-Specific

ETV1 – ETS Variant 1

ETV4 – ETS Variant 4

ETV5 – ETS Variant 5

FDA – Food and Drug Administration

GS – Gleason Score

HBOC – Hereditary Breast and Ovarian Cancer Syndrome

HGPIN – High Grade Prostatic Intraepithelial Neoplasia

HPCa – Hereditary Prostate Cancer

IFT – Intraflagellar transport

LGPIN - Low Grade Prostatic Intraepithelial Neoplasia

LS – Lynch Syndrome

mCRPC – Metastatic Castration Resistant Prostate Carcinoma

mCSPC – Metastatic Castration-Sensitive Prostate Carcinoma

MMR – Mismatch repair

mpMRI – Multiparametric magnetic resonance imaging

MRI – Magnetic Resonance Imaging

NCCN – Nacional Comprehensive Cancer Network

NSCLC – Non-small Cell Lung Cancer

PBS – Phosphate Buffered Saline

PCa – Prostate cancer

PIN – Prostatic Intraepithelial Neoplasia

PSA – Prostate Specific Antigen

RP – Radical Prostatectomy

RPMI – Roswell Park Memorial Institute medium

RT – Radiotherapy

SPDEF – Prostate-Derived ETS Factor

TCGA – The Cancer Genome Atlas

TKIs – Tyrosine Kinase Inhibitors

ABSTRACT

Abstract

Prostate cancer (PCa) is a significant health concern worldwide, ranking second in cancer-incidence and fifth in cancer-related deaths among men. The molecular mechanisms underlying PCa development are largely unknown, with ETS genomic rearrangements, leading to overexpression of the involved ETS genes, namely, *ERG* and *ETV1*, being the single well-established molecular drivers of prostate carcinogenesis. On another note, primary cilia loss is a common event in the development of different types of cancer, including PCa. Primary cilia are non-motile structures found at the surface of most human cells, essential in the regulation of cell polarity and cell cycle, anchoring multiple oncogenic signalling pathways. Recently, several drugs, namely, EGFR inhibitors, have been described to be able to restore ciliogenesis in cancer cells. Interestingly, a recent study from our research group uncovered EGFR as a downstream effector of oncogenic ETS signalling in PCa.

In this project, we aimed to explore a potential link between ETS overexpression and loss of primary cilia and assess the utility of EGFR inhibition in the restoration of primary cilia in PCa cells with differential ETS overexpression. For that purpose, we used PCa cell models derived from the non-tumorigenic PNT2 cells with *de novo* overexpression of ΔERG or ETV1. We started by characterizing primary cilia frequency and length, using immunofluorescence staining for Arl13B (a marker of the cilia membrane) and Centrin1 (a marker of the cilia basal body), at different cell growth conditions, and then evaluated the impact of Erlotinib, an EGFR inhibitor, in the restoration of primary cilia in the presence or absence of serum.

We uncovered a clear association between ETS overexpression and primary cilia loss, and that primary cilium assembly and disassembly is differentially regulated by ETS-specific cellular mechanisms. While PNT2-ΔERG cells displayed cilia characteristics related to ciliary instability, namely, shorter cilia, low Arl13B signal intensity, and predominant loss of Centrin1, PNT2-ETV1 cells exhibited primary cilia characteristics similar to those of the non-tumorigenic parental cells. Moreover, treatment with sub-cytotoxic concentrations of Erlotinib showed greater impact in restoring primary cilia assembly in both ETS-overexpressing cells than in the parental non-tumorigenic cells, independently of the presence of growth factors.

This study unveils a direct link between overexpression of ΔERG or ETV1 and primary cilia loss in PCa and supports the potential utility of EGFR inhibitors in the

restoration of ciliogenesis in PCa cells overexpressing ETS, opening a novel therapeutic avenue in PCa.

RESUMO

Resumo

O cancro da próstata é um significativo problema de saúde a nível mundial, sendo o segundo cancro mais incidente e a quinta causa de morte relacionada com cancro nos homens. Os mecanismos moleculares subjacentes ao desenvolvimento de cancro da próstata são, em grande parte, desconhecidos. Os rearranjos genómicos envolvendo os genes ETS, que levam à sobre-expressão dos fatores de transcrição ETS neles envolvidos, nomeadamente de ΔERG e ETV1, são os únicos propulsores moleculares bem estabelecidos da carcinogénese da próstata. Por outro lado, a perda do cílio primário é um evento comum no desenvolvimento de diferentes tipos de cancro, incluindo o cancro da próstata. O cílio primário é uma estrutura não móvel encontrada na superfície da maioria das células humanas, essencial na regulação da polaridade celular e do ciclo celular, que serve de âncora a diversas vias oncogénicas. Recentemente, vários fármacos, nomeadamente, inibidores do EGFR, têm sido descritos como capazes de restaurar a ciliogénese em células cancerígenas. Curiosamente, um estudo recente do nosso grupo de investigação identificou o EGFR como um efetor da sinalização oncogénica mediada pelos ETS em cancro da próstata.

Neste projeto, tivemos como objetivo explorar uma possível ligação entre a sobre-expressão de ETS e a perda do cílio primário, bem como avaliar a utilidade da inibição do EGFR na restauração de cílios primários em células de cancro da próstata com sobre-expressão diferencial de ETS. Para tal, utilizámos modelos celulares de cancro da próstata derivados das células não tumorigénicas PNT2 com sobre-expressão *de novo* de ΔERG ou ETV1. Começámos por caracterizar a frequência e o comprimento dos cílios primários em diferentes condições de crescimento celular, utilizando coloração por imunofluorescência para Arl13B (um marcador da membrana ciliar) e Centrina 1 (um marcador do corpo basal dos cílios), e depois avaliámos o impacto de um inibidor do EGFR (Erlotinib) na restauração dos cílios primários, na presença ou ausência de soro no meio de cultura.

Descobrimos uma clara associação entre a sobre-expressão dos ETS e a perda de cílios primários, e que a formação e a desagregação dos cílios primários é regulada diferencialmente por mecanismos celulares específicos dos ETS. Enquanto as células PNT2-ΔERG apresentaram características associadas à instabilidade da ciliogénese, nomeadamente cílios mais curtos, baixa intensidade de sinal de Arl13B e perda predominante de Centrina 1, as células PNT2-ETV1 exibiram cílios primários com características semelhantes às células parentais não tumorais. Além disso, o tratamento com concentrações sub-citotóxicas de Erlotinib mostrou maior impacto na restauração da

ciliogénese em ambas as células com sobre-expressão de ETS do que nas células parentais não tumorais, independentemente da adição de fatores de crescimento.

Este estudo revela uma ligação direta entre a sobre-expressão de ΔERG ou ETV1 e a perda de cílios primários no cancro da próstata e sustenta o potencial dos inibidores de EGFR na restauração da ciliogénese em células de cancro da próstata com sobre-expressão de ETS, abrindo a possibilidade de uma nova via terapêutica para o tratamento do cancro da próstata.

INTRODUCTION

1. Prostate

1.1.Anatomy and histology

The prostate is a walnut-sized accessory gland of the male reproductive system that plays a crucial role in male fertility by producing the seminal fluid, a mixture of functionally diverse substances that support sperm activity (Hopkins et al., 2017; Verze et al., 2016). Located below the urinary bladder and in front of the rectum (Ittmann, 2018), the prostate can be anatomically and histologically divided into 4 major zones: peripheral zone, central zone, transition zone and anterior fibromuscular stroma (Figure 1) (McNeal, 1981; Rebello et al., 2021).

The peripheral zone, the outermost part of the prostate, constitutes ~70% of the glandular tissue and is located posteriorly, surrounding the central and transition zones. This zone is the most susceptible to inflammation, thus being the most frequent site for prostate cancer (McNeal, 1968, 1969, 1981). The central zone, comprising 20-25% of the glandular tissue, surrounds the ejaculatory ducts, and is described as being “immune to cancer” due to the infrequent occurrence of prostate cancer (PCa) in this zone (McNeal, 1981). The transition zone, making up to 5% of the prostate gland, lies between the peripheral zone and the central zone, and consists of two small lobules. This is the region where benign prostatic hyperplasia (BPH) typically arises. Finally, the anterior fibromuscular stroma is a nonglandular, thick sheath of tissue providing structural support to the prostate gland (Holland et al., 2003; Ittmann, 2018; Lee et al., 2011; McNeal, 1981).

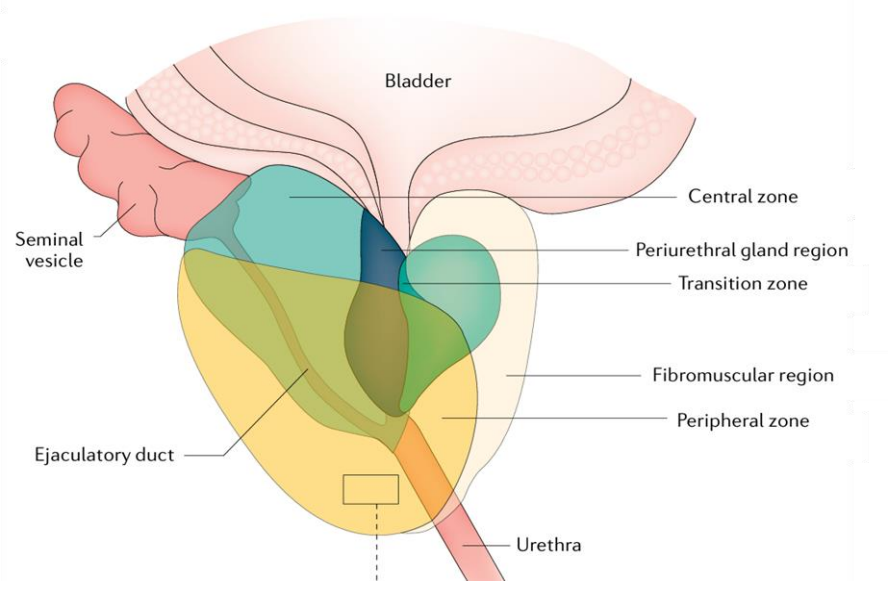

Figure 1. Anatomic structure of the prostate gland, showing the location of the peripheral, central and transition zones [adapted from (Rebello et al., 2021)].

Histologically, the prostate, as an exocrine gland, comprises acini and ducts. The epithelial tissue is divided into two layers based on cell type (Figure 2). The luminal layer is composed of tall columnar cells and is responsible for secreting various compounds, including prostate-specific antigen (PSA), prostatic acid phosphate and human kallikrein 2. On the other hand, the basal layer, which supports the luminal layer, consists of cuboidal epithelial cells and neuroendocrine cells. This basal layer is supported by a basement membrane that physically separates the epithelial cells from the stroma, a connective tissue that provides mechanical and nutritional support to the epithelial cells (Ittmann, 2018; Verze et al., 2016).

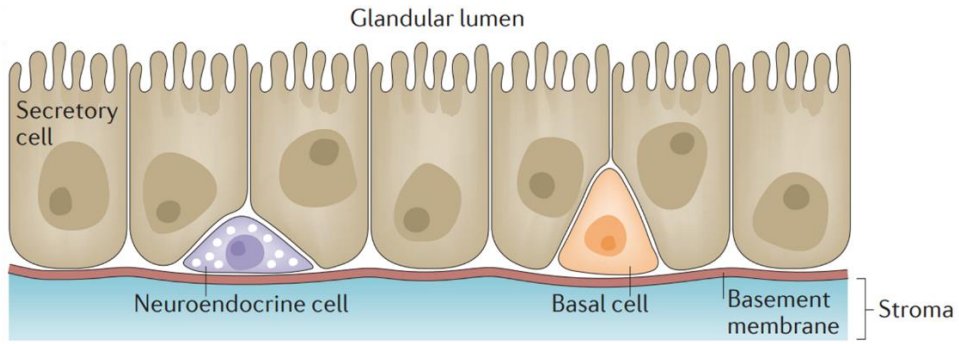

Figure 2. Histological organization of human prostate gland epithelium [adapted from (Verze et al., 2016)].

1.2.Prostatic lesions

Benign prostatic hyperplasia (BPH) is a non-malignant condition characterized by an enlarged prostate (Roehrborn, 2005). Although not considered a premalignant lesion itself, it often accompanies PCa development (Malins et al., 1997). BPH is frequent among ageing men, typically starting around the age of 40 and arises from the proliferation of both stromal and epithelial cells in the transition zone of the prostate, resulting in glandular enlargement. This enlargement exerts pressure on the urethra, potentially leading to lower urinary tract symptoms (LUTS), that include increased urinary frequency, a weakened or interrupted urine stream, nocturia, urinary incontinence and pain after ejaculation or during urination (Chughtai et al., 2016; Roehrborn, 2005). The precise cause of BPH remains unknown, but current theories focus on the deregulation of dihydrotestosterone (DHT), a male hormone involved in prostate development and growth (Roehrborn, 2005). Recent studies have revealed a significant correlation between higher DHT levels and larger prostates in patients with BPH, although the exact relationship remains unclear (Pejčić et al., 2017).

In contrast to BPH, prostatic intraepithelial neoplasia (PIN) is a premalignant prostatic lesion, that can be classified into Low Grade (LGPIN) or High Grade (HGPIN) (Bostwick & Qian, 2004; Brawer, 2005; Joniau et al., 2005), with the latter considered the most established precursor of PCa (Bostwick et al., 1996; Bostwick & Qian, 2004). HGPIN is characterized by an abnormal epithelial proliferation within preexisting benign acini and ducts, without stromal invasion (Bostwick & Qian, 2004; Brawer, 2005). Moreover, HGPIN exhibits specific cytological changes, including nuclear and nucleolar enlargement (Brawer, 2005). Correctly identifying HGPIN lesions is crucial, as the presence of HGPIN in a needle biopsy sample indicates a roughly 25% risk of detecting prostate carcinomas in subsequent biopsies (Zhou, 2018).

Once a PIN lesion is established, it can progress to an *in situ* adenocarcinoma, eventually evolving into a locally advanced carcinoma. Ultimately, the tumour may invade surrounding tissues and grow independently of androgen stimuli, culminating in metastatic castration-resistant prostate carcinoma (mCRPC) (Figure 3) (Sekhoacha et al., 2022).

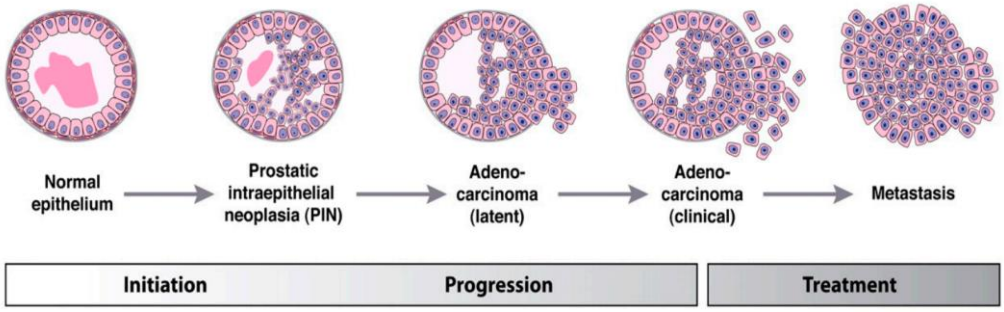

Figure 3. Schematic representation of human PCa progression - PCa starts with the development of a PIN lesion within the prostate ducts. Eventually, this lesion evolves into a localized adenocarcinoma, which may progress to advanced adenocarcinoma and, later, to metastatic PCa [adapted from (Sekhoacha et al., 2022)].

2. Prostate cancer

2.1.Epidemiology

Currently, prostate cancer (PCa) is the second most incident cancer and the fifth leading cause of cancer-related deaths among men (Ferlay J, 2024). In 2022, 1,466,718 new cases of PCa were diagnosed worldwide, representing 14.2% of new male cancer cases (Figure 4), and 397,430 reported deaths were attributed to PCa, accounting for 7.3% of cancer-related deaths in men worldwide (Figure 5) (Ferlay J, 2024).

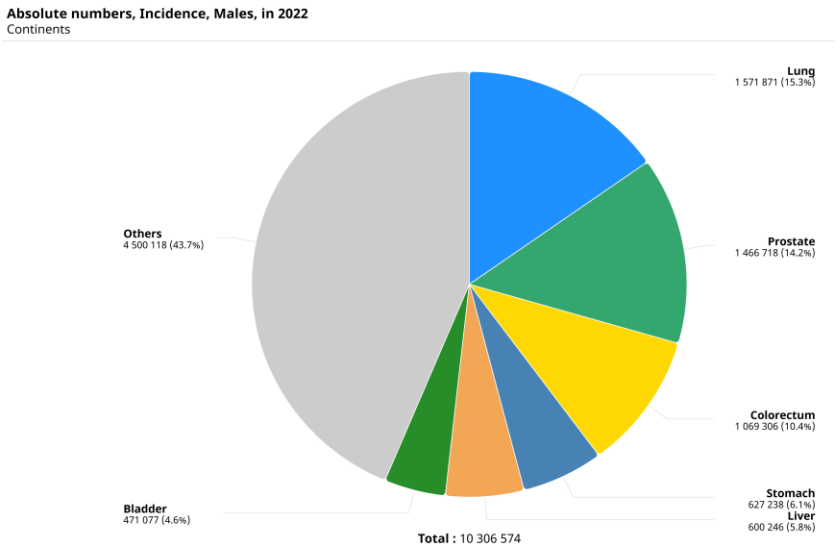

Figure 4. Worldwide incidence of male cancers in 2022 [adapted from GLOBOCAN 2022, available at https://gco.iarc.fr/].

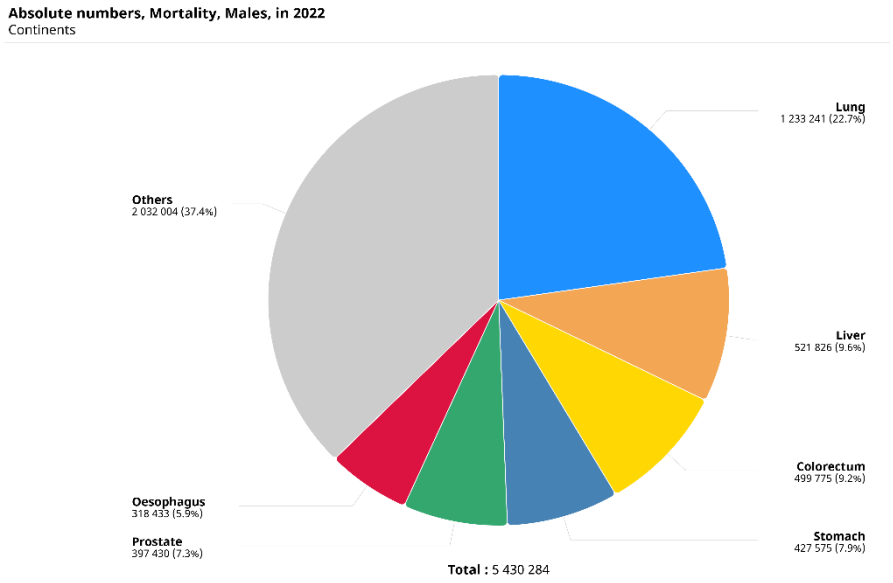

Figure 5. Worldwide mortality rated of male cancers in 2022 [adapted from GLOBOCAN 2022, available at https://gco.iarc.fr/].

Globally, PCa exhibits higher incidence rates in Western and Northern Europe, the Caribbean, Northern America, South Africa and Oceania, and a lower incidence rate in Asia and Northern Africa (Figure 6) (Culp et al., 2020; Sung et al., 2021; Wang et al., 2022). Conversely, mortality rates from PCa have decreased over the years in high-income countries due to early detection and the development of effective therapies (Culp et al., 2020; Wang et al., 2022).

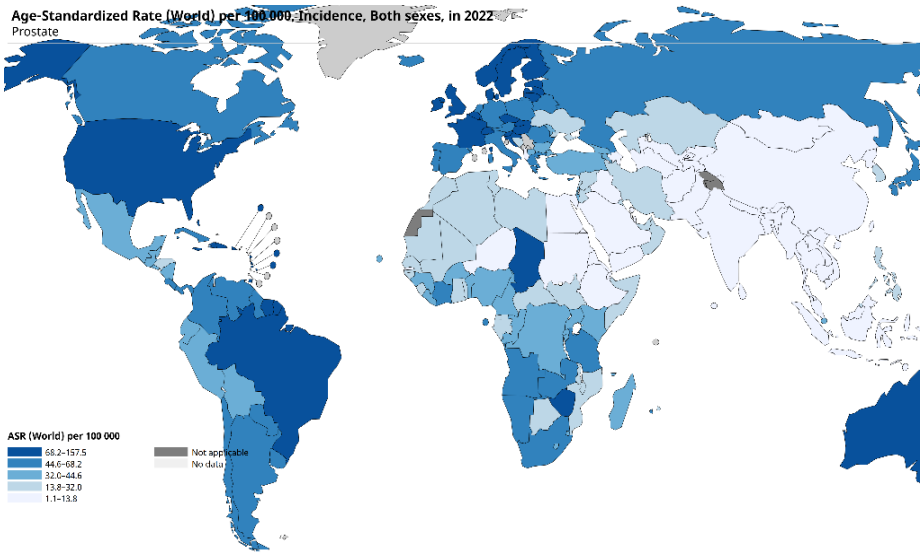

Figure 6. Age-standardized PCa incidence rates (ASR) worldwide [adapted from GLOBOCAN 2022, available at https://gco.iarc.fr/].

In Portugal, PCa stands as the most incident cancer in men, with 7,529 new cases diagnosed in 2022. Regarding mortality, PCa ranks as the third most fatal cancer for men, with 2,083 reported deaths in 2022 (Ferlay J, 2024). According to the latest projections for 2050, 2,637,926 new cases and 913,744 deaths are estimated to be attributed to PCa worldwide (Ferlay J, 2024).

2.2.Etiology and risk factors

Although PCa ranks among the most incident cancers worldwide, the precise etiology surrounding this disease is still unknown. Nevertheless, certain risk factors have been associated to PCa development, and these include advanced age, ethnicity, family history of the disease, specific inherited genetic alterations and some lifestyle and dietary factors (Allott et al., 2013; Center et al., 2012; Ferlay J, 2024).

Age is consistently identified as the most influential risk factor for PCa development. PCa incidence notably increases with age, particularly after the age of 50, and increases exponentially with each successive decade of life (Perdana et al., 2016). Moreover, survival rates decline with advanced age, with 26% of men the age of 75 years presenting high-risk disease (*SEER Cancer Stat Facts: Prostate Cancer. National Cancer Institute*).

On another note, ethnicity has a well-documented impact on PCa incidence and mortality. More specifically, African American men have the highest incidence of PCa in the

world, being 1.7 times more likely to be diagnosed with PCa and facing a ~2-fold higher risk of mortality due to more aggressive disease than Caucasian men (Perdana et al., 2016; Siegel et al., 2022). In contrast, Asian and Hispanic men generally show lower PCa incidence rates compared to Caucasian men (Perdana et al., 2016). These disparities are mostly attributed to genetic factors associated with ancestry or geographic origin, but can also be due to access to healthcare and/or environmental factors (Das & Rodriguez, 2020; Nair et al., 2022).

The risk of developing PCa is directly influenced by a family history of PCa. Notably, the risk of developing PCa increases by 2-fold in men with first-degree relatives with PCa when compared to men with no family history of this disease (Perdana et al., 2016). The risk also increases with the number of affected relatives, the closer the relatives are, and the younger the family members are at diagnosis and/or death (Bergengren et al., 2023). Moreover, the occurrence of other types of cancer in the family, including breast and ovarian cancer, also increases the risk of developing PCa (Bergengren et al., 2023; Perdana et al., 2016). Thus, understanding the patient's family history of cancer is crucial for risk assessment and better-informed screening practices. In line with this, certain genetic alterations, including those in the *BRCA1* and *BRCA2* genes, or familial genetic conditions such as Lynch Syndrome (LS) and Hereditary Breast and Ovarian Cancer (HBOC), also influence PCa risk (Brandão et al., 2020; Vietri et al., 2021). Additionally, environmental and lifestyle factors, such as smoking, alcohol consumption, excess weight and exposure to chemicals, have been described to increase the risk of developing the disease (Bergengren et al., 2023; Sung et al., 2021; Wilson & Mucci, 2019).

Given the multifactorial nature of PCa, integrating various factors into risk assessment, utilizing early detection strategies, and developing personalized management plans are crucial for individuals at an increased risk of developing the disease.

2.3.Diagnostic methods

PCa is predicted to begin developing at a very early age (around 20-30 years) and may progress slowly over several years before becoming clinically significant (Bax et al., 2018; Phan et al., 2020). Symptoms of PCa often appear in the advanced stages of the disease, underscoring the importance of screening programs for early detection. These programs play a crucial role in identifying PCa at its earliest stages when treatment outcomes are generally more favourable (Nevalainen et al., 2024).

According to the National Comprehensive Cancer Network (NCCN) and the European Society of Medical Oncology (ESMO) guidelines, the first step in early detection involves the evaluation of an individual's risk of PCa. This assessment includes documenting the patient's detailed medical history and considers various factors such as family cancer history, prior occurrences of prostate disease and cancer, ethnicity (with a focus on Black/African American individuals), medications taken, and exposure to environmental factors. This risk stratification helps to identify those who may benefit most from PCa screening (National Comprehensive Cancer Network, 2024).

For men aged 45-75, especially those at higher risk, screening typically includes PSA testing and a digital rectal examination (DRE). Individuals with abnormal screening results, such as elevated PSA levels (PSA>3ng/mL for those aged 45-75 or PSA≥4ng/mL for those over 75), or with very suspicious findings on DRE, are assigned for further evaluation, and a prostate biopsy may be recommended. Moreover, other complementary exams, such as a repeated PSA test, Magnetic Resonance Imaging (MRI), or additional biomarkers assessment, may also be considered (Figure 7) (National Comprehensive Cancer Network, 2024; Parker et al., 2020).

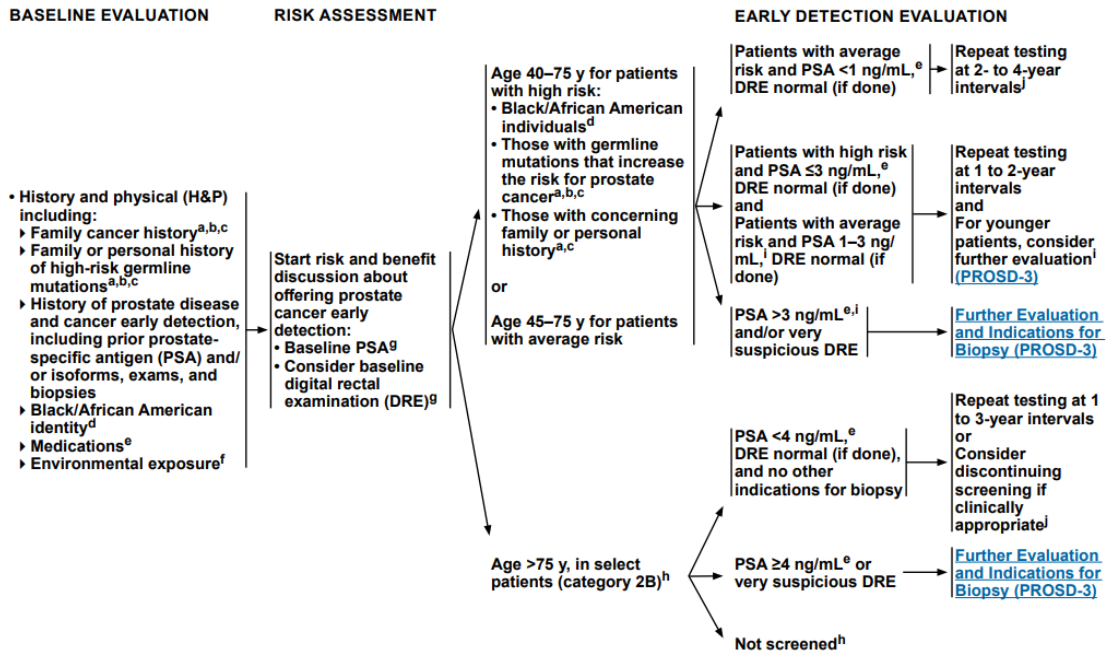

Figure 7. Guidelines for PCa early detection - NCCN Clinical Practice Guidelines in Oncology, version 1.2024 [adapted from (National Comprehensive Cancer Network, 2024)].

Throughout this process, healthcare providers engage in shared decision-making with eligible individuals. These discussions involve explaining the potential benefits, limitations

and uncertainties associated with PCa screening. Ultimately, the decision to undergo screening is made by the patient, based on their preferences (Miller et al., 2022).

2.3.1. Prostate-specific antigen (PSA)

Prostate-specific antigen (PSA) is a protein produced exclusively by prostatic epithelial cells, capable of hydrolysing the coagulum of the ejaculate and, consequently, increasing sperm motility (Aronson & deKernion, 2007; Sandhu & Schlegel, 2004). While most PSA remains in the semen, a small portion can enter the bloodstream, where its levels are indicative of an abnormal condition in the prostate (Sandhu & Schlegel, 2004).

PSA testing, which consists of the quantification of PSA levels in the blood, was first proposed in 1991 by Catalona et al., who stated that this screening tool could identify localized PCa more effectively than DRE or transrectal ultrasound (TRUS) (Catalona et al., 1991). Although this technique showed real potential due to its minimal invasiveness and low cost, it also drastically increased the incidence of PCa due to its low specificity, since high PSA levels can also result from other benign lesions, namely BPH or prostatitis, resulting in overdiagnosis and subsequent overtreatment of clinically non-relevant PCa (Bray et al., 2018; Van Poppel et al., 2021), (Guimaraes et al., 2020; Jia et al., 2022). Consequently, PSA is no longer used as a specific biomarker of PCa but is widely used for risk assessment, disease monitoring and treatment efficacy (Duffy, 2020).

A recent study by Schröder et al. evaluated PSA screening's impact on PCa incidence and mortality, showing a 25% relative reduction in PCa mortality among men aged 55-69 (Schröder et al., 2014). Based on this, current ESMO guidelines recommend PSA screening for men over 50 years of age. Additionally, PSA testing is advised for men aged over 45 with a family history of PCa, African-Americans over 45, and individuals over 40 carrying *BRCA1/2* mutations (Parker et al., 2020). Finally, PSA screening is not recommended for asymptomatic men with a life expectancy lower than 10 years, as the potential benefits of detecting PCa through PSA testing in these individuals may not outweigh the risks associated with unnecessary treatment (Parker et al., 2020).

2.3.2. Digital rectal examination (DRE)

The digital rectal examination (DRE) is one of the most frequently used tests to assess anatomic changes in the prostate gland, mostly due to its inexpensiveness, ease of

performance and association with a low false-positive rate. During this examination, a lubricated gloved finger is gently inserted into the patient's rectum to detect any abnormalities, such as prostate enlargement, nodules, lumps, or areas of hardness (Ragsdale et al., 2014).

Although DRE serves as a frequent screening tool for PCa, its accuracy as a standalone test is limited, as its effectiveness relies on the skill and experience of the examiner (Ragsdale et al., 2014).

Nowadays, DRE is often combined with PSA testing to improve the detection of PCa. A recent study revealed that a combination of PSA and DRE provides higher sensitivity, specificity and accuracy in the diagnosis of PCa, compared to either test alone (Barry & Simmons, 2017; Moses et al., 2023; Ozah & Imasogie, 2023).

2.3.3. Biopsy and Gleason score

As previously mentioned, a prostate biopsy is recommended for individuals with high PSA levels and/or suspicious findings on the DRE, representing the best diagnostic tool for PCa (Litwin & Tan, 2017; National Comprehensive Cancer Network, 2024). During the biopsy procedure, which is typically guided by trans-rectal ultrasonography (TRUS), approximately 10-12 small tissue samples are extracted from the prostate gland using a thin needle. After the samples are collected, they are observed under a microscope and a Gleason Score is assigned based on the histological patterns observed (Kasivisvanathan et al., 2018; Shariat & Roehrborn, 2008).

The Gleason Score (GS), introduced in 1974 by Donald Gleason and the Veterans Administration Cooperative Urologic Research Group, is determined by microscopically evaluating the two most predominant histological patterns observed in the biopsy tissue. Each pattern is graded on a scale of 1 to 5, with 1 being the most differentiated and 5 the least differentiated pattern. These grades are then combined to generate the GS, ranging from 2 to 10 (Gleason & Mellinger, 1974). Thus, a GS of 7 can represent either a mostly well differentiated tumour (3+4=7) or a predominantly poorly differentiated tumour (4+3=7), with different implications for disease management.

Advancements in understanding PCa biology and improvements in diagnostic techniques have prompted the development of a new grading system, known as the Grade Group, introduced in 2014 (Epstein, Egevad, et al., 2016; Pierorazio et al., 2013). The

Grade Group system simplifies PCa grading by categorizing tumours into five groups based on their histological architecture and aggressiveness. Grade Group 1 corresponds to Gleason scores of 6 or lower, indicating low-grade cancer with a favourable prognosis. Grade Group 2 includes Gleason scores of 3+4=7, representing intermediate-grade cancer. Grade Groups 3, 4 and 5 encompass Gleason scores of 4+3=7, 8 and 9-10, respectively, indicating aggressive cancer with increasing progression risk and poorer outcomes (Epstein, Zelefsky, et al., 2016; Pierorazio et al., 2013). This novel grading system has demonstrated efficacy in preventing overtreatment for patients with grade 1 prostate carcinomas (GS≤6), which are associated with a favourable prognosis (Epstein, Zelefsky, et al., 2016).

Even though ultrasound-guided prostate biopsy is the most frequently used technique for PCa diagnosis, it misses approximately 21-28% of prostate carcinomas (Litwin & Tan, 2017). As a result, pre-biopsy multiparametric magnetic resonance imaging (mpMRI) has emerged as the first approach to locate suspicious lesions. Recent studies showed that pre-biopsy mpMRI can reduce the number of patients undergoing TRUS-guided biopsy by 27-49% (Ippoliti et al., 2022). Additionally, MRI is increasingly used as a guidance tool during the biopsy procedure as it offers detailed anatomical images of the prostate gland, allowing precise targeting of suspicious areas (Ahdoot et al., 2020; Ippoliti et al., 2022). MRI images can be fused with TRUS for a guided biopsy. A prospective study demonstrated that targeted prostate biopsy using the MRI-ultrasound fusion significantly increased the detection of high-risk prostate carcinomas (GS≥4+3) while decreasing the detection of low-risk prostate carcinomas (GS=3+3) (Litwin & Tan, 2017; Siddiqui et al., 2015).

2.4.Treatment modalities and challenges

Selecting therapy for a patient involves a well-considered process that takes into account the tumour characteristics, such as PSA levels and Gleason Score; patient characteristics, which include patient age, co-morbidities and life expectancy; and the patient's preferences (Berg, 2016). PCa treatment can lead to side effects, including erectile dysfunction, infertility and urinary problems. Hence, it is crucial to educate the patient comprehensively about all aspects of the treatment, including its benefits and potential side effects, to promote a fully informed and deliberate decision-making process (Parker et al., 2020).

2.4.1. Approaches for localized or locally advanced prostate cancer

Localized PCa is a disease stage where the tumour remains confined to the prostate gland without invading the surrounding tissues (Wilt et al., 2021). According to the ESMO guidelines, patients with localized PCa should be classified into three risk categories: low, intermediate or high (Table 1) (Parker et al., 2020).

For patients with localized PCa, treatment options include watchful waiting (WW), active surveillance (AS), radical prostatectomy (RP), external beam radiotherapy (RT), low-dose-rate brachytherapy (BT), androgen deprivation therapy (ADT), and chemotherapy (CT). WW is typically recommended for patients who are not suitable candidates for or are reluctant to undergo treatment. RP alone is the only treatment with curative intent and is an option for both low- or high-risk PCa. ADT is the most widely used treatment approach. It works by suppressing the production of testosterone in the body (either chemically of physically through castration), thereby inhibiting prostate tumour cells from using testosterone as a growth factor, and ultimately leading to tumour regression (Sekhoacha et al., 2022). In WW patients it can be used for symptoms control. AS consists of closely monitoring the disease by performing recurrent PSA testing, biopsies and MRIs, and is also an option for low- or high-risk PCa, as well as BT, a radiotherapy technique where the radiation source is placed in or near the target issue. Patients with intermediate-risk tumours may also benefit from neoadjuvant ADT in combination with radical RT (Parker et al., 2020; Stish et al., 2018).

For patients with high-risk tumours, long-term ADT combined with radical RT has shown benefits. This was confirmed by the Trans Tasman Radiation Oncology Group 96-01 trial, which demonstrated that the use of hormone therapy improved overall mortality (Denham et al., 2005), and the Radiation Therapy Oncology Group trial 8610, which showed an improvement in 10-year mortality for patients treated with neoadjuvant and concurrent ADT (Pilepich et al., 2001). Additionally, these patients may benefit from neoadjuvant CT, and RP along with lymphadenectomy (Parker et al., 2020).

For patients suffering from locally advanced disease, neoadjuvant and adjuvant ADT combined with radical RT is recommended, as this approach has shown significant improvements in overall survival (Incrocci et al., 2016; Roach et al., 2008). These patients may also benefit from neoadjuvant CT or RP combined with pelvic lymphadenectomy (Parker et al., 2020).

Table 1. ESMO Guidelines regarding treatment options for localized PCa [adapted from (Parker et al., 2020)].

Localized disease	**Low-risk**	Active surveillance Brachytherapy RP Radical RT
	Intermediate-risk	RP Radical RT ± neoadjuvant ADT Brachytherapy Active surveillance
	High-risk	Long-term ADT + radical RT ± neoadjuvant docetaxel RP + pelvic lymphadenectomy
Locally advanced disease	Neoadjuvant ADT + radical RT + adjuvant ADT ± neoadjuvant docetaxel RP + pelvic lymphadenectomy	

ADT – Androgen Deprivation Therapy; RP – Radical Prostatectomy; RT – External Beam Radiotherapy

2.4.2. Approaches for metastatic prostate cancer

Metastatic PCa develops when PCa cells spread beyond the prostate gland to other parts of the body, including distant lymph nodes, bones, liver or lungs. Patients with metastatic PCa have a significantly shorter life expectancy compared to those with localized PCa (Freedland et al., 2023), underscoring the urgent need for developing new and effective therapeutic approaches to improve outcomes and extend survival for these patients.

Metastatic PCa can be classified as metastatic castration-sensitive PCa (mCSPC) or metastatic castration-resistant PCa (mCRPC). CSPC tumours are still hormone-sensitive, making ADT a highly recommended, and initially effective, treatment. For patients with CSPC, the treatment options include ADT complemented with other androgen pathway inhibitors as abiraterone, apalutamide, or enzalutamide, or with the chemotherapeutic agent docetaxel (Parker et al., 2020). Moreover, for patients with limited metastatic disease, ADT combined with focused RT directed at the primary tumour is other viable treatment option (Schaeffer et al., 2022).

Although PCa tumours are initially hormone-sensitive, most patients eventually develop resistance to ADT within 2-3 years, resulting in mCRPC (Cai et al., 2011). For these patients, ADT is still advised to control testosterone levels, in combination with additional therapies. These include secondary hormone therapies, chemotherapies, immunotherapies, radiopharmaceuticals and/or targeted therapies (Schaeffer et al., 2022).

Recently, PARP inhibitors have emerged as potential therapeutic approaches for PCa. Studies have shown that patients with mCRPC whose tumours harbour mutations in homologous recombination repair (HRR) genes, which include *BRCA1*, *BRCA2*, *ATM*, and *PALB2*, among others, may benefit from PARP inhibitors (Schaeffer et al., 2022). Olaparib and rucaparib, two PARP inhibitors, have already received FDA approval for use in PCa and are currently being studied as a front-line therapy for patients with mutations in HRR genes (Barsouk et al., 2020; Schaeffer et al., 2022).

3. Genetic alterations in prostate cancer

One of the main changes governing cancer initiation and progression involves alterations in the DNA sequence. These alterations include point mutations, single nucleotide polymorphisms (SNPs), and copy number variations (CNVs) (Fraser & Rouette, 2019; Shlien & Malkin, 2009; Vogelstein et al., 2013).

Point mutations trigger malignant transformation by disrupting the balance of regulatory mechanisms governing tumour suppressor genes and/or oncogenes, leading to uncontrolled cellular proliferation and/or decreased cell death (Hanahan & Weinberg, 2011). *SPOP* (speckle type BTB/POZ protein), *FOXA1* (forkhead box protein A1), *PTEN* (phosphatase and tensin homolog), and *TP53* (tumour protein P53) are the most frequently mutated genes in primary PCa (~15% of the cases), suggesting a role in early carcinogenesis ("The Molecular Taxonomy of Primary Prostate Cancer," 2015).

The presence of SNPs adds another layer of complexity to cancer predisposition. These subtle DNA sequence variations can influence gene expression and/or protein function, thereby modulating the risk of developing various malignancies, including PCa (Antoniou et al., 2009; Vinothkumar et al., 2020). Studies have shown that SNPs collectively contribute to over 28% of the inherited risk of developing PCa (Fraser & Rouette, 2019).

Additionally, CNVs significantly shape the genomic landscape of cancer. These involve duplications, deletions or other changes that can affect large DNA segments, resulting in

gene dosage imbalances that disrupt cellular homeostasis. In the context of PCa, research indicates a notable accumulation of CNVs throughout the genome, particularly affecting genes such as *PTEN* and *RB1*, which are involved in PCa progression (Wang et al., 2013).

3.1.Germline variants

Germline variants are inherited genetic alterations originated in germ cells, thus, being present in all cells of an individual's body, and can be transmitted from one generation to the next. These alterations significantly affect the susceptibility to develop PCa and can also influence the disease's aggressiveness (Chatrath et al., 2021).

Hereditary factors contribute to the development of approximately 5-15% of PCa cases, making it the cancer with the highest heritability among men. Individuals with hereditary PCa (HPCa) tend to develop more aggressive tumours at an earlier age and face a higher risk of recurrence following surgery when compared to those with non-hereditary (somatic) PCa. Nevertheless, no differences in overall survival have been reported between the two groups (Heidegger et al., 2019; Vietri et al., 2021).

The majority of the known mutations associated with HPCa susceptibility affect homologous recombination genes, such as *BRCA1*, *BRCA2*, *ATM*, and *CHEK2*, or DNA mismatch repair (MMR) genes, including *MLH1*, *MSH2*, *MSH6*, and *PMS2* (Heidegger et al., 2019; Vietri et al., 2021). Homologous recombination genes participate in a molecular DNA repair mechanism characterized by the exchange of genetic information between two closely related DNA sequences (Creeden et al., 2021). Deleterious *BRCA2* variants have been described to contribute to approximately 5% of the HPCa cases, while *CHEK2* variants for about 2%, *ATM* variants for ~1.5% and *BRCA1* variants for ~1% (Khan & Cheng, 2022; Pritchard et al., 2016; Vietri et al., 2021). Additionally, deleterious variants in these genes have been correlated with Hereditary Breast and Ovarian Cancer (HBOC), an inherited genetic condition characterized by an increased risk of developing breast, ovarian, prostate, and other cancers (Yoshida, 2021).

Deleterious variants in *BRCA1* (breast cancer gene 1) and *BRCA2* (breast cancer gene 2) genes, although rare in the population, significantly elevate the risk of developing certain types of cancer, including prostate, ovarian and breast cancer. For PCa, variants in *BRCA1* or *BRCA2* genes can increase the risk by 1.8- to 3.8-fold and 2.5- to 8.6-fold, respectively, by the age of 65 years old (Brandão et al., 2020; Ni Raghallaigh & Eeles, 2022). Additionally, studies have revealed that individuals with tumours harbouring deleterious *BRCA2* variants

tend to develop PCa at earlier ages, exhibit tumours with higher Gleason grades, face elevated risks of disease recurrence, and exhibit poorer responses to radical treatment, namely surgery and RT, when compared to non-carriers (Brandão et al., 2020; Cheng et al., 2019; Ni Raghallaigh & Eeles, 2022; Wang et al., 2018). Moreover, a 2015 study conducted by Castro et al. demonstrated that individuals harbouring *BRCA1/2* mutations had higher rates of metastases at 3, 5 and 10 years post-treatment, when compared to non-carriers (Castro et al., 2015).

CHEK2 (Checkpoint kinase 2) and *ATM* (ataxia telangiectasia mutated) are genes that encode for proteins involved in the cellular response to DNA damage, namely DNA-double strand break repair mechanisms (Brandão et al., 2020; Vietri et al., 2021). When DNA damage occurs, especially from ionizing radiation and/or other stressors, ATM serine threonine kinase plays a pivotal role by phosphorylating downstream proteins involved in DNA repair and/or cell-cycle regulation. Among the downstream activated proteins is CHEK2, which, when phosphorylated, can activate DNA repair pathways or induce cell cycle arrest (Brandão et al., 2020; Toss et al., 2021). Both *CHEK2* and *ATM* mutations have been associated with HBOC syndrome and, in the case of *CHEK2*, Li-Fraumeni syndrome (Vietri et al., 2021). In a recent study performed by Paulo et al., 94 genes associated with cancer predisposition were sequenced in a series of 121 PCa patients, using next generation sequencing (NGS). The results revealed that 14.9% of the cases had potentially pathogenic germline variants predisposing for PCa, with *ATM* (5.8%) and *CHEK2* (3.3%) being the most frequently mutated genes (P. Paulo et al., 2018).

MMR genes, namely, *MLH1* (mutL homologue 1), *MSH2* (mutS homologue 2), *MSH6* (mutS homologue 6), and *PMS2* (postmeiotic segregation increased 2), are critical components of the cellular machinery responsible for preserving the genome integrity by correcting errors that occur during DNA replication. These genes play a vital role in identifying and repairing mismatch base pairs, insertion-deletion loops, and other DNA replication errors that can lead to mutations and genomic instability if left unrepaired (Harfe & Jinks-Robertson, 2000; Li, 2008). In fact, mutations in MMR genes, especially *MLH1* and *MSH2,* are associated with Lynch syndrome (LS), previously known as hereditary non-polyposis colon cancer (HNPCC) (Brandão et al., 2020; Harfe & Jinks-Robertson, 2000; Li et al., 2021). LS is a hereditary condition primarily associated with an increased risk of colorectal and endometrial cancer, although several extracolonic cancers, including gastric, small bowel, pancreatic, brain and urothelial cancers, have been reported within the Lynch tumour spectrum (Cerretelli et al., 2020; Li et al., 2021). Furthermore, recent epidemiological studies have established an association between LS and the risk for PCa

development (Huang et al., 2018). In fact, PCa was formally included in the LS spectrum after a systematic review and meta-analysis performed in 2014 by Ryan et al. This analysis showed that 73% of the prostate tumours in mutation carriers exhibited MMR deficiency and that men with LS had an elevated overall risk of developing PCa (Ryan et al., 2014). Nevertheless, despite these findings, the link between Lynch syndrome and an increased risk of PCa remains a subject of debate, as conflicting results have been reported in different studies (Aarnio et al., 1999; Brandão et al., 2020; Pande et al., 2012).

While much attention has been directed towards understanding the role of homologous recombination genes and DNA MMR genes in PCa susceptibility, recent research has highlighted the importance of additional genetic factors, such as *HOXB13* (Homeobox B13). *HOXB13*, a gene encoding a transcription factor crucial for prostate gland development, is known to interact with the androgen receptor (AR) and regulate gene expression in the prostate (Dupont et al., 2021; Norris et al., 2009). Among the various mutations within *HOXB13*, the G84E variant stands out for its higher prevalence among individuals with a family history and early-onset PCa, when compared to those with non-familial late-onset PCa (Ewing et al., 2012). In fact, a study conducted in 2014 showed that individuals carrying the G84E variant of *HOXB13* had a 3.5-fold increased risk of developing PCa (Karlsson et al., 2014). Nevertheless, this variant appears to be predominantly present in men of European ancestry (Chen et al., 2013). Furthermore, aside from G84E, other *HOXB13* variants such as G135E, A128D and F240L have been identified, albeit in specific populations (Brandão et al., 2020).

In a study from 2018, Paulo et al. performed a study, using NGS, to identify germline mutations in individuals with early-onset or familial PCa, aiming to elucidate the genetic basis of this subset of PCa. By focusing on a panel of genes known to be associated with cancer predisposition, the researchers aimed to uncover novel genetic determinants contributing to PCa susceptibility. The results showed mutations in *ATM* and *CHEK2*, previously linked to PCa predisposition, along with the discovery of five novel candidate PCa-associated genes: *RAD51C*, *FANCD2*, *FANCI*, *CEP57* and *RECQL4*. In fact, similar to *BRCA1*, *BRCA2* and *ATM*, *RAD51C*, *FANCD2* and *FANCI* are genes linked to Fanconi anaemia, while, *CEP57* and *RECQL4* are linked to other recessive disorders (Paula Paulo et al., 2018).

Despite ongoing research efforts to uncover new mutations associated with PCa development, the current understanding remains limited. In fact, only 7-21% of gene mutation frequencies have been identified to date, leaving a substantial fraction of genes yet to be discovered (Vietri et al., 2021). Therefore, it is crucial to continue searching for

novel genes to expand our understanding of the genetic landscape of PCa and gain insights into the underlying molecular mechanisms of the disease.

3.2.Somatic variants

Somatic variants are spontaneous mutations that occur in the DNA of somatic cells. Unlike germline mutations, which are inherited and present in every cell of an individual's body, somatic mutations are acquired during a person's lifetime and are typically localized to specific tissues or organs. These mutations can arise from various exogenous factors, such as ultraviolet light, ionizing radiation and certain chemicals, as well as endogenous factors, including reactive oxygen species, aldehydes, or errors during cell division that are inadequately repaired. When left unrepaired, somatic mutations persist, disrupting the normal regulation of cell growth, proliferation, and metastasis, thereby conferring a selective advantage to the mutated cells (Martincorena & Campbell, 2015).

In 2015, The Cancer Genome Atlas (TCGA) undertook a comprehensive study involving 333 primary prostate carcinomas to explore the molecular and genetic characteristics of these tumours. The findings revealed that 74% of the tumours could be categorized into one of seven groups based on distinct gene fusions (*ERG*, *ETV1*, *ETV4* or *FLI1*) or mutations (*SPOP*, *FOXA1* or *IDH1*). Notably, 53% of all tumours harboured an ETS-family gene fusion, while mutations in *SPOP*, *FOXA1*, and *IDH1* were less frequent (11%, 3% and 1%, respectively) ("The Molecular Taxonomy of Primary Prostate Cancer," 2015).

SPOP is a gene responsible for encoding a protein involved in DNA double strand break repair. Consequently, mutations in *SPOP* disrupt this DNA repair mechanism, resulting in genomic instability (Boysen et al., 2015). Studies have shown that *SPOP* mutations and ETS alterations are mutually exclusive, while tumours with both *SPOP* and *FOXA1* mutations can been found ("The Molecular Taxonomy of Primary Prostate Cancer," 2015). In fact, tumours with both *SPOP* mutation and *CHD1* deletion exhibit elevated levels of methylation (Lin, 2021; "The Molecular Taxonomy of Primary Prostate Cancer," 2015). Despite studies have reported that tumours with *SPOP* mutations tend to respond better to androgen deprivation therapy (ADT) (Nakazawa et al., 2022), the prognostic impact of *SPOP* mutations remains a subject of ongoing investigation, with some studies suggesting a poor prognosis associated with *SPOP*-mutant PCa (García-Flores et al., 2014), while others have reported conflicting results (Shoag et al., 2020).

FOXA1, also known as hepatocyte nuclear factor 3-alpha (HNF3A), serves as a transcriptional factor engaged in regulating the expression of transthyretin and α_1-antitrypsin in the liver. Within the prostate, FOXA1 plays a pivotal role in AR-mediated gene regulation and signalling, a pathway fundamental to prostate development and homeostasis. Specifically, FOXA1 can bind directly to DNA, facilitating DNA transcription by loosening compacted chromatin. Previous studies have already reported FOXA1 to be implicated in tumorigenesis, acting both as an oncogene and a tumour suppressor gene, depending on the cancer type. In PCa, elevated levels of FOXA1 correlate with poor prognosis (Robinson et al., 2013).

IDH1 encodes for a key enzyme involved in cellular metabolism, particularly in the tricarboxylic acid (TCA) cycle, where it catalyses the oxidative decarboxylation of isocitrate to α-ketoglutarate. Mutations in *IDH1* have been identified in various types of cancer, including acute myeloid leukaemia and gliomas. In the prostate, mutations in *IDH1* are linked to early-onset PCa and are characterized by an increased methylation status (Kaffenberger & Barbieri, 2016; "The Molecular Taxonomy of Primary Prostate Cancer," 2015).

DNA fusions regarding the ETS family will be discussed in greater detail in Chapter 5.

4. Epigenetic alterations in prostate cancer

Although much attention has been given to the genetic pattern of prostate tumours, recent studies have highlighted the important role of epigenetic modifications in PCa development.

According to the National Cancer Institute, an epigenetic alteration is “a change in the chemical structure of DNA that does not change the DNA coding sequence” (Institute, 2021). These modifications include DNA methylation, histone modifications, chromatin remodelling, and regulation via non-coding RNAs. Dysregulation of these epigenetic mechanisms can result in aberrant gene expression profiles, which may lead to tumour initiation, progression and even therapeutic resistance in PCa (Kgatle et al., 2016; Sugiura et al., 2021).

DNA hypermethylation is the most predominant epigenetic alteration found in PCa. This alteration is mediated by DNA methyltransferases (DNMTs), which are responsible for methylating gene promoter regions, leading to gene inactivation. In fact, genes involved in

DNA repair (*GSTP1*, *MGMT*), cell cycle (*CDKN2*, *RASSF1*), growth suppression (*APC*, *RAR*β), apoptosis (*DCR1*, *DCR2*, *XAF1*, *TMS1*) and cell adhesion (*CDH1*, *CD44*) are among the most frequently hypermethylated genes in PCa (Kgatle et al., 2016; Sugiura et al., 2021).

GSTP1, a member of the Gluthathione-S-transferases (GSTs) enzyme family, is responsible for detoxifying xenobiotics to protect DNA against potential carcinogens and reactive oxygen species (Cui et al., 2020; Henrique & Jerónimo, 2004). In PCa, *GSTP1* silencing through promoter hypermethylation stands as the most frequent epigenetic alteration, present in over 90% of the prostate carcinomas (Henrique & Jerónimo, 2004). This alteration can also be found in HGPIN, the precursor lesion of PCa. Since *GSTP1* hypermethylation is absent in normal tissue, it holds promise as a potential biomarker for PCa (Cui et al., 2020; Sugiura et al., 2021).

Besides *GSTP1*, other genes classified as tumour suppressor genes or “caretaker” genes may also undergo silencing due to hypermethylation. Consequently, DNMT inhibitors, which block promoter hypermethylation, have emerged as promising therapeutics for PCa. Azacitidine and decitabine are two DNMT inhibitors with demonstrated anti-tumour efficacy in PCa xenografts (Baumgart & Haendler, 2017; Naldi et al., 2014).

Contrarily, certain genes as *PLAU*, *HPSE* and *CYP1B1*, can be found hypomethylated in PCa. Although this is less frequent and the underlying molecular mechanisms are not yet understood, hypomethylation typically appears in late stages of PCa, such as metastasis (Sugiura et al., 2021).

Additionally, gene expression can also be influenced by histone modifications, a series of molecular mechanisms that impact the chromatin structure, thereby altering the accessibility to transcriptional machinery and changing the gene expression pattern. Histones undergo various modifications, including acetylation, methylation, phosphorylation and ubiquitination (Nowacka-Zawisza & Wiśnik, 2017; Sugiura et al., 2021). In this chapter, only histone acetylation and methylation will be briefly mentioned in the context of PCa given that these are the most well studied histone modifications.

Histone acetylation is a molecular process mediated by histone acetyltransferases (HATs) and histone deacetylases (HDACs), which add or remove acetyl groups from histones, respectively. Generally, histone acetylation is associated to gene transcription whereas deacetylation leads to gene silencing. In PCa, studies have shown that HATs are hyperactivated in tumours, correlating with high PSA levels and increased invasiveness.

HAT inhibitors are currently being used as a potential treatment option to control PCa growth (Albany et al., 2011; Nowacka-Zawisza & Wiśnik, 2017).

Histone methylation is a molecular process catalysed by methyltransferases, in which one, two or three methyl groups are added to histones. This modification can either activate or repress gene expression, depending on the methylation level and also the position of the amino acids involved (Ngollo et al., 2014; Nowacka-Zawisza & Wiśnik, 2017). In PCa, a reduction in the levels of histone 3 lysine 4 (H3K4) dimethylation is frequently observed, however, patients exhibiting PCa with lower H3K4 dimethylation have a poorer prognosis and an increased risk of relapse when compared to those with higher levels (Chervona & Costa, 2012; Seligson et al., 2009).

MicroRNAs (miRNAs) are a class of small non-coding RNAs capable of regulating gene expression at the post-translational level by either degrading or repressing the translation of target mRNAs. In recent years, miRNAs have garnered significant interest due to their pivotal role in regulating numerous biological processes, with their dysregulation being associated with various diseases, including PCa (Doghish et al., 2022; Rana et al., 2022). In fact, cancer cells exhibit different miRNA expression patterns compared to normal cells, emphasizing the important role of miRNAs in cancer development and progression, and highlighting their potential as cancer biomarkers, prognostic indicators and even therapeutical targets (Jorge et al., 2021; Rana et al., 2022). In 2007, Porkka et al. investigated the expression of 319 human miRNAs in PCa cell lines and PCa xenografts, generating, for the first time, a miRNA expression profile for PCa. Their findings revealed 37 down-regulated miRNAs and 14 over-expressed miRNAs in PCa samples (Porkka et al., 2007). Subsequent studies have confirmed and expanded upon these results, identifying additional dysregulated miRNAs in PCa. A study performed in 2008 demonstrated that miR-141 is upregulated in PCa and can accurately distinguish patients with PCa from healthy controls, with miR-141 levels correlating with PSA levels (Mitchell et al., 2008). Overall, miRNAs play a crucial role in PCa development, providing valuable insights into disease progression and potential therapeutic targets. Nevertheless, gaps remain in the current understanding of specific miRNA biological roles and their clinical utility as diagnostic or prognostic biomarkers.

5. Role of the ETS family in prostate cancer

5.1.ETS subfamilies

The E26 transformation-specific (ETS) family of transcription factors is a group of 28 human transcription factors divided into 12 subfamilies, according to the homology of the "ETS domain", a DNA binding domain composed of 84 to 90 conserved amino acids, capable of recognizing and binding to DNA 5'-GCA(A/T)-3' motifs (Dhara et al., 2022; Nicholas et al., 2019; Qian et al., 2022). Upon binding to DNA, these transcription factors can either activate or repress gene expression. The ETS family is involved in multiple molecular pathways, namely haematopoiesis, immune cell maturation, neuronal and vascular development, and oncogenesis (Dhara et al., 2022; Gina M. Sizemore et al., 2017).

Among the ETS subfamilies, the oncogenic ERG and PEA3 subfamilies have gathered significant attention due to their roles in different carcinomas, namely, in PCa development (Qi et al., 2020). The ERG subfamily is composed of ERG, FLI1 and FEV while the PEA3 subfamily comprises ETV1, ETV4 and ETV5 (Figure 8) (Qi et al., 2020).

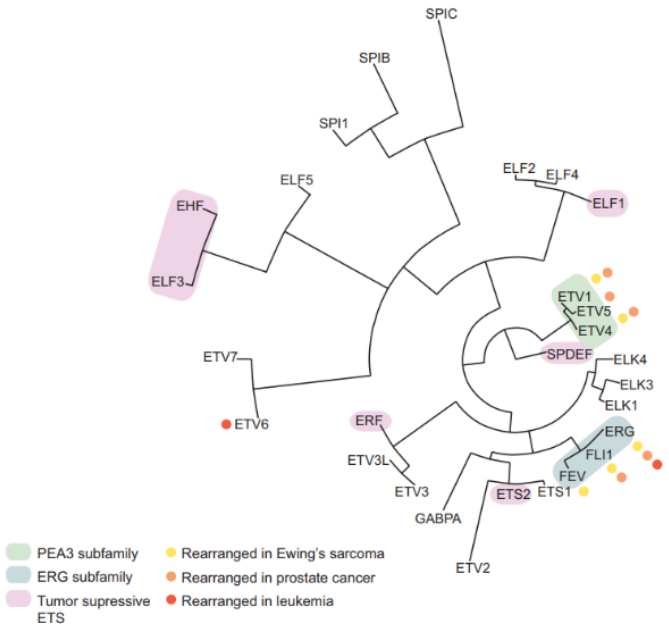

Figure 8. Hierarchical representation of the ETS family members based on the homology of the DNA-binding domain - PEA3 subfamily members are highlighted in green, the ERG subfamily in blue and the tumour suppressive ETS subfamily in pink. Red, orange and yellow dots highlight ETS genes found rearranged in leukaemia, PCa and Ewing's sarcoma, respectively [adapted from (Nicholas et al., 2019)].

Despite variations in expression across different tissues, ETS transcription factors are expressed in all cell types. In the prostate, the SPDEF, also known as PDEF (prostate-derived ETS factor) is the most expressed ETS transcription factor. Unlike others, the *SPDEF* gene is not involved in gene fusions and, along with ELF3 and EHF, plays a tumour-suppressor role in the prostate (Nicholas et al., 2019).

5.2.ETS rearrangements

ETS rearrangements are the most frequent genetic alterations found in PCa cells, but are also found in Ewing's sarcoma and myeloid leukaemia (Qi et al., 2020; G. M. Sizemore et al., 2017). In PCa, these rearrangements generally involve the fusion of the 5' region of an androgen-regulated promoter with the 3' region of the ETS transcription factor gene, leading to ETS overexpression (Nicholas et al., 2019).

Rearrangements involving *ERG* are the most frequent, being present in approximately 50% of all prostate carcinomas. Nevertheless, chromosomal rearrangements involving other members of the ETS family, namely the PEA3 subfamily, are also recurrent, with *ETV1* rearrangements present in 8-10% of the prostate carcinomas. Genomic rearrangements leading to *ETV4*, *ETV5* and *FLI1* overexpression are more infrequent (2-5% of all prostate carcinomas). Although ERG and PEA3 rearrangements are generally mutually exclusive, some rare cases have been reported in which patients harbour both *ERG* rearrangements and *ETV1* or *ETV4* fusions, although in different tumour foci (Nicholas et al., 2019).

The most frequent ETS fusion partner is the *TMPRSS2* gene, an androgen responsive gene which encodes for a transmembrane serine protease highly expressed by epithelial cells in different tissues, including prostate (Nicholas et al., 2019; Qian et al., 2022). Multiple genomic breakpoints have been described for the *TMPRSS2-ERG* fusion, although the most typical involve the fusion of the non-coding intron 1 of *TMPRSS2* and the coding introns 3, 4 or 5 of *ERG*, which result in 5' truncated ERG proteins (Qian et al., 2022). Since the discovery of the *TMPRSS2-ERG* and *TMPRSS2-ETV1* fusions by Tomlins et al. in 2005 (Tomlins et al., 2005), multiple other ETS fusion partners have been reported, although the majority of them in isolated PCa cases. These include *SLC45A3*, *NDRG1*, and *HERPUD1* for *ERG*, *SLC45A3*, *HERV-K*, *HERVK17*, *C15ORF21*, *HNRPA2B1*, *OR51E2*, *EST14*, *FLJ35294*, *FOXP1*, and *ACSLS* for *ETV1*, and *SLC45A3*, *CANT1*, *KLK2*, *DDX5*, *HERVK17*, and *UBTF* for *ETV4* (Nicholas et al., 2019).

5.3.Oncogenic functions

The ETS family of transcription factors is involved in numerous cellular processes, including proliferation, cell cycle regulation, differentiation and apoptosis. Thus, alterations in ETS expression can disrupt cellular homeostasis, leading to tumour development, progression and even metastasis.

In PCa, ETS rearrangements are described as an early event in carcinogenesis, detectable in precursor lesions such as HGPIN, but absent in benign lesions, such as BPH. However, a second oncogenic event, such as *PTEN* inactivation or *TP53* loss, is described to be necessary for tumour development (Nicholas et al., 2019).

In addition to mediating cancer cell self-renewal and survival, ETS factors also play roles in regulating DNA repair, maintaining genomic stability, modulating the chromatin landscape, influencing the tumour microenvironment, and altering cellular metabolism (Gina M. Sizemore et al., 2017). A study performed in 2011 by Brenner et al. demonstrated that the product of *TMPRSS2-ERG* fusion directly interacts with the enzyme poly (ADP-ribose) polymerase 1 (PARP1) and DNA protein kinases (DNA-PKcs), ultimately leading to cell invasion and PCa progression (Brenner et al., 2011). Additionally, overexpression of ΔERG can modulate the chromatin landscape by upregulating the expression of histone lysine *N*-methyltransferase enhancer of zeste homologue 2 (EZH2), which methylates histone H3 lysine 27 (H3K27), resulting in gene silencing (Brenner et al., 2011; Yu et al., 2010). Additionally, the ETS family of transcription factors also regulates genes involved in the extracellular matrix (ECM), including those encoding for matrix metalloproteinases (MMPs), collagenases, serine proteases and glycoproteins. Specifically, the product of *TMPRSS2-ERG* fusion activates the transcription of certain genes, namely *MMP9* and plexin A2 (*PLXN2*), which enhance cellular invasiveness in PCa cells (Brenner et al., 2011). Lastly, ETS factors are described to alter the metabolism of PCa cells. Cells with *TMPRSS2-ERG* fusion exhibit dysregulated fatty acid, sphingolipid and polyamine signalling (Baena et al., 2013; Brenner et al., 2011; Meller et al., 2016).

5.4.Prognostic value

Rearrangements involving the ETS family of transcription factors have emerged as potential clinical biomarkers of a cancerous prostate. Nevertheless, the prognostic value of oncogenic ETS, especially rearrangements involving *ERG*, is not well established, since there's still some controversy around this theme (Barwick et al., 2010; Nicholas et al., 2019).

A 2007 study by Wang et al. reported that various rearrangements involving *ERG* were associated with aggressive PCa and poor outcome following radical prostatectomy (Wang et al., 2006). Another study from the same year found a significant association between the *TMPRSS2-ERG* fusion and disease relapse in patients with clinically localized PCa, indicating poorer outcomes (Nam et al., 2007). Of note, a cohort study conducted in 2007 concluded that the *TMPRSS2-ERG* fusion was significantly associated with PCa-specific death, further correlating the fusion with poor prognosis (Demichelis et al., 2007). Later, in 2015, Font-Tello et al. reported that fusion-positive tumours were linked to a higher Gleason Score (GS), a more aggressive phenotype and poor prognosis (Font-Tello et al., 2015), while Kulda and colleagues, in 2016, suggested that higher expression of *TMPRSS2-ERG* was linked to shorter disease-free survival (Kulda et al., 2016). More recently, in 2020, Zhou and colleagues showed that tumours with *TMPRSS2-ERG* fusion exhibited reduced immune infiltration, which is associated with tumour development and worse prognosis. (Zhou et al., 2020).

Conversely, other studies have reported no correlation between *TMPRSS2-ERG* fusion and worse prognosis. For instance, a study performed by FitzGerald et al. showed that the presence of this fusion in PCa was not associated with reduced survival. However, there was a trend suggesting higher PCa-specific mortality in patients with multiple copies of *TMPRSS2-ERG* (FitzGerald et al., 2008). Additionally, several studies have suggested an association between *TMPRSS2-ERG* fusion and a better prognosis. In 2005, Petrovics et al. showed that fusion-positive tumours were correlated with longer PSA recurrence-free survival, indicating a less aggressive behaviour of tumours overexpressing *ERG* (Petrovics et al., 2005). These findings were supported by subsequent studies, namely one performed in 2007 by Winnes et al. and other performed in 2008 by Saramäki (Saramäki et al., 2008; Winnes et al., 2007).

The discrepancies between studies may be attributed to different factors, including differences in the study design, population differences, the inherent heterogeneity of PCa, or the inter-tumour heterogeneity characteristic of ERG overexpression in PCa (Baena et al., 2013). Therefore, it is crucial to conduct further research to accurately determine the prognostic significance of *TMPRSS2-ERG* fusion, which could then be applied to clinical settings to better patient stratification.

In contrast to *ERG* fusions, various studies have shown that overexpression of ETV1 or ETV4 transcription factors is associated with poor prognosis in PCa. In 2008, Attard and colleagues showed that tumours harbouring *ETV1* rearrangements correlated with higher GS and higher PSA levels at diagnosis, both indicators of worse prognosis. However, an

association between the presence of these rearrangements and poorer survival was not found (Attard et al., 2008). The link between ETV1 overexpression and increased disease aggressiveness and poor prognosis was later confirmed by others, including the study from Baena et al. in 2013, and that from Segalés et al. in 2019 (Baena et al., 2013; Segalés et al., 2019). Additionally, in 2015, Qi and colleagues demonstrated that ETV4 overexpression was an unfavourable prognostic factor, as tumours overexpressing ETV4 were associated with higher GS and advanced pathological stage (Qi et al., 2015). Recent studies, performed by our research group, have shown that ETV1 overexpression contributed to increased cellular proliferation and invasion in prostate-derived cell lines (Mesquita et al., 2015).

5.5.Therapeutic implications

Given their role as oncogenic factors in PCa, ETS transcription factors have emerged as potential targets for inhibiting PCa development and progression. Nevertheless, developing effective therapeutic drugs targeting ETS factors is challenging due to their nuclear localization and the lack of “binding pockets”, which makes them difficult to target. Additionally, it is crucial to avoid disrupting the normal physiological roles of both oncogenic and non-oncogenic ETS factors, as some of these factors play vital roles in essential cellular functions (Nicholas et al., 2019).

YK-4-279 is a small-molecule that has been studied as an inhibitor of ETS factors, including FLI1, ERG and ETV1. A study performed by Rahim et al. in 2011 demonstrated that YK-4-279 can inhibit ERG and ETV1 transcriptional activity and significantly decrease invasion in PCa cell lines harbouring *ERG* or *ETV1* rearrangements. Moreover, this compound showed greater cytotoxicity in cell lines with ETS-rearrangements compared to those without (Rahim et al., 2011). Following these *in vitro* results, Rahim and colleagues tested YK-4-279 *in vivo* using mouse xenograft models. LNCaP cells, which are *ETV1* fusion-positive cells, were subcutaneously injected into the dorsal flank of SCID/beige mice, which were then treated with YK-4-279. The treatment led to an inhibition in both tumour growth and development of lung metastasis (Rahim et al., 2014). Furthermore, when tested in combination with docetaxel, a chemotherapeutic drug used as first-line treatment for castration-resistant PCa, YK-4-279 synergistically inhibited the growth of LNCaP and PC3 cell lines, induced apoptosis and decreased motility and invasion (Yu et al., 2017).

Other compounds, namely BRD32048 and CIT-0312 have shown real potential in targeting ETS fusion-positive cells *in vitro*. By using small-molecule microarrays, Pop and

colleagues identified BRD32048, a small-molecule that directly binds to ETV1, impacting its transcriptional activity in LNCaP cells and inhibiting invasion in PCa cell lines harbouring *ETV1* rearrangements (Pop et al., 2014), however, clinical trials have not yet been performed. Additionally, in 2019, Currie and colleagues showed that the compound CIT-0312 had the ability to disrupt the interaction between ETS transcription factors and DNA. Consequently, CIT-0312 inhibited the growth of cell lines overexpressing ERG or ETV1, suggesting its potential as a therapeutic drug. Nevertheless, due to its lack of high specificity, further refinement of this compound is necessary (Currie et al., 2018).

Given the significant interest in developing novel therapeutic compounds targeting ETS factors and the inherent challenges in doing so, our research group has shifted focus toward identifying ETS-downstream effectors that could serve as therapeutic targets. In 2012, Paulo et al. conducted a study that identified and validated specific and shared target genes of ETS transcription factors in PCa, particularly ERG and ETV1. While using VCaP and LNCaP knockdown cell line models they confirmed that *KCNH8*, *GRPR* and *TMEM45B* are downstream effectors of both ERG and ETV1, making these promising therapeutic targets (Paulo et al., 2012). Additionally, recent studies performed by our research group led to the identification of a positive feedback loop between EGFR and ETV1 in PCa, highlighting the EGFR-STAT3 pathway as a promising therapeutic target (Paiva, Orr, Azeredo, et al., *submitted*).

6. EGFR signalling in prostate cancer

6.1.EGFR gene, protein and receptor

The epidermal growth factor receptor (EGFR) gene, also known as *HER1*, and *ERBB1* (among others), encodes a tyrosine kinase that belongs to the human epidermal receptor (HER) family, alongside with HER2, HER3 and HER4. EGFR plays vital roles in cell growth, proliferation, apoptosis, angiogenesis and cancer development (Burgess, 2008; Sabbah et al., 2020; Sigismund et al., 2018).

Located at the short arm of chromosome 7 (7p11.2), the *EGFR* gene is composed of 31 exons that encode for a transmembrane glycoprotein that belongs to the protein kinase superfamily (Sabbah et al., 2020). Structurally, EGFR is composed of three main domains, namely, an extracellular domain responsible for ligand biding, an hydrophobic alpha-helix transmembrane domain that anchors the receptor to the cell membrane, and an intracellular tyrosine kinase domain containing a C-terminal tail with multiple tyrosine residues, activated

by phosphorylation upon ligand binding (Sabbah et al., 2020; Sigismund et al., 2018). While the tyrosine kinase domain is conserved across the HER family members, differences exist between the extracellular and C-terminal domains of these receptors (Figure 9) (Normanno et al., 2006; Sabbah et al., 2020; Sigismund et al., 2018).

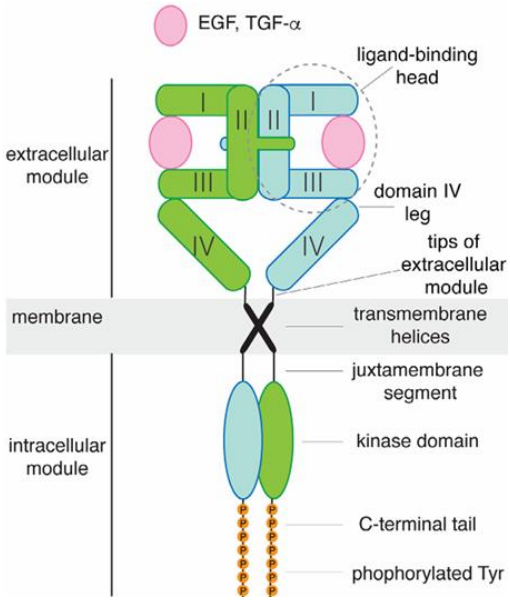

Figure 9. Schematic representation of the EGFR structure – The EGFR is a receptor constituted by an extracellular domain with a ligand-binding head (domains I-IV), a hydrophobic transmembrane domain (composed of transmembrane helices), and an intracellular tyrosine kinase domain containing a C-terminal tail rich in tyrosine residues [adapted from (Huang et al., 2021)].

6.2.EGFR signalling pathways

The EGFR can bind to various ligands with different affinities, including amphiregulin, betacellulin, epidermal growth factor (EGF), heparin-binding EGF-like growth factor, and transforming growth factor-alpha (TGF-α) (Quesnelle et al., 2007). Ligand binding occurs at the receptor's extracellular domain, causing a conformational change that triggers receptor dimerization. This dimerization can occur with other EGFR receptor (homodimerization) or with a different member of the HER family (heterodimerization). As a result of dimerization, the intracellular tyrosine kinase is activated, resulting in the autophosphorylation of specific tyrosine residues located in the C-terminal region. Once phosphorylated, these tyrosine residues lead to activation of several downstream signalling cascades, including RAS/RAF/MAPK, PI3K/AKT, PLC/PKC and JAK/STAT (Figure 10) (Huang & Fu, 2015; Sabbah et al., 2020; Sigismund et al., 2018).

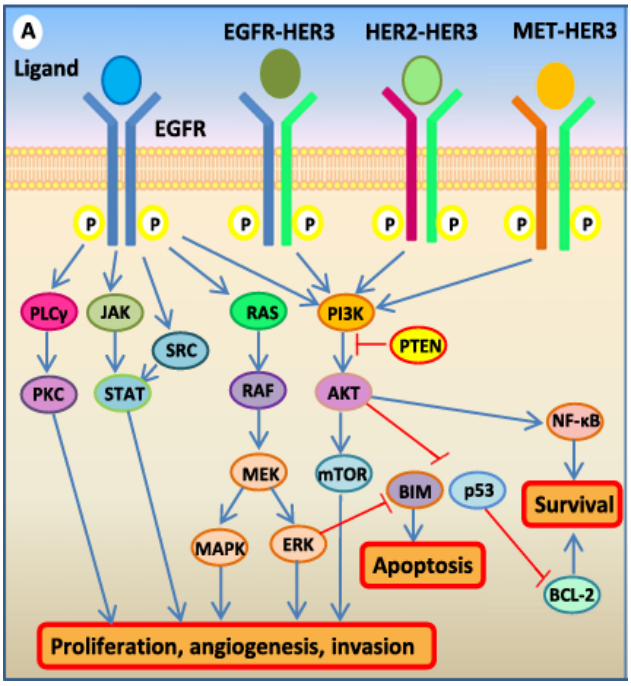

Figure 10. Signalling pathways activated by EGFR and/or other HER family receptor – Autophosphorylation of the tyrosine residues in the intracellular domain of EGFR activates several oncogenic pathways, including RAS/RAF/MAPK, PI3K/AKT, PLC/PKC and JAK/STAT. Activation of these downstream cascades alters gene expression, ultimately promoting proliferation, angiogenesis, invasion and survival, while inhibiting apoptosis [adapted from (Leto & Trusolino, 2014)].

6.3.Mutations and oncogenic functions of EGFR

Due to its involvement in various signalling pathways, dysregulation of EGFR can lead to oncogenic transformation and tumour development. This dysregulation can result from gene amplification, point mutations or in-frame deletions. *EGFR* amplification results in an increased number of EGFR receptors on the cell surface, enhancing cells' responsiveness to growth signals, stimulating receptor dimerization, and activating multiple signalling pathways. On the other hand, point mutations can affect the receptor ubiquitination and degradation, or alter the extracellular domain of the receptor (Sabbah et al., 2020; Sigismund et al., 2018). The L858R point mutation in exon 21 and small in-frame deletions in exon 19 (ΔLRE) are the most frequent EGFR mutations. In non-small cell lung cancer (NSCLC), these mutations are associated with constitutive activation of EGFR signalling, increased aggressiveness and development of metastasis. Moreover, they are also correlated with poor prognosis in other types of cancer, including breast, lung, bladder, ovarian, oesophageal, brain and head and neck cancers (Hong et al., 2014; Sabbah et al.,

2020; Sharma et al., 2007). In light of these evidences, several EGFR targeted therapies have been developed and are currently used in clinical practice.

6.4.EGFR inhibitors and resistance mechanisms

EGFR inhibitors are classified in two main categories: monoclonal antibodies (mAbs) and tyrosine kinase inhibitors (TKIs). mAbs target the extracellular domain of the receptor, preventing ligand binding, whereas TKIs target the intracellular domain, inhibiting EGFR phosphorylation and blocking the activation of downstream signalling pathways. Despite their different mechanisms of action, both types of EGFR inhibitors effectively block EGFR activation and its downstream signalling (Sabbah et al., 2020; Sigismund et al., 2018; Wu et al., 2022).

The first mAb developed to specifically bind EGFR was cetuximab, also known as C225, which not only inhibits EGFR signalling but also promotes EGFR internalization, thus reducing receptor activation (Baselga, 2001; Reynolds & Wagstaff, 2004). Cetuximab has shown potent antitumor activity in various types of cancer, including non-small cell lung cancer (NSCLC), head and neck squamous cell carcinoma (HNSCC), and metastatic colorectal cancer (mCRC), with the two latest receiving approval from the Food and Drug Administration (FDA) and the European Medicines Agency (EMA) in 2004 (Reynolds & Wagstaff, 2004). Since then, other EGFR-targeted mAbs have been developed and approved, namely, panitumumab for the treatment of mCRC, necitumumab for metastatic NSCLC and nimotuzumab for HNSCC (Guardiola et al., 2019; Wu et al., 2022).

Regarding TKIs, there are currently six FDA-approved options, that can be divided into three generations: the first generation of EGFR-TKIs includes gefitinib and erlotinib, the second generation includes afatinib and dacomitinib, and the third generation includes osimertinib (Wu et al., 2022). Gefitinib was the first TKI to be approved for patients with NSCLC in 2004 (Cohen et al., 2003), followed by other TKIs. Despite their initial effectiveness, most patients eventually develop resistance to first generation EGFR-TKIs, relapsing after several months (Guardiola et al., 2019; Wu et al., 2022). This resistance can arise from various mechanisms, including secondary *EGFR* mutations, point mutations in downstream effectors as KRAS, BRAF or PI3K, or activation of alternative signalling pathways through other receptors, such as HER3, c-MET, IGFR, PDGFR, or VGEFR (Huang & Fu, 2015). The most frequent resistance mutation is the T790M located in exon 20, which increases ATP binding and leads to constitutive EGFR activation. In such cases, second generation TKIs are more effective (Wu et al., 2022).

Erlotinib is currently approved as monotherapy for the treatment of NSCLC and in combination with gemcitabine for pancreatic cancer. The recommended daily dose of erlotinib for patients suffering from pancreatic cancer is 100mg, whereas for patients with NSCLC is 150mg, which is considered the maximum tolerated dose. The most frequent side effect of erlotinib are skin rash, diarrhoea and fatigue (Cohen et al., 2005).

6.5.EGFR and its role in prostate cancer progression

PCa development is a complex, multistep process, under which various molecular mechanisms, signalling pathways and cascades play a role. Understanding these pathways and the receptors involved is crucial for the development of novel therapeutic drugs.

As previously mentioned, EGFR is a receptor involved in multiple signalling pathways and plays a significant role in the development and progression of different types of cancer (Hong et al., 2014; Sabbah et al., 2020; Sharma et al., 2007). Given its activity in cancer progression, in general, numerous studies have been conducted to elucidate EGFR's role in PCa. In a 2002 study by Di Lorenzo et al., it was shown that EGFR was overexpressed in the majority of the prostate carcinomas, including those who underwent radical prostatectomy as first-line therapy, those who received hormone-therapy before radical prostatectomy and those with metastatic and hormone-refractory PCa. Moreover, tumours overexpressing EGFR were significantly associated with higher Gleason Scores and disease relapse (Di Lorenzo et al., 2002). Four years later, Shah and colleagues demonstrated that EGFR overexpression was linked with the transition to androgen unresponsiveness in PCa progression (Shah et al., 2006). Furthermore, in 2011, Peraldo-Neia et al. showed that patients with tumours overexpressing EGFR were associated with disease relapse. Therefore, determining EGFR expression status in tumours could aid in better stratifying PCa patients in the clinic (Peraldo-Neia et al., 2011).

Previous studies performed by our research group explored the possible association between ETS overexpression in prostate-derived cell lines and EGFR activation. Analysis of the results led to the conclusion that ETV1 overexpression alone is sufficient to induce activation of EGFR-regulated pathways, suggesting the potential utility of therapies targeting EGFR as novel approaches for carcinomas harbouring ETV1 overexpression. Furthermore, *in vitro* studies showed that treating ETS-overexpressing cell lines with the EGFR inhibitor erlotinib resulted in both growth impairment and increased apoptosis in an ETS-dependent manner. Despite these findings, the specific molecular pathways involved in this response remain unknown, underscoring the need for further investigation.

7. Primary cilia in prostate cancer

7.1.Structure and function of primary cilia

Primary cilia are non-motile, microtubule-based organelles that protrude from the surface of most eukaryotic cells. Structurally, they are comprised of 9 outer microtubules with no inner microtubules (9+0 microtubule rearrangement) and are anchored to the cell by the basal body, a structure nucleated by the mother centriole (Figure 11). Contrary to motile cilia, primary cilia do not have the ability to move, but they function as sensory organelles, capable of receiving, transmitting and translating mechanical and chemical stimuli from the extracellular environment (Carvalho-Santos et al., 2011; Higgins et al., 2019; Mill et al., 2023).

Primary cilia assembly, disassembly and function is closely controlled by intraflagellar transport (IFT). IFT proteins can be involved in two different protein complexes, namely, the IFT complex A and the IFT complex B, which are responsible for the retrograde and anterograde transport of ciliary proteins, respectively. This transport system is essential for the delivery of structural components and signalling molecules to the cilium but also for the removal of turnover products (Lechtreck, 2015; Lin et al., 2021; Scholey, 2003).

Apart from promoting molecular shuttling, primary cilia also anchors multiple signalling receptors, including those of hedgehog (Hh), platelet-derived growth factor (PDGF), Notch, Wnt, and mTOR pathways. The localization of these receptors within the ciliary membrane enables primary cilia to function as signalling hubs, integrating and converting diverse external signals into intracellular responses (Higgins et al., 2019; Pala et al., 2017; Saternos et al., 2020).

Multiple studies have focused on ciliary proteins and their role in regulating ciliogenesis. Aurora quinase A (AURKA), a key protein in cell cycle regulation, is activated at the basal body of primary cilia when cells exit the G0 phase in response to growth factors. This activation can be promoted by different proteins, including NEDD9 (Neural Precursor Cell Expressed, Developmentally Down-Regulated 9) and TCHP (Trichoplein, keratin filament-binding protein). Once activated, AURKA subsequently activates HDAC6 (Histone deacetylase 6), which promotes the destabilization of primary cilia microtubules, stimulating primary cilia disassembly (Pugacheva et al., 2007; Zhang et al., 2019). On another note, the intraflagellar transport 88 (IFT88) protein, was the first ciliary protein directly associated with the development of polycystic kidney disease. As part of the IFT complex B, IFT88 plays a crucial role in regulating ciliogenesis and ensuring proper mitotic spindle orientation,

essential for a correct mitotic division. In fact, reduced expression of IFT88 is correlated with shortened primary cilia, underscoring its importance in maintaining cilia homeostasis (Fujii et al., 2021; Hua & Ferland, 2018). Furthermore, Arl13b (ADP-ribosylation factor-like protein 13b) is a small guanosine triphosphate exclusively located in the primary cilium, where it stabilizes the IFT-A and IFT-B complexes. Research has shown that the absence of Arl13b results in shortened cilia and defects in the ciliary axoneme, highlighting its critical role in ciliary structure and function (Larkins et al., 2011; Zhang et al., 2019). Although significant research has been conducted on the main functions of ciliary proteins, there is still a considerable knowledge gap regarding the role of many ciliary proteins.

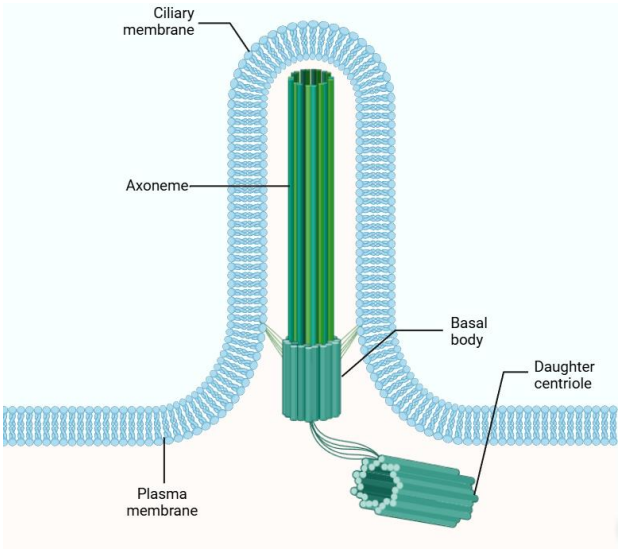

Figure 11. Schematic representation of primary cilium structure – Primary cilia are structures present in the membrane of human cells and attached to the basal body. They are structured by microtubules, which, all together, form the axoneme [created with Biorender.com].

Primary cilia assembly and disassembly are tightly coordinated with the cell cycle. Cilia typically assemble during the G0 and G1 phases and are resorbed before cell enters mitosis, allowing the centrosome to detach from the basal body and act as a mitotic spindle pole, essential for proper chromosome alignment during mitosis (Plotnikova et al., 2009). Serum deprivation/starvation is a technique frequently used in cell culture to promote primary cilia assembly, as the absence of serum induces cell cycle arrest, enabling cells to enter into a state of differentiation, and stimulating ciliogenesis. In contrast, the reintroduction of serum triggers cell cycle re-entry and leads to primary cilia disassembly (Kasahara & Inagaki, 2021; Lim et al., 2015).

In addition to cell cycle regulation, primary cilia can also sense and respond to other changes in the extracellular environment, such as pH and oxygen levels. In a study performed in 2019 by Atkinson et al., it was shown that lower extracellular pH can increase the length of primary cilia, which could modulate the activity of pH-sensitive ion channels and, consequently, the signalling pathways within the ciliary compartment (Atkinson et al., 2019). However, the response of primary cilia to hypoxia appears to be cell type-dependent (Lavagnino et al., 2016; Shamloo et al., 2017).

Another important aspect of primary cilia function is their ability to act as mechano-sensors. Although non-motile, primary cilia can detect and transduce mechanical stimuli like fluid motion or tissue deformation in certain tissues, such as kidney, bone, cartilage and the vasculature (Prasad et al., 2014; Saternos et al., 2020). This ability is typically mediated by the presence of mechanosensitive ion channels, such as Polycistin-1 (PC1) and Polycistin-2 (PC2). Bending of the primary cilium triggers the opening of these channels, allowing calcium ions to enter the ciliary compartment and activate downstream signalling cascades. (Pala et al., 2017; Saternos et al., 2020).

Moreover, cell confluence and cell-to-cell contact have also been shown to affect primary cilia dynamics. Interestingly, 3T3-L1 cells, a preadipocyte cell line, can be differentiated into adipocytes *in vitro*, when cells reach confluence. In 2009, a study by Zhu and colleagues demonstrated that, during this process, the cells undergo growth arrest and assemble primary cilia (Xu et al., 2016; Zhu et al., 2009). Recently, in 2020, Ma et al. showed that human mesenchymal stem cells (MSCs) cultured *in vitro* under confluent conditions also produced primary cilia (Ma et al., 2020).

In summary, primary cilia are highly specialized sensory organelles that can detect and transduce a wide range of mechanical, chemical and environmental signals into intracellular responses. Nevertheless, the specific molecular mechanisms by which the cell cycle, extracellular factors and various signalling pathways regulate primary cilia assembly, disassembly and function are still largely unknown and remain an active area of ongoing research (Kasahara & Inagaki, 2021).

7.2.Primary cilia alterations in cancer development

Given their diverse functions and impact on various signalling pathways, the regulation and proper function of primary cilia are essential for maintaining cellular homeostasis. Malfunctions in primary cilia disassembly can act as a brake on the cell cycle, inducing cells

to enter a dormant state. On the other hand, defects in cilium formation can accelerate the re-entry in the cell cycle and lead to the development of various diseases, collectively known as ciliopathies. These disorders, which encompass over 30 human diseases, are mostly inherited in an autosomal recessive manner. They typically manifest in childhood or adolescence and can affect multiple tissues in the human body, including the eye, kidney, liver, brain and heart (Braun & Hildebrandt, 2017; Fabbri et al., 2019; Mill et al., 2023).

Because primary cilia play a crucial role in preventing uncontrolled cell growth and maintaining a normal epithelial phenotype, there has been growing interest in understanding their role in cancer progression. Nevertheless, the effect of primary cilia in tumorigenesis appears to be cell type and tissue-specific, as it can both stimulate or suppress cancer development (Carotenuto et al., 2023; Lee, 2023).

Primary cilia loss is a frequent event in different types of cancer, including cholangiocarcinoma, melanoma, ovarian cancer, colon cancer, breast cancer, medulloblastoma, renal cancer, and PCa (Figure 12) (Eguether & Hahne, 2018; Lee, 2023). For instance, in cholangiocarcinoma, inhibiting HDAC6 in cancer cells lacking primary cilia leads to ciliogenesis restoration and inhibits cancer growth (Peixoto et al., 2020). On another note, the *VHL* (Von Hippel-Lindau) gene encodes a tumour suppressor protein that plays an important role in ciliogenesis, and germline mutations in *VHL* are associated with the development of clear-cell renal cell carcinoma (ccRCC). Similarly to HDAC6 inhibition in cholangiocarcinoma, VHL re-expression in ccRCC restores primary cilia assembly (Esteban et al., 2006). In ovarian cancer, overexpression of AURKA, induces cilia disassembly and disrupts Hh signalling, ultimately promoting ovarian cancer development (Egeberg et al., 2012).

Contrary to the majority of other cancers, Emoto and colleagues showed that primary cilia are present in pancreatic cancer cells, and associate with increased metastasis and worse prognosis (Emoto et al., 2014). However, recent studies have demonstrated that, during tumorigenesis progression, primary cilia are gradually lost in pancreatic cancer cells, but, in contrast, are increased in the surrounding stroma (Carotenuto et al., 2023; Schimmack et al., 2016). Additionally, basal cell carcinoma and a subtype of medulloblastoma, are characterized by having more ciliated cells than the non-tumorigenic tissue (Eguether & Hahne, 2018). Basal cell carcinoma is the most frequent form of skin cancer, and its development is correlated with the activation of Hh signalling, a pathway exclusively linked to the primary cilia in epidermal keratinocytes. Notably, loss of primary cilia in keratinocytes has been shown to halt tumour development in a mouse model (Eguether & Hahne, 2018; Wong et al., 2009). Regarding medulloblastoma, a study

performed in 2015 by Gate and colleagues demonstrated that, when analysing primary cilia presence in 24 biopsies from medulloblastoma patients, primary cilia was present in tumours with activated Hh and Wnt signalling pathways (Gate et al., 2015).

Overall, targeting primary cilia offers a new and promising avenue for cancer therapy, potentially leading to more effective treatments.

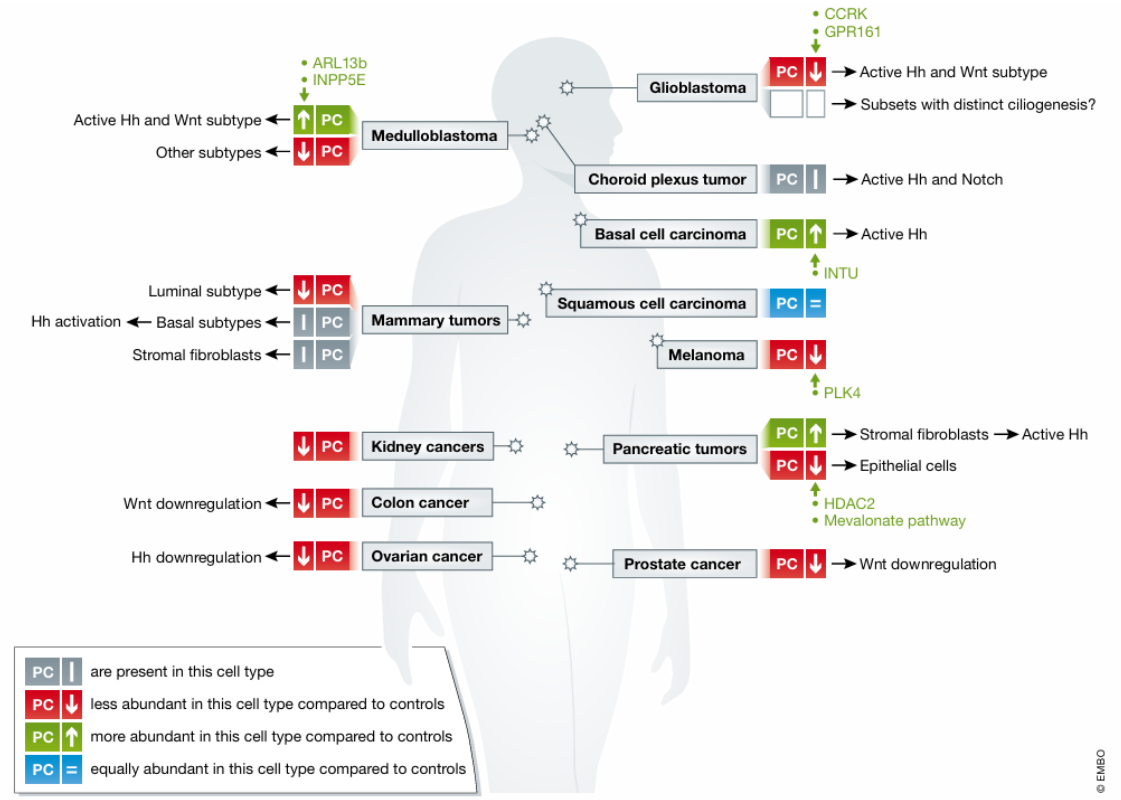

Figure 12. Overview of primary cilia abundance in different types of cancer – Primary cilia are lost in various types of cancer, including, medulloblastoma, melanoma, glioblastoma, breast, kidney, colon, ovarian, prostate and pancreatic cancers. Nevertheless, an increase in primary cilia is observed in basal cell carcinoma, a subtype of medulloblastoma and a subtype of pancreatic cancer, compared to controls [adapted from (Eguether & Hahne, 2018)].

7.3.Primary cilia alterations in prostate cancer

The frequency and length of primary cilia in PCa was first thoroughly characterized in 2013 by Hassounah et al. This study analysed various prostate-related tissues, including normal prostatic tissue, prostatic intraepithelial neoplasia (PIN), PCa tissue, and perineural invasion lesions. Using acetylated tubulin to stain primary cilia, the results demonstrated a loss of primary cilia in both preinvasive and invasive tissues, with a gradual decrease in

ciliated cells being observed with increasing aggressiveness of prostate tissues. However, when examining stromal cells surrounding cancer, there were no significant differences in the frequency of primary cilia between the different stages of prostate lesions, indicating that primary cilia loss is specific to cancer cells and not the surrounding stroma (Hassounah et al., 2013). It was also evident that both cancer cells and the surrounding stromal cells, both in preinvasive and invasive PCa, had abnormally short primary cilia, which was correlated with ciliary dysfunction. To confirm this, the authors measured nuclear β-catenin signals, a marker of activated canonical Wnt signalling (Hassounah et al., 2013). Previous studies have shown that primary cilia can suppress the canonical Wnt signalling pathway (Corbit et al., 2008; Lancaster et al., 2011), so a loss of primary cilia would typically be associated with an increase in nuclear β-catenin. However, a decrease in nuclear β-catenin was observed, likely due to lack of canonical Wnt ligands or other pathway components in the tissue (Hassounah et al., 2013).

Later, in 2009, study performed by Zhang and colleagues demonstrated that PCa cell lines, namely LNCaP, PC3, DU145 and 22Rv1, failed to assemble primary cilia, even under conditions that promote ciliogenesis, such as serum starvation and high cell confluence (Zhang et al., 2009). Jamal et al. also reported the absence of primary cilia in DU145 cells, and a very low percentage of primary cilia in PC3 cells (Jamal et al., 2020).

Given the consistent reports on the loss and dysfunction of primary cilia in PCa, restoration of primary cilia emerges as a potential strategy to induce cell cycle arrest in cancer cells and control PCa progression.

7.4.Primary cilia and EGFR signalling

As previously mentioned, EGFR is a receptor tyrosine kinase involved in numerous signalling pathways and its dysregulation is frequently observed in different types of cancer (Hong et al., 2014; Sabbah et al., 2020; Sharma et al., 2007). Interestingly, recent studies have highlighted a complex interaction between EGFR signalling and primary cilia formation.

In a recent study (2021), Kasahara and Inagaki demonstrated that, when activated, EGFR kinase has the ability to phosphorylate and, consequently, activate the ubiquitin specific peptidase 8 (USP8). Once activated, USP8 deubiquitinates and stabilizes TCHP, which binds to AURKA leading to ciliogenesis suppression. Nevertheless, under serum starvation conditions, EGFR is not activated, preventing USP8 from deubiquitinating TCHP.

Consequently, TCHP is degraded, AURKA remains inactive, and primary cilia assembly occurs. The authors also showed that knockdown of *EGFR* in RPE1 cells (an hTERT-immortalized retinal epithelial cell line) is sufficient to induce ciliogenesis (Kasahara et al., 2018). This study was the first to associate EGFR activation with primary cilia regulation, opening new possibilities for using EGFR-targeting drugs to restore ciliogenesis and regulate cell growth.

Given the recent interest in discovering pharmacological agents capable of regulating ciliogenesis, numerous studies have been conducted to screen clinically approved drugs for their effects on primary cilia assembly. In a 2016 study, Khan et al. performed a high-content analysis-based screening and identified several small molecules that could restore primary cilia assembly. Of the 1600 compounds tested in CFPAC-1 cells (a pancreatic cancer cell line), 118 were found to enhance ciliogenesis. Interestingly, gefitinib, an EGFR inhibitor, was among these ciliogenic drugs. Further verification showed that gefitinib significantly stimulated primary cilia assembly in several other cell lines, including a lung cancer cell line (A549), a kidney cancer cell line (UMRC2), a breast cancer cell line (SUM159), and another pancreatic cancer cell line (L3.6) (Khan et al., 2016).

More recently, in other compound screening to identify drugs that stimulate or inhibit ciliogenesis, a panel of 178 kinase inhibitors was tested in RPE1 cells. The EGFR inhibitor erlotinib was found to block primary cilia disassembly when cells were exposed to serum, suggesting that EGFR activation is involved in cilia disassembly. However, when exploring the ability of erlotinib in restoring ciliogenesis in different cell lines, results were heterogeneous, suggesting that the cilia-restoration effect of erlotinib appears to be cell type-specific (Kiseleva et al., 2019).

Nevertheless, primary cilia regulation by EGFR inhibitors represents a promising avenue for cancer therapy that deserves further investigation.

AIMS

Aims

Previous studies have demonstrated that EGFR-targeted therapies hold great potential for restoring ciliogenesis in cancer cells. Given that PCa cells exhibit a defective ciliogenesis phenotype, the main aim of this thesis project is to investigate the impact of *de novo* ΔERG or ETV1 overexpression in the ciliogenesis of prostate-derived cells, and whether EGFR inhibition is capable of restoring ciliogenesis in an ETS-specific cell context.

To accomplish this, we propose to address the following aims:

1. Uncovering a link between *de novo* ETS overexpression and primary cilia loss in prostate carcinogenesis;

2. Exploring ETS-specific characteristics of primary cilia in PCa cells;

3. Evaluate the potential utility of the EGFR inhibitor, Erlotinib, in primary cilia restoration in an ETS-specific cell context.

MATERIALS AND METHODS

Methods

1. Cell lines

In this study, clonal cell populations derived from the non-tumorigenic prostate-derived cell line PNT2 were used. PNT2 cells, originally derived from a normal prostate of a 33-year-old male at *post mortem* (Berthon et al., 1995), were obtained from the European Collection of Authenticated Cell Cultures (Sigma-Aldrich, St. Louis, MO, USA). Additionally, stable clonal PNT2 cell populations with *de novo* expression of ΔERG or ETV1, previously established by the Cancer Genetics Group (CGG) (Paulo et al., 2012), were used (Table 2). Validation of ΔERG and ETV1 expression levels in these cell models was performed by quantitative reverse transcription PCR (Appendix 1).

The Lenti-X 293T cell line, a highly transfectable subclone of the transformed human embryonic kidney cell line HEK 293, was previously acquired from Takara Bio (Mountain View, CA, USA).

PNT2 Neo, PNT2 ETV1-C1 and PNT2 ΔERG-C3 were grown in RPMI-1640 medium (Gibco, Invitrogen™, Carlsbad, CA, USA) whereas Lenti-X 293T cells were grown in DMEM (PAN-Biotech GmbH, Aidenbach, Germany). All cell lines were maintained in standard growth medium supplemented with 10% fetal bovine serum (FBS; Gibco, Thermo Fisher Scientific, Carlsbad, CA) and 1% penicillin/streptomycin solution (Gibco, Thermo Fisher Scientific, Carlsbad, CA), and grown at 37°C, in a humidified atmosphere with 5% CO_2.

Cell lines were regularly tested for *Mycoplasma spp.* contaminations using a PCR Mycoplasma Detection Set (Clontech Laboratories, Mountain View, CA, USA).

Table 2. Cell line models used in this study

Cell Line	Model	Description
PNT2	PNT2 Neo	Control cells obtained after transfection of PNT2 cells with a pMSCV-Neo empty vector; expresses low levels of ETV1 and ERG, similar to the parental, *wild-type* cells
	PNT2 ETV1-C1	*ETV1* overexpressing clone obtained after transfection of PNT2 cells with a pMSCV-Neo vector carrying full-length *ETV1* (resembling the expected protein consequence resulting from the most common *ETV1* rearrangement)
	PNT2 ΔERG-C3	*ERG* overexpressing clone obtained after transfection of PNT2 cells with a pMSCV-Neo vector carrying a 5' truncated *ERG* sequence (resembling the expected protein consequence resulting from the most common *TMPRSS2-ERG* fusion)

2. Primary cilia characterization

2.1. Modulation of primary cilia assembly and disassembly

To investigate and characterize primary cilia in prostate-derived cell lines, we developed an immunofluorescence-based workflow to assess changes in both cilia assembly and disassembly (Figure 13). Briefly, PNT2-derived cell populations were cultured in regular growth conditions – RPMI 1640 medium supplemented with 10% (v/v) FBS and 1% (v/v) Penicillin/Streptomycin – on 20x20mm glass coverslips (Normax, Portugal) placed in 6-well plates (SPL Life Sciences, Seoul, South Korea), to reach ~80% confluency after 24 hours. Then, four distinct end-points were assessed and analysed:

I. Baseline (BL): PNT2-derived cell lines were cultured in regular growth conditions for additional 24 hours.

II. Serum Starved (SS): PNT2-derived cell lines were cultured in "serum starvation" growth conditions – RPMI 1640 medium supplemented with 1% (v/v) Penicillin/Streptomycin only – for 24 hours.

III. SS+2h: PNT2-derived cell lines, following serum starvation for 24 hours, were cultured in regular growth conditions for 2 hours.

IV. SS+18h: PNT2-derived cell lines, following serum starvation for 24 hours, were cultured in regular growth conditions for 18 hours.

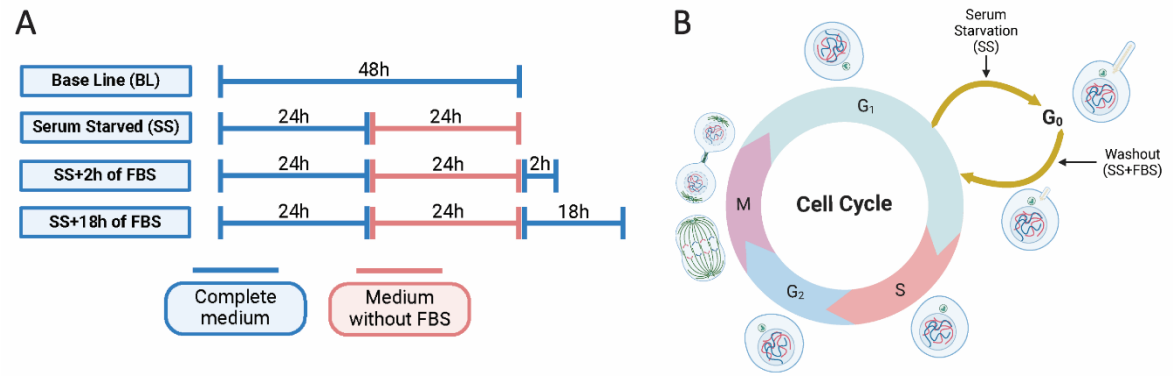

Figure 13. Experimental design for modulating primary cilia assembly and disassembly. [A] Schematic representation of the workflow used for the immunofluorescence assay. Cells were subjected to four different conditions: Baseline (BL) with complete medium, Serum Starvation (SS) for 24 hours, and two post-starvation recovery periods with FBS (SS+2h of FBS and SS+18h of FBS) [created with Biorender.com]. **[B]** Schematic representation of the cell cycle and ciliogenesis in response to media with and without FBS, highlighting cilia assembly during serum starvation and disassembly upon reintroduction of FBS [created with Biorender.com].

2.2. Immunofluorescence staining

Immunofluorescence staining is a technique that allows for the quantitative detection and visualization of a wide variety of proteins/antigens, with increased sensitivity and signal amplification when compared with immunohistochemistry.

For this purpose, cells were grown on coverslips in 6-well plates, and at each end-point, cell media was removed, and cells were fixed using 1mL of 4% paraformaldehyde (PFA, Alfa Aesar, Haverhill, MA, USA), diluted in 1x Phosphate Buffered Saline (PBS) (GRiSP, Porto, Portugal) for 10 minutes, at room temperature (RT). After this, extraction was performed by washing twice with Tris-buffered saline containing 0,5% Triton® X-100 (Merck) (TBST) for 8 minutes each, with agitation. Cells were, then, incubated with 50µL of IF Block solution, containing 10% FBS in PBS with 0.1% Tween® 20 (Sigma-Aldrich) (PBST), for 30 minutes at RT, in a humidified chamber. Following this, IF Block solution was replaced with 50µL of a primary antibody mixture, in which cells incubated for 2 hours at

RT, in a humidified chamber. Since our main goal was to visualize ciliated cells, a mixture of a mouse anti-Arl13B monoclonal antibody (1:400 dilution; clone N295B/66, NeuroMab, UC Davis) and a rabbit anti-Centrin1 monoclonal antibody (1:100 dilution; #12794-1-AP, Proteintech) diluted in IF Block was used. The anti-Arl13B antibody is described to target a GTPase located in the cilia membrane (Prasad et al., 2014), allowing for the visualization of the axoneme, while an anti-Centrin1 antibody targets a calcium-binding protein localized in the basal body (Vonderfecht et al., 2011).

Following incubation with primary antibodies, cells were washed three times, for 5 minutes each, with PBST and incubated with 50µL of a secondary antibody mixture for 1h at RT, in a humidified chamber and protected from light. Two secondary antibody mixtures were used: goat anti-mouse Alexa Fluor 488 polyclonal antibody (1:1000 dilution; #A11029, Invitrogen, Thermo Fisher), and goat anti-rabbit Alexa Fluor 569 polyclonal antibody (1:1000 dilution; #A11011, Invitrogen, Thermo Fisher), both diluted in IF Block. The first was used in cells formerly incubated with anti-Centrin 1 antibody, and the second in cells formerly incubated with anti-Arl13B antibody. Following incubation with secondary antibodies, cells were washed, for 5 minutes, twice with 0.1% PBST and once with DAPI (1:50 000 dilution; #D9542, Sigma-Aldrich) diluted in 1x PBS. Finally, slides were mounted with a homemade mounting media containing 0.5% n-propylgallate, 90% Glycerol and 20mM Tris-HCl (pH 8), and sealed with nail varnish.

To increase the output level of the assay, allowing testing of multiple conditions simultaneously, a similar immunofluorescence protocol was adapted for 96-well plate assays (#89607, Ibidi, Gräfelfing, Germany). The procedure followed the same steps as on coverslips, but the volumes of each solution used were adjusted. Briefly, cell media was first replaced with 100µL of 4% PFA diluted in 1x PBS, followed by washing with TBST. Blocking was performed with 50µL IF Block per well, and 30µL were used for each incubation of primary and secondary antibodies, as well as of DAPI solution. In the end, the wells were filled with 25µL of homemade mounting media and the plate was sealed with parafilm to prevent evaporation.

3. Pharmacological modulation of primary cilia with Erlotinib

Erlotinib, an EGFR inhibitor, was selected to investigate the effect of EGFR inhibition on ciliogenesis in PNT2-derived cell lines. Erlotinib hydrochloride (Sigma-Aldrich, Merck,

Massachusetts, USA), was obtained as a solid form, and was dissolved in DMSO to make a stock concentration of 5mM.

PNT2-derived cell lines were seeded in glass bottom 96-well plates (Ibidi, Gräfelfing, Germany) at a cell density of 200 000 cells/mL in complete growth medium (100µL/well), and incubated overnight in a humidified chamber, at 37°C with 5% CO_2. In the following day, medium was replaced with either fresh complete growth medium or growth medium without FBS. After 24 hours, medium was replaced with Erlotinib-containing medium (either complete or without FBS) at different concentrations: 5, 10 or 20µM. As "controls"/vehicle, cells were treated with equivalent growth media (either complete or without FBS) containing 0.4% DMSO, corresponding to the DMSO concentration at the highest Erlotinib concentration used. Cells were exposed to treatments for 24 hours, after which they were fixed and processed for immunofluorescence staining, as described in section 2.2 (Figure 14). The number of ciliated cells and cilia length were quantified and the impact of Erlotinib treatment in the different ETS backgrounds was assessed.

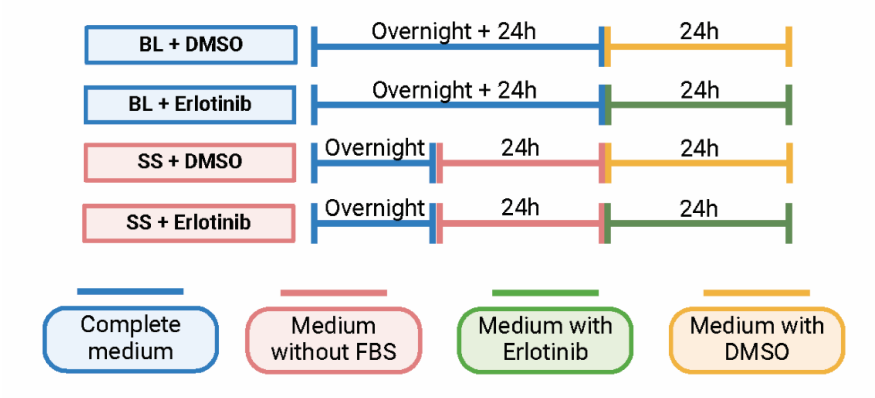

Figure 14. Experimental design for pharmacologically modulating primary cilia using Erlotinib. Cells were exposed to different combinations of growth conditions and treatments: Baseline (BL) with complete medium, or Serum Starvation (SS), each treated with either DMSO (vehicle control) or Erlotinib [created with Biorender.com].

4. Image analysis

4.1. Image acquisition and analysis

All fluorescently stained cells, either on coverslips or in multi-well plates, were analysed on a BioTek Cytation C10 Confocal Imaging Reader which is equipped with fluorescent

filters suitable for detecting “green” (GFP – Arl13b), “red” (Texas Red – Centrin1) and “blue” (DAPI) fluorescence signals.

In order to capture as many cells as possible to obtain a homogenous result, at least 12 images were acquired from each condition, accounting for at least 500 cells per condition. Images were acquired with a 40x objective. The BioTek Gen5 Software was used to automatically identify and count the number of cells in each image based on DAPI staining. The software, designed for imaging and microscopy, identifies and counts fluorescently labelled cells, enabling unbiased automated cell quantification across different conditions.

Image brightness and contrast were adjusted using Fiji software (ImageJ, version 1.54f) and image panels were assembled using Adobe Illustrator (Adobe Systems Inc.).

4.2. Manual quantification of primary cilia

Initially, the number of ciliated cells and cilia length were quantified manually using the BioTek Gen5 Software. We established a set of criteria for identifying primary cilia, which included: 1. Positive Arl13B signal; 2. Cilia length greater than 1µm; 3. Have a cilia-like structure; and 4. Proximity to a nucleus. Consequently, dot-like structures and cilia-like formations not adjacent to a cell, likely considered debris, were excluded from the count.

4.3. Automated quantification of primary cilia

To enable future high-throughput assays, automated quantification of primary cilia was optimized using the BioTek Cytation C10 Confocal Imaging Reader and the BioTek Gen5 Software. Images previously used for manual quantification were reanalysed automatically to allow for result comparison. The software was configured to identify nuclei and primary cilia based on predefined criteria, including a minimum and maximum object size and an intensity threshold (for nuclei or cilia). These settings were fine-tuned on one representative image to maximize detection of cilia-like structures, and then applied consistently to all subsequent images, providing robust, unbiased quantifications.

5. Statistical analysis

Statistical significance for the percentage of ciliated cells and cilia length between groups was determined using the unpaired *t*-test and Mann-Whitney test, respectively, with $p<0.05$ considered statistically significant. For each assay, three independent experiments were performed. For the Erlotinib assays, each experiment included at least two biological replicates (wells) per condition.

RESULTS

Results

1. Modulation of primary cilia assembly/disassembly in PNT2-derived cells

Given that mitotic cell division and ciliogenesis are interdependent, yet mutually exclusive processes, we analysed the number of mitotic figures in PNT2-Neo cells under different conditions, namely, Baseline (BL), Serum Starved (SS), SS+2h of FBS and SS+18h of FBS (Figure 15). This analysis was conducted to determine if the presence or absence of serum would affect the mitotic index, as a surrogate marker of cell cycle modulation. The results showed a tendency for a decrease in the index of mitotic cells upon 24h of serum starvation (SS), comparing with BL cells, likely due to cells entering the G0 phase and halting division. Two hours after the cell culture medium was replaced by complete growth medium (containing FBS; SS+2h), a significant drop in the mitotic index is observed, eventually as a cause of cellular adaptation to medium exchange, thus preventing mitotic entry. After an additional 16 hours (SS+18h), the mitotic index was increased, reflecting cells' adaptation to the new growth conditions. Overall, these observations confirm that the chosen workflow and time-points significantly impact cell cycle dynamics in PNT2-Neo cells. A similar pattern was observed for the PNT2-derived cell models with *de novo* ΔERG or ETV1 overexpression, although, globally, the mitotic index of both ETS-overexpressing cells seems to be less sensitive to growth media changes than PNT2-Neo cells (Appendix 2).

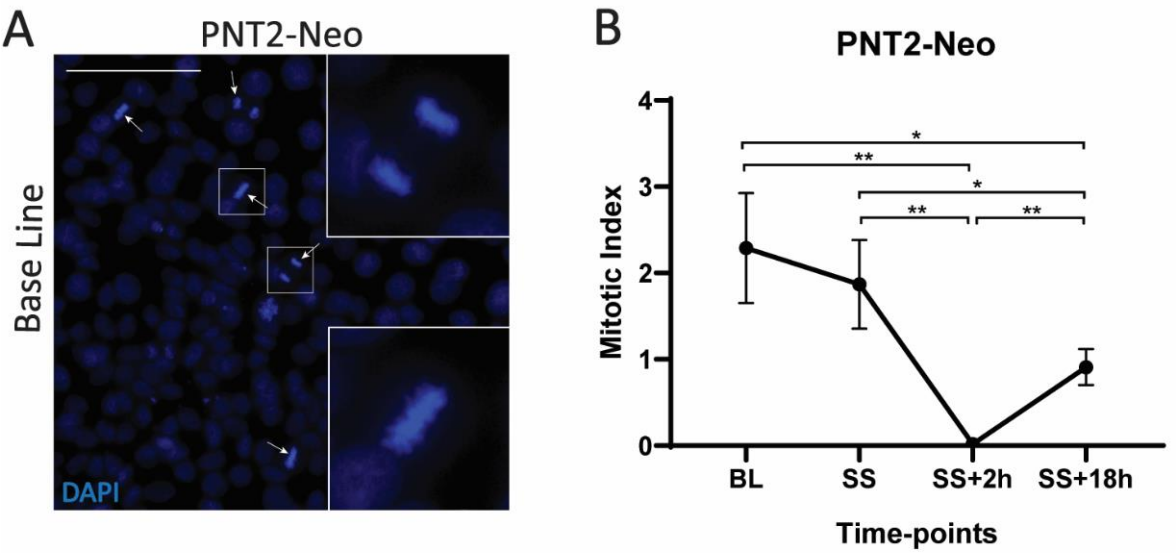

Figure 15. The mitotic index is modulated by the defined growth conditions and time-points in culture in PNT2 cells. [A] Representative immunofluorescence image of PNT2-Neo cells stained to reveal mitotic figures in Baseline conditions. Nuclei are stained with DAPI (blue). Cells were grown on coverslips and images were acquired with the Cytation C10 confocal microscope (40x magnification). White arrows indicate mitotic figures in representative cells. Scale

bar: 100μm. Insets show 4x magnifications of cells in metaphase (lower panel) or late anaphase (upper panel). **[B]** The mitotic index of PNT2-Neo cells was quantified under various conditions: Baseline (BL), Serum Starved (SS), Serum Starved plus 2 hours of complete growth medium (SS+2h of FBS), and Serum Starved plus 18 hours of complete growth medium (SS+18h of FBS). Data were obtained from three independent experiments. In each experiment, at least 1300 cells were analysed per condition. Unpaired two-tailed *t*-test was used for statistical analysis (*p<0.05; **p<0.01).

After assessing the mitotic index, the percentage of PNT2 ciliated cells subjected to the different growth conditions was also analysed (Figure 16). The results demonstrate that, in complete growth medium, PNT2-Neo cells exhibit ~10% of ciliated cells. This percentage increased to ~17% when cells were exposed to medium without FBS (SS), confirming the effect of serum starvation in stimulating cilia assembly. When cells were again exposed to serum-containing growth medium (SS+2h of FBS), the percentage of ciliated cells decreased to levels equivalent to those observed in BL, thus reflecting complete inhibition of ciliogenesis. Curiously, an increased percentage of ciliated cells was observed after 18 hours of medium exchange (SS+18h of FBS), which can be attributed to the increase in cell-cell contact as a result of increased cell density. Indeed, a positive correlation was found between cell density (measured by the number of cells per frame) and the percentage of ciliated cells, explaining the increased percentage of ciliated cells recorded in the SS+18h of FBS time-point. These effects on ciliogenesis were also seen for the cells overexpressing ETS, although some variation may be observed after 18 hours of the addition of FBS-containing growth medium (Appendix 3).

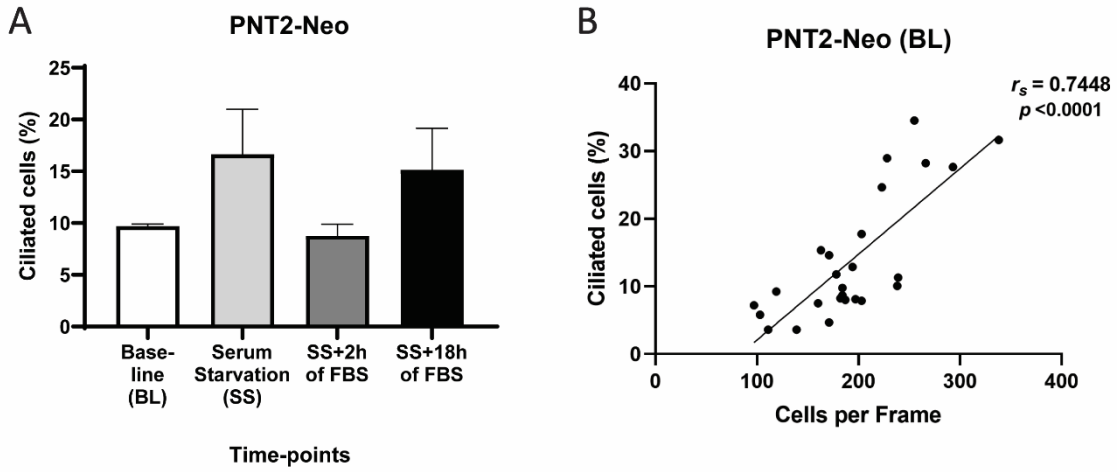

Figure 16. Primary cilia assembly/disassembly in PNT2 cells is modulated by both the presence of serum and cell density. **[A]** The percentage of ciliated PNT2-Neo cells was quantified under various conditions: Baseline (BL), Serum Starved (SS), Serum Starved plus 2 hours

of complete growth medium (SS+2h of FBS), and Serum Starved plus 18 hours of complete growth medium (SS+18h of FBS). Data were obtained from two independent experiments. Unpaired two-tailed t-test was used for statistical analysis. **[B]** Spearman correlation analysis between cell density (measured by the number of cells per frame) and the percentage of ciliated cells. A total of 26 frames from three independent experiments (≥6 frames per experiment) were analysed.

2. Primary cilia characterization in PNT2-derived cells

2.1. Impact of *de novo* ETS overexpression on the percentage of ciliated cells

To characterize primary cilia in prostate-derived cell lines with ETS overexpression, immunofluorescence staining was performed on PNT2-derived cell lines with *de novo* ΔERG or ETV1 overexpression, as well as in the control PNT2-Neo cell population. This was performed using antibodies specific for Arl13B and Centrin1, which localise to the primary cilia membrane and basal body, respectively, upon modulation of the cell cycle using different cell culture conditions. We observed a significant decrease in the number of ciliated cells in prostate-derived cell lines with *de novo* ETS overexpression across different time-points in culture (Figure 17). Notably, the ΔERG-overexpressing cell line exhibited the lowest percentage of ciliated cells (approximately 1.9%), which is statistically different from ETV1-overexpressing cells upon serum starvation (approximately 2.8%). These findings strongly support the hypothesis of a link between oncogenic overexpression of ETS transcription factors and loss of primary cilia in PCa.

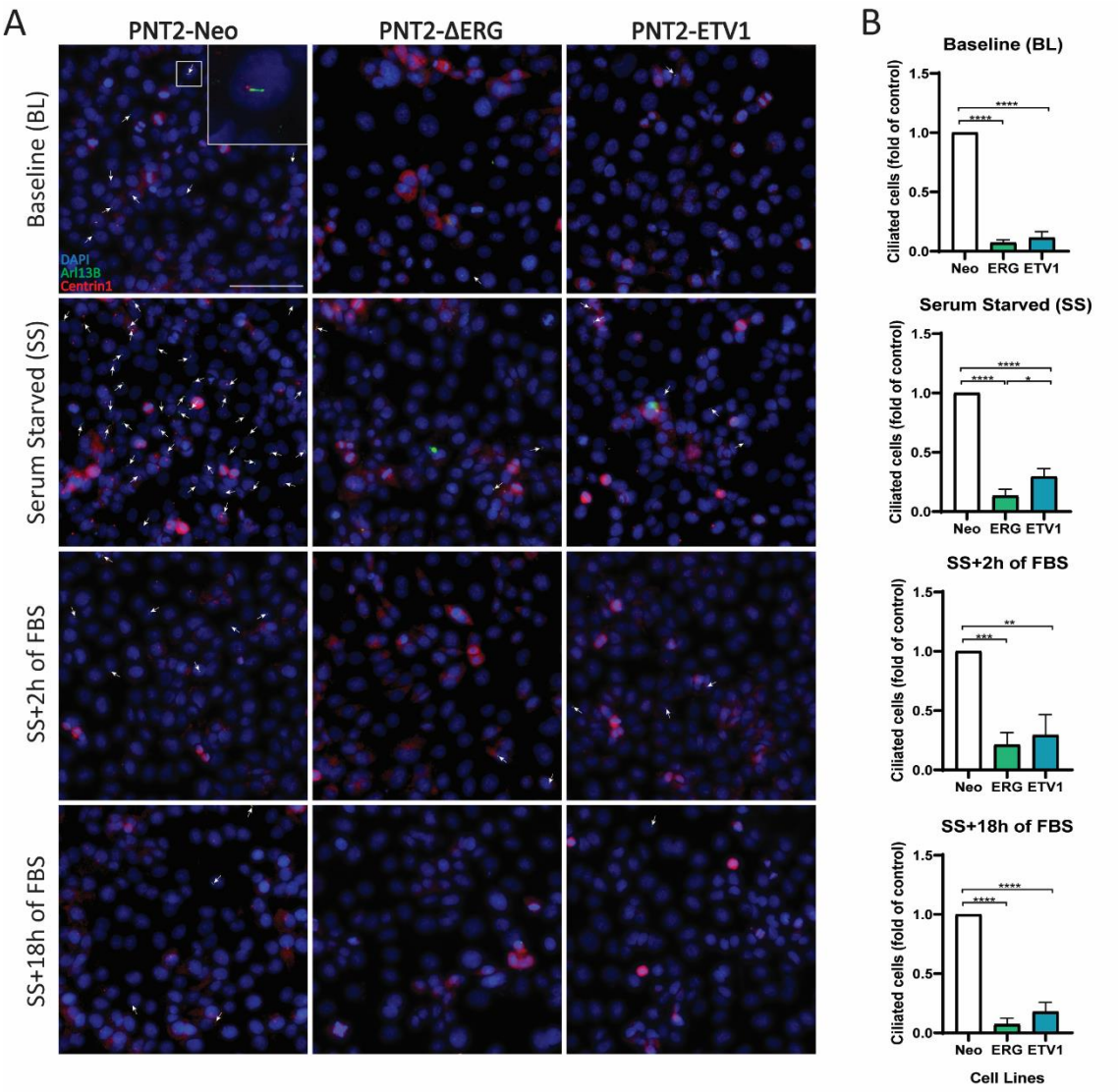

Figure 17. De novo ETS overexpression is associated with a significant decrease in the percentage of ciliated cells. [A] Representative immunofluorescence images of primary cilia in PNT2-derived cells (PNT2-Neo, PNT2-ΔERG and-PNT2 ETV1) at different growth conditions: Baseline (BL), Serum Starved (SS), Serum Starved plus 2 hours of complete growth medium (SS+2h of FBS), and Serum Starved plus 18 hours of complete growth medium (SS+18h of FBS). Nuclei are stained with DAPI (blue), primary cilia are stained with Arl13B (green), and the basal body is stained with Centrin1 (red). White arrows indicate primary cilia in representative cells. For this experiment, cells were grown on glass coverslips and images were acquired with the Cytation C10 confocal microscope (40x magnification). Scale bar: 100μm. Inset show 4x magnification of *a* selected region. **[B]** Quantification of the percentage of ciliated cells in each condition, expressed as fold-change compared to the control cell line (PNT2-Neo). Data were obtained from three independent experiments. Unpaired two-tailed *t*-test was used for statistical analysis. In each experiment, at least 1300 cells were analysed per condition. Only statistically significant differences are shown (**p*<0.05; ***p*<0.01; ****p*<0.001; *****p*<0.0001).

2.2. Impact of *de novo* ETS overexpression on primary cilia length

To assess differences in primary cilia length, we measured the length of each primary cilia manually using the “Measure objects” tool in Agilent Gen5 software (Figure 4). In the PNT2-Neo cells, the average cilia length was 4.1 ± 1.6µm in the presence of serum (BL) and 4.5 ± 1.6µm in its absence (SS) (Figure 18). Our results show that PNT2 cells overexpressing ΔERG exhibit a tendency for shorter primary cilia at every time-point analysed compared to the control (PNT2-Neo), with an average cilia length of 3.2 ±1.6µm and 3.9 ± 1.9µm in BL and SS, respectively. Conversely, a tendency for increased cilia length is observed in PNT2-ETV1 cells, which showed an average cilia length of 4.3 ± 2.3µm under BL conditions and 5.0 ± 2.1µm under SS. Moreover, all cell lines exhibited a similar pattern of cilia length changes over time, with an increase in cilia length under SS conditions, followed by a decrease when re-exposed to complete medium (Appendix 4). Thus, while both cell lines exhibit defects in ciliogenesis, the observed differences in cilia length suggest that ciliogenesis deregulation is not only ETS-mediated but also ETS-specific.

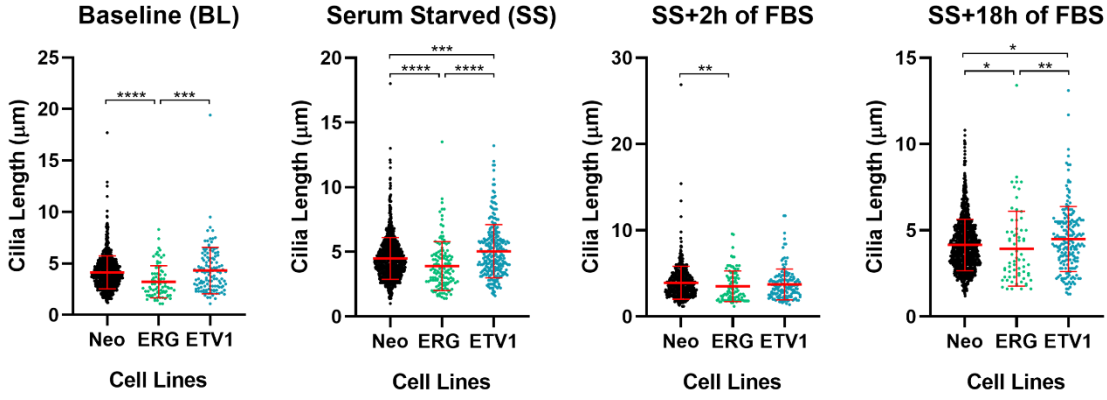

Figure 18. ETS overexpression impacts primary cilia length in an ETS-specific manner. The quantification of primary cilia length exhibited by PNT2-derived cells (PNT2-Neo, PNT2-ΔERG and PNT2-ETV1) was performed under the different growth conditions: Baseline (BL), Serum Starved (SS), Serum Starved plus 2 hours of complete growth medium (SS+2h of FBS), and Serum Starved plus 18 hours of complete growth medium (SS+18h of FBS), using Arl13B signal. Data were obtained from three independent experiments. For each condition, at least 70 cilia were measured. Mann-Whitney test was used for statistical analysis. Only statistically significant differences are shown (*p<0.05; **p<0.01; ***p<0.001; ****p<0.0001).

2.3. Impact of *de novo* ETS overexpression on the percentage of ciliated cells with Centrin 1

When examining the expression of Centrin1 in the basal body of primary cilia, we observed differences in the frequency of primary cilia lacking Centrin1 signal among the different PNT2-derived cell models. The data shown in Figure 19 clearly indicate that the PNT2-ΔERG cell line demonstrates a substantial increase of 1.4-4.0 fold in the percentage of primary cilia lacking Centrin1 signal compared to the control (PNT2-Neo cells), at every time-point analysed. In contrast, PNT2-ETV1 cells exhibit a trend toward a decrease in the percentage of cilia without Centrin1 compared to PNT2-Neo when cells are exposed to FBS-containing growth medium upon serum starvation, reaching statistical significance at 18 hours (1.3-1.9 fold decrease).

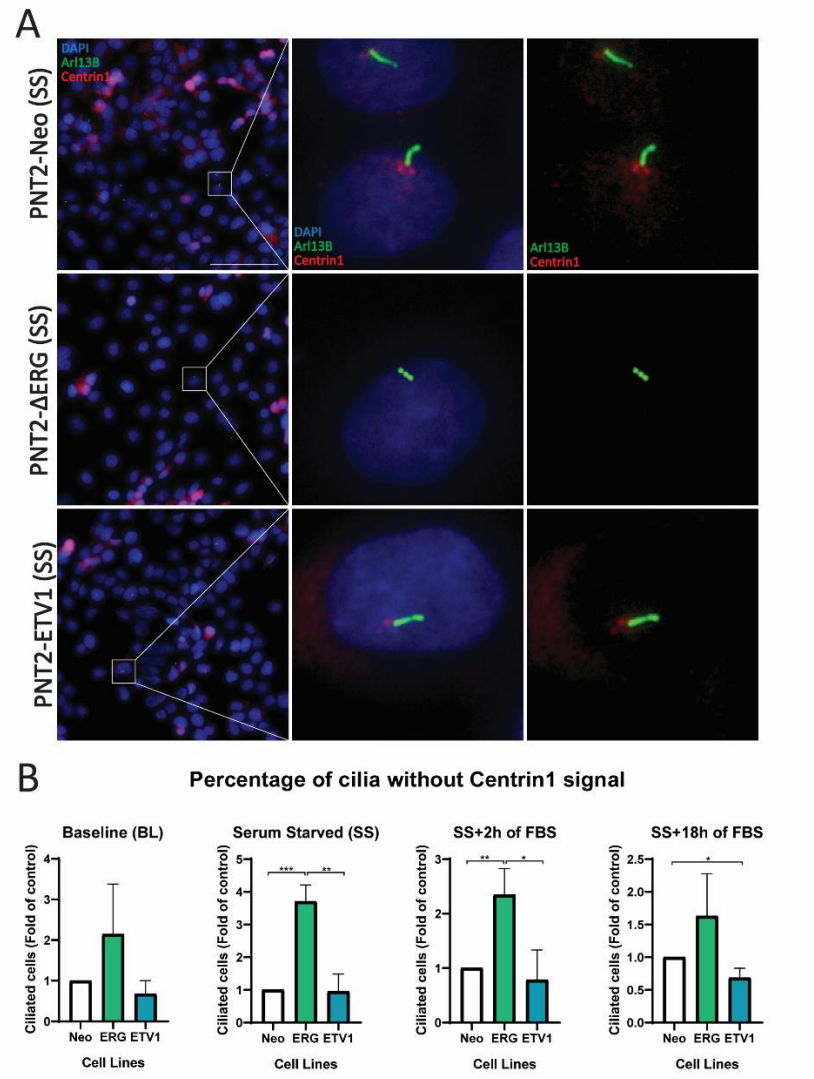

Figure 19. PNT2 cells overexpressing ΔERG exhibit a higher percentage of primary cilia lacking Centrin1. [A] Representative immunofluorescence image of PNT2 cell lines (PNT2-

Neo, PNT2-ΔERG and PNT2-ETV1) stained to reveal primary cilia membrane and basal body at the different growth conditions: Baseline (BL), Serum Starved (SS), Serum Starved plus 2 hours of complete growth medium (SS+2h of FBS), Serum Starved plus 18 hours of complete growth medium (SS+18h of FBS). Nuclei are stained with DAPI (blue), primary cilia are stained with Arl13B (green), and the basal body is stained with Centrin1 (red). Cells were grown on glass coverslips and images were acquired with the Cytation C10 confocal microscope (40x magnification). Scale bar: 100µm. Insets show 10x magnifications of selected regions. **[B]** Quantification of the percentage of ciliated cells lacking Centrin1 signal in their basal body in each condition, expressed as fold change compared to the control cell line (PNT2-Neo). Data were obtained from three independent experiments. In each experiment, at least 1300 cells were analysed per condition. Unpaired two-tailed *t*-test was used for statistical analysis. Only statistically significant differences are shown (**p*<0.05; ***p*<0.01; ****p*<0.001).

2.4. Impact of *de novo* ETS overexpression on the levels of Arl13B on primary cilia

The levels of Arl13B detected on primary cilia were also analysed and manually classified into “high”, “medium” or “low” signal. We observed that cells overexpressing ΔERG exhibit a higher proportion of cilia with low Arl13B signal, and few cilia with high Arl13B signal in the ciliary membrane (Figure 20). This pattern is particularly more pronounced at both “Serum Starved” and “Serum Starved+2h of FBS” time-points, where it represents 61-66% and 16-28% of the ciliated cells from PNT2-ΔERG and PNT2-Neo cell lines, respectively. In contrast, in cells overexpressing ETV1, the levels of Arl13B at primary cilia exhibit patterns similar to those of control cells, in every time-point analysed.

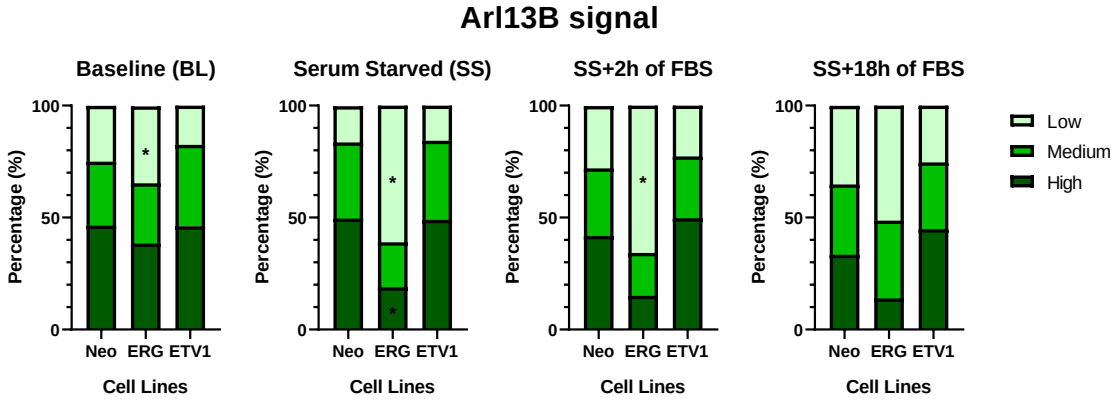

Figure 20. PNT2 cells overexpressing ΔERG display decreased Arl13B levels at ciliary membranes. The qualitative assessment of Arl13B signal in the ciliary membrane of primary cilia in PNT2-derived cells (PNT2-Neo, PNT2-ΔERG and PNT2-ETV1) was performed under

the different growth conditions: Baseline (BL), Serum Starved (SS), Serum Starved plus 2 hours of complete growth medium (SS+2h of FBS), and Serum Starved plus 18 hours of complete growth medium (SS+18h of FBS). Primary cilia were categorized as “High”, “Medium” or “Low” based on the intensity of the Arl13B signal in their ciliary membrane. Specifically, signals that appeared nearly overexposed were classified as “High”, signals that were difficult to visualize without increasing the exposure were classified as “Low”, and the remaining signal intensities were classified as “Medium”. Data were obtained from three independent experiments. *In each experiment, at least 1300 cells were analysed per condition.* Unpaired two-tailed *t*-test was used for statistical analysis. Only statistically significant differences are shown (*p<0.05).

3. Assessing the effectiveness of EGFR inhibition in reversing ETS-mediated ciliogenesis impairment

To investigate whether the oncogenic ETS signalling driving loss of ciliogenesis could be reverted by EGFR inhibition, we treated the PNT2-derived cell lines with Erlotinib concentration below the previously determined IC50 value and assessed the effects on ciliogenesis using immunofluorescence-based assays.

According to previous studies performed by our research group, the determined Erlotinib IC50 in PNT2 cells is ~17μM (Paiva, Orr, Azeredo, et al., *submitted*). Thus, to validate that lower Erlotinib concentrations would not impact cell viability, we started by evaluating the effect of different concentrations of Erlotinib (5, 10 and 20μM) on cell viability. For that purpose, we quantified cell density (number of cells per frame) after 24 hours of treatment in complete growth medium (Baseline) or serum starved medium (Figure 21). The results revealed a significant decrease in the number of cells/frame with increasing Erlotinib concentrations, reaching statistical significance at 20μM, in agreement with the previously determined IC50 value (17μM).

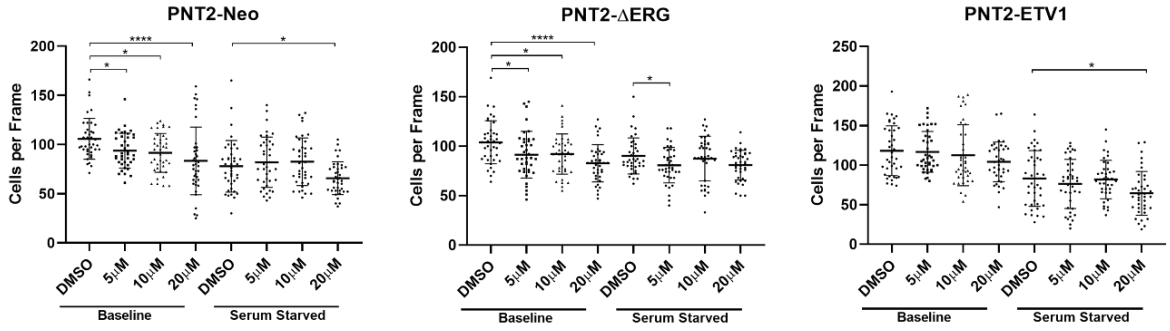

Figure 21. Quantification of cell density in PNT2-derived cells treated with different concentrations of Erlotinib. Cell viability, indirectly inferred from the quantification of the number of cells/frame, was quantified in PNT2-derived cells (PNT2-Neo, PNT2-ΔERG and PNT2-ETV1) after 24h of treatment with different concentrations of Erlotinib (5, 10 and 20μM) under two growth conditions: Baseline (complete growth medium) and Serum Starved (without FBS). A total of 39 frames and ≥2,500 cells were analysed per condition. Mann-Whitney test was used for statistical analysis (**p*<0.05; ***p*<0.01; ****p*<0.001; *****p*<0.0001).

Then, to determine the impact of EGFR inhibition on ciliogenesis, we quantified the prevalence of ciliated cells in those PNT2-derived cell lines treated with 5, 10 and 20μM of Erlotinib. We observed a significant increase in the percentage of ciliated cells across all cell models (Figure 22), which was more pronounced when cells were exposed to Erlotinib concentrations below the defined IC50 – 5μM and 10μM. In fact, at 20μM of Erlotinib all cell lines showed a percentage of ciliated cells equivalent to that observed in control cells treated with vehicle only (DMSO). Notably, PNT2-derived cell lines overexpressing ETS showed a greater impact on ciliogenesis following Erlotinib treatment compared to the control PNT2-Neo cells, independently of the growth conditions. The differences reach statistical significance at 5μM Erlotinib for PNT2-ETV1 cells, and at 10μM Erlotinib for PNT2-ΔERG cells. Additionally, under BL conditions, no differences were observed between the two ETS-overexpressing cell lines. However, under SS conditions, ETV1-overexpressing cells exhibited a lower fold-change increase in the percentage of ciliated cells in response to Erlotinib than ΔERG-overexpressing cells. This may be explained by the fact that cells overexpressing ETV1 show a greater increase in ciliogenesis under SS conditions compared to PNT2-ΔERG cells (Appendix 5), resulting in a smaller relative fold-change increase in response to Erlotinib.

Altogether, our results suggest that, although the Erlotinib effect in promoting ciliogenesis may be ETS-associated and some ETS-specificity may exist, it is not ETS-dependent.

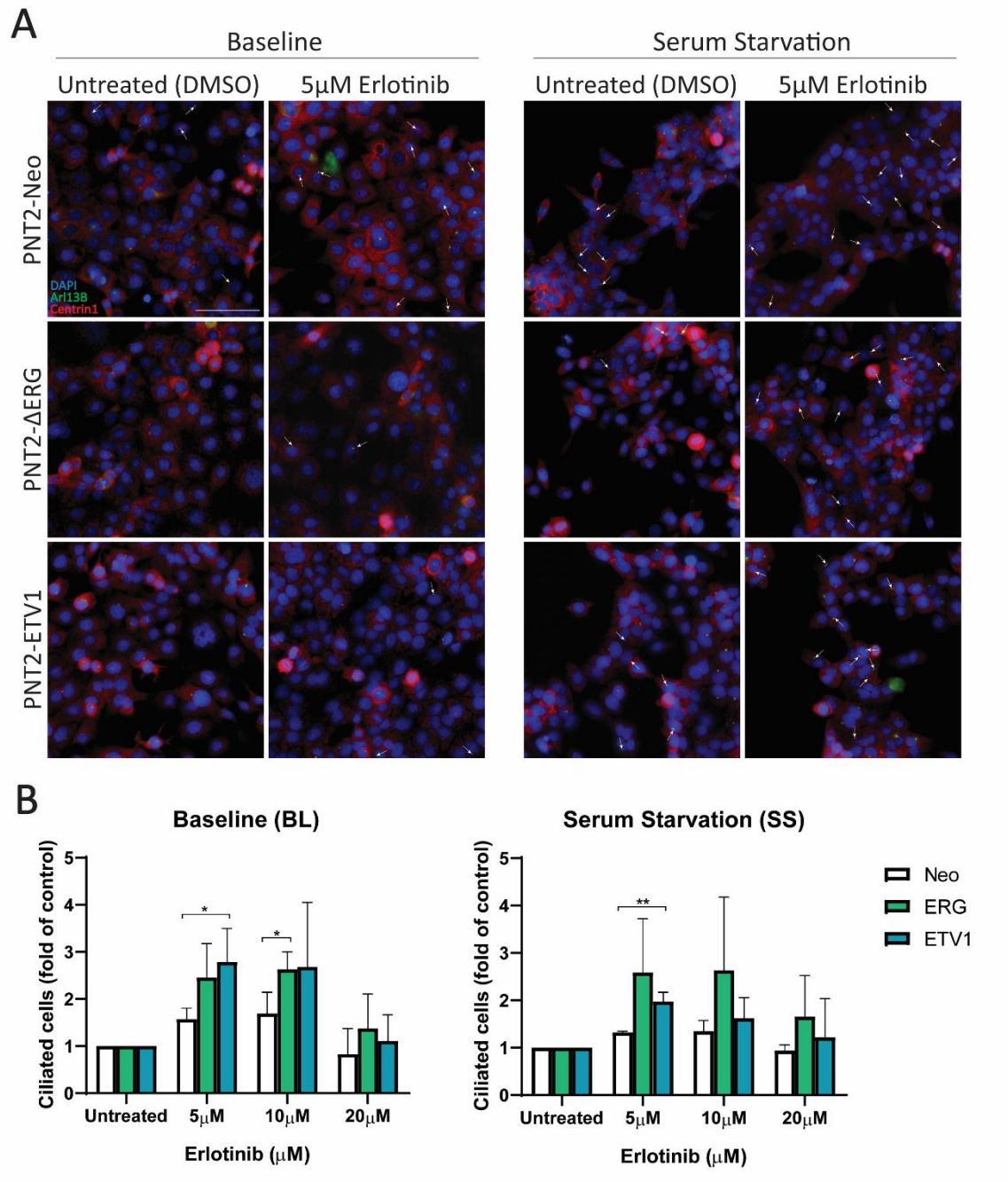

Figure 22. Erlotinib treatment induces restoration of primary cilia loss in PNT2-derived cell lines with *de novo* ETS overexpression independently of the presence of serum. [A] Representative immunofluorescence images of PNT2-derived cells (PNT2-Neo, PNT2-ΔERG and PNT2-ETV1), untreated (DMSO) and treated with 5μM Erlotinib at different growth conditions: Baseline and Serum Starved. Nuclei are stained with DAPI (blue), primary cilia are stained with Arl13B (green), and the basal body is stained with Centrin1 (red). White arrows indicate

primary cilia. Cells were grown in 96-well plates and images were acquired with the Cytation C10 confocal microscope (40x magnification). Scale bar: 100µm. **[B]** Quantification of the percentage of ciliated cells in PNT2-derived cells upon treatment with different concentrations of Erlotinib (5, 10 and 20µM) at different growth conditions: Baseline and Serum Starved. For each cell line and growth conditions, levels in treated cells were normalized to those of untreated (DMSO) cells. Data were obtained from three independent experiments. In each experiment, at least 500 total cells were analysed per condition. Unpaired two-tailed *t*-test was used for statistical analysis. Only statistically significant differences are shown (**p<0.05; **p<0.01*).

We also analysed the length of primary cilia assembled in response to Erlotinib treatment, as a possible additional readout of changes in primary ciliogenesis. As shown in Figure 23, there were no significant differences in primary cilia length upon Erlotinib treatment.

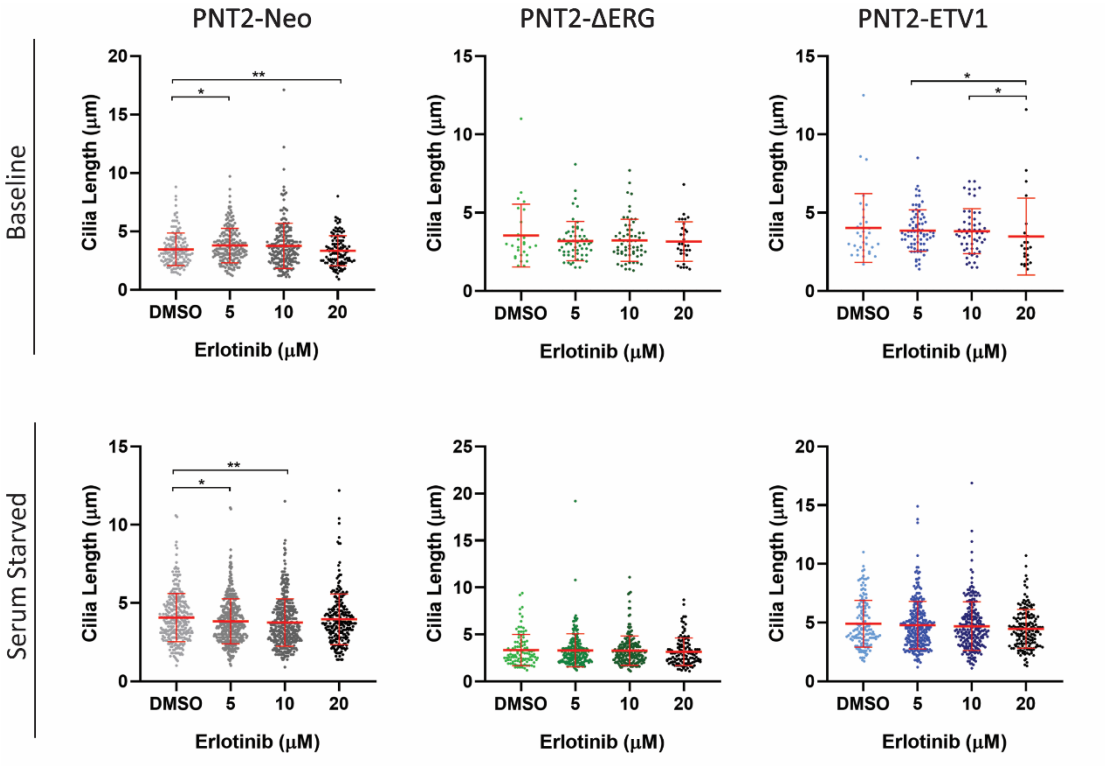

Figure 23. Primary cilia assembly induced by Erlotinib treatment has no impact on cilia length. Quantification of the length of primary cilia exhibited by PNT2-derived cells (PNT2-Neo, PNT2-ΔERG and PNT2-ETV1) after treatment with different concentrations of Erlotinib (5, 10 and 20µM) was performed under different growth conditions: Baseline (BL) and Serum Starved (SS). Control cells were treated with DMSO. Data were obtained from three independent experiments. In each experiment, at least 500 total cells were analysed per condition. Mann-Whitney test was used for statistical analysis. Only statistically significant differences are shown (**p*<0.05; ***p*<0.01).

4. Optimization of automated quantification of primary cilia

Given that, in the near future, we intend to perform high-throughput and high-content screenings of drugs influencing ciliogenesis, we aimed to develop an automated quantification method for faster and unbiased quantification of primary cilia using the Agilent Gen5 Software.

Exploiting the capacity of the Gen5 software to count objects, namely nuclei and primary cilia, we established precise thresholds for object intensities and defined minimum and maximum sizes for both DAPI (DNA) and GFP (Arl13B) channels. Using these settings, we identified the total number of nuclei as well as the total number of primary cilia. Identified objects were automatically outlined with a yellow mask, facilitating the identification and adjustment of size and intensity thresholding (Figure 24). When we compared the primary cilia counted manually with the results obtained with the automated quantification (in the same images), minimal differences were observed between the two quantification methods. Thus, we demonstrate that automated quantification of primary cilia is accurate, paving the way for high-throughput studies of primary cilia function in the future.

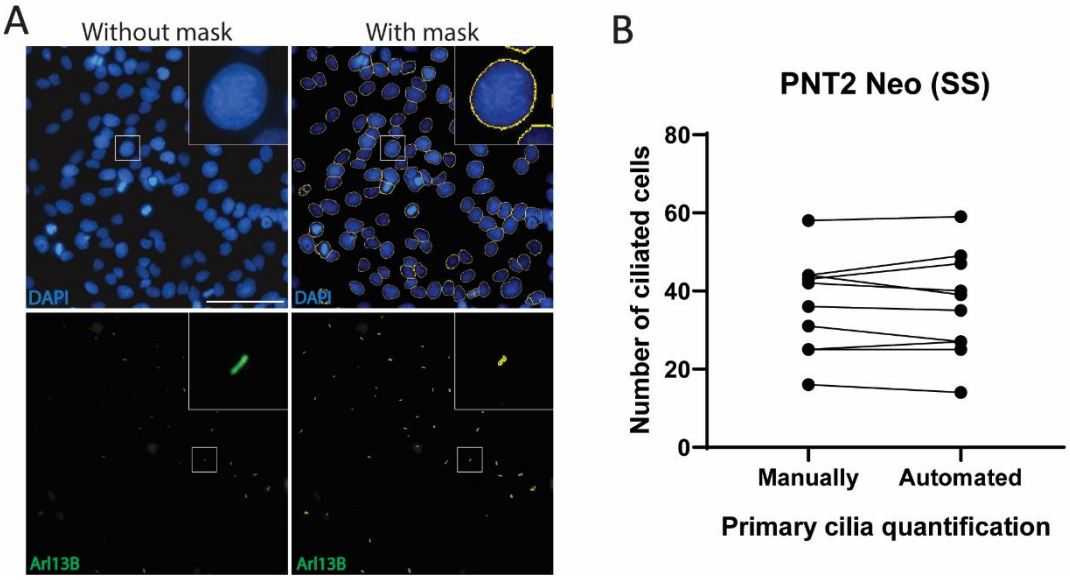

Figure 24. Reproducibility between automatic and manual quantification of primary cilia in Cytation C10. **[A]** Representative immunofluorescence images showing nuclei and primary cilia of PNT2 Neo cells upon Serum Starvation, with and without "mask" object identification. Cells were grown in glass coverslips and images were acquired at 40x magnification. Scale bar: 100µm. **[B]** Comparison between the number of ciliated cells determined by manual and automated counting methods. A total of 10 frames and 1,560 cells were analysed.

DISCUSSION

Discussion

As previously stated, the main aim of this study was to unveil and explore a putative link between *de novo* ETS oncogenic overexpression in prostate-derived models and loss of ciliogenesis, with the ultimate goal of restoring primary cilia in ETS-overexpressing cells. To achieve this, we started by characterizing ciliogenesis by immunofluorescence considering multiple parameters, namely, the percentage of ciliated cells, cilia length, and both Arl13B and Centrin1 staining, in prostate-derived cell models with or without *de novo* overexpression of ΔERG or ETV1, using modulation of growth conditions. Subsequently, in light of recent studies of our group pinpointing the EGFR pathway as a downstream target of ETV1 oncogenic signaling, we questioned whether inhibition of EGFR would restore primary ciliogenesis in an ETS-dependent manner. Thus, we treated our prostate-derived cell models with different concentrations of Erlotinib, an EGFR inhibitor, to assess its effects on primary cilia restoration.

In the following section, we will dissect the significance of our findings, focusing on how ETS overexpression impacts ciliogenesis, and the potential of EGFR inhibition to reverse primary cilia loss in a specific ETS-overexpressing cell context.

1. Uncovering a link between *de novo* ETS overexpression and primary cilia loss in prostate carcinogenesis

Primary cilia loss is a common event in several types of cancer, including PCa. Considering that primary cilia act as important sensors for extracellular signals, their dysfunction can lead to aberrant signalling, which promotes tumour growth. In fact, this loss is described to occur early in carcinogenesis, in general. In breast cancer, primary cilia are lost during early stages of cancer development, even in premalignant lesions (Menzl et al., 2014). Similarly, in melanoma, the absence of primary cilia is observed across different stages, from melanoma *in situ* to primary invasive and metastatic disease (Kiseleva et al., 2023). Regarding PCa, primary cilia loss is also described to occur in early oncogenesis, being already observed in premalignant (PIN) lesions (Hassounah et al., 2013).

On the other hand, ETS rearrangements, occurring in approximately 50-70% of PCa cases, are recognized as driver events of prostate carcinogenesis. In fact, gene fusions involving ETS members are detected in premalignant PIN lesions and early-stage tumours, indicating that they occur early in the oncogenic process (Rubin, 2012).

Given the limited research on ciliogenesis in PCa cells, we questioned whether primary cilia loss could be associated with oncogenic ETS overexpression in PCa. To answer this question, a detailed characterization of primary cilia in prostate-derived cell lines overexpressing ETS was conducted through immunofluorescence, using Arl13B as a well-established marker of primary cilia membrane (Zhang et al., 2019). Although acetylated tubulin is also commonly used for studying primary cilia, as tubulin acetylation is one of the most prominent post-translational modification found in microtubules (Rahimi et al., 2021), it can lead to misleading results by also labelling the midbody, a structure that is formed during the final stages of cell division, particularly during cytokinesis. In fact, the structure created during this stage is structurally very similar to primary cilia, which can lead to misinterpretation of the results.

Primary cilia characterization was performed in PNT2-derived cell lines with and without ΔERG or ETV1 overexpression at different time-points and growth conditions, designed to promote cilia assembly and disassembly. These included: evaluation at “Baseline” (BL) conditions, in which cells were exposed to regular growth conditions (complete growth medium, containing FBS); evaluation at “Serum Starvation” (SS) conditions, in which cells were exposed for 24 hours to growth medium without FBS, expected to induce cell cycle arrest at G0 and, thus, stimulate primary cilia assembly; and evaluation at two “G0 Release” time-points, the first, 2 hours after addition of FBS-containing growth medium to Serum Starved cells (SS+2h of FBS), and the second, 18 hours after (SS+18h of FBS), expecting to potentiate cell cycle progression, and thus, to stimulate primary cilia disassembly. Using DAPI staining we confirmed a decrease in the number of mitotic figures when cells were exposed to medium without FBS, suggestive of cell cycle arrest in G0 phase. However, to more accurately validate the enrichment of cells in the G0 phase, flow cytometry would be an essential tool. Overall, our DAPI-based observations support that the selected workflow and the growth conditions established effectively influence the dynamics of the cell cycle, sustaining growth conditions to modulate ciliogenesis.

Globally, we observed that the percentage of ciliated cells is highly dependent on the cell line analysed, as well as the culture conditions used, and the timing of the experimental endpoints. Regarding the control cell line – PNT2 Neo – 4-10% of the cells in complete growth medium (Baseline) exhibit primary cilia, and this percentage increases to 10-17% under serum starvation conditions. When FBS is reintroduced, the percentage of ciliated cells declines, consistent with ciliary disassembly.

When comparing the “Baseline” percentage of ciliated cells between PNT2-Neo and cells overexpressing ETS (PNT2-ΔERG and PNT2-ETV1), a significant decrease in the

percentage of ciliated cells was observed in the cell models with ETS overexpression. This reduction persisted across all cell culture conditions, indicating that, even in the absence of FBS in the growth medium, these cell lines were unable to assemble primary cilia as effectively as the PNT2-Neo control cells. Although ΔERG-overexpressing cells tended to exhibit the lowest percentage of ciliated cells, this difference was not statistically significant from that of ETV1-overexpressing cells, suggesting no measurable differences between the impact of ΔERG or ETV1 overexpression on the percentage of ciliated cells. Nevertheless, ETS-overexpressing cells still exhibited sensitivity to FBS, showing a slight increase in primary cilia assembly and disassembly in response to FBS removal and addition, respectively (Appendix 3). These findings suggest that *de novo* ETS overexpression impairs overall primary cilia formation, leading to a dramatic 60-95% decrease in the percentage of non-tumorigenic prostate cells that assemble and disassemble primary cilia in the time window analysed. Taken together, these results strongly support a link between ETS-driven oncogenic transformation and primary cilia loss in early prostate carcinogenesis. Given that ETS overexpression is the single introduced oncogenic alteration in PNT2-ΔERG and PNT2-ETV1 clonal cell populations, and that no major differences were observed when comparing the percentage of ciliated cells between the two ETS cell models, it is possible that ETS-shared downstream molecular pathways govern, at least in part, cilia formation and maintenance in PCa.

2. Exploring ETS-specific characteristics of primary cilia in PCa cells

In addition to assessing the overall percentage of primary cilia, an analysis regarding specific primary cilia characteristics was performed in the different PNT2-derived cell models. This included evaluation of cilia length, intensity of Arl13B signal in the ciliary membrane, and the presence of Centrin1 in the basal body of primary cilia.

Cilia length was manually quantified using the Biotek Gen5 Software. In all PNT2-derived cell models, a statistically significant increase in cilia length was observed with serum deprivation (Appendix 3). This finding aligns with previous studies, namely, a 2023 study performed by Steidl et al., which demonstrated that multiple cell lines, including MEF (mouse embryonic fibroblasts), hRPE (human retinal pigment epithelial cells), mIMCD3 (murine inner medullary collecting duct cells) and MDCK (Madin-Darby Canine Kidney cells) exhibited a significant increase in cilia length after 24 hours of exposure to FBS-free medium (Steidl et al., 2023). Additionally, Goméz et al. observed a similar increase in cilia length in ARPE-19 and hTERT RPE-1 cells (Gómez et al., 2022).

When comparing cilia length across the cell lines, the PNT2-ΔERG cell line showed a consistent tendency to exhibit shorter cilia when compared to control cells, independently of the growth conditions analysed. In fact, statistical significance is only lost when primary cilia are measured 18 hours after “G0 Release” with FBS (SS+18h of FBS), probably associated with a significantly lower number of primary cilia available to measure at this time-point, thereby decreasing statistical power. On the other hand, PNT2-ETV1 cells showed a tendency to exhibit longer primary cilia when compared to both PNT2-Neo and PNT2-ΔERG cells, reaching statistical significance when cells are serum-starved, specifically the time-point at which we recorded the highest proportion of ciliated cells.

As previously mentioned, cilia length is described to be directly correlated to the proper functioning of primary cilia. Therefore, the reduced length of primary cilia in the ΔERG-overexpressing cell line, independently of the modulation of the growth conditions, may suggest unstable primary cilia dynamics, under which assembly and disassembly of primary cilia are not tightly dependent on the presence of growth factors (FBS) in the cell culture medium and, consequently, elongation and absorption are weekly controlled. In contrast, the longer primary cilia observed in SS in PNT2-ETV1 cells, may suggest increased stability of primary cilia dynamics, with assembly and disassembly processes being tightly regulated and dependent on the availability of external stimuli. Nevertheless, it is important to take into account that the high statistical significance observed was only possible due to the large number of primary cilia examined in each cell line, sustaining the high statistical power of our observations.

Another parameter that increased the robustness of our study was the characterization of the primary cilia basal body. The initial guidelines that we followed for counting primary cilia relied on positive Arl13B signal, cilia length, and the presence of Centrin1 in the basal body. However, during the analysis of ΔERG-overexpressing cells, it became evident that many cilia lacked a Centrin1 signal at the basal body. Then, we decided to change our criteria for identifying primary cilia, which included: labelling of Arl13B in the ciliary membrane, a cilia-like structure, a cilia length greater than 1.0μm, and being in close proximity to the cell nucleus.

Centrin1 belongs to the centrin family of proteins, which are characterized by a C-terminal domain that localizes to the basal body. This observation places centrins as major players in basal body assembly and stability, being crucial for primary cilia formation and maintenance (Vonderfecht et al., 2011). Thus, the absence of Centrin1 in the basal body of primary cilia, observed in the ΔERG-overexpressing cell line suggests potential defects in cilia assembly and stability due to compromised centrin function. Again, this observation is

in line with the hypothesis of lack of ciliogenesis robustness evidenced by both the lower percentage of primary cilia, and the shorter cilia length observed in ΔERG-overexpressing cells. On other hand, PNT2-ETV1 cells did not show any differences in the Centrin1 signal in the basal body of the primary cilia when compared to the control cell line, again supporting the hypothesis of stable control of cilia dynamics in this cell model. Nevertheless, since other centrins may also regulate cilia assembly and maintenance, it would be important to assess the expression/localization of other centrins tightly associated with the basal body, namely, Centrin3 (Ning et al., 2023).

Additionally, we categorized the intensity of Arl13B signal in the ciliary membrane as “high”, “medium” or “low”. The results revealed that ΔERG-overexpressing cells exhibited the highest proportion of primary cilia with "low” Arl13B signal in their ciliary membrane, particularly under SS growth conditions, compared to both the control cell line and cells overexpressing ETV1. Since Arl13B is a protein crucial for proper primary cilia functioning and signalling, a reduced Arl13B signal also suggests instability and potential dysfunction in the primary cilia. Contrarily, in PNT2-ETV1 cells, the Arl13B signal was consistently similar to that observed in the control cell line, across all time-points, again supporting the hypothesis of stable and robust ciliogenesis in ETV1-overexpressing cells, despite the percentage of primary cilia being much lower than that in the non-tumorigenic PNT2-Neo cells.

3. Evaluate the potential utility of the EGFR inhibitor, Erlotinib, in primary cilia restoration in an ETS-specific cell context

Given our initial findings that PNT2-derived cell lines overexpressing ETS exhibit a significant decrease in the number of ciliated cells, we sought to explore whether we could restore ciliogenesis in an ETS-specific oncogenic cell background. Interestingly, other research groups have shown that EGFR inhibitors, namely Erlotinib, may be effective in restoring primary cilia in cancer cells (Kiseleva et al., 2023). In light of our previous discovery of an ETS-specific EGFR activation axis in PCa cells, we chose Erlotinib as a potential modulator of ciliogenesis in our PNT2-derived cell lines with *de novo* ETS overexpression.

The results showed that treatment with 5μM Erlotinib was sufficient to partially promote ciliogenesis in all cell lines. This effect was observed both in the presence and absence of FBS, suggesting that the treatment had an addictive effect to the serum starvation and was able to counteract the inhibitory effect of FBS on ciliogenesis. Although the PNT2 Neo cells

exhibited more ciliated cells in absolute terms, cells lines overexpressing ΔERG and ETV1 experienced a major increase in the percentage of ciliated cells, up to 4-fold, when treated with Erlotinib.

On the other hand, no significant differences were found in the percentage of ciliated cells induced by Erlotinib treatment between the ΔERG- and ETV1-overexpressing cell lines. Therefore, while the effect of Erlotinib on ciliogenesis appears to be ETS-dependent, it does not seem to show ETS-specificity. Nevertheless, the ability shown by Erlotinib to partially restore ciliogenesis in ERG and ETV1-overexpressing cell lines opens new avenues for its application in PCa therapy. While traditionally used for targeting EGFR in NSCLC, Erlotinib's role in ciliogenesis suggests that it may have broader applications in cancers where ciliary dysfunction is a contributing factor. Additionally, by partially restoring ciliogenesis, Erlotinib could potentially enhance the sensitivity of PCa to other therapies. This restoration of primary cilia might re-establish proper Hedgehog and Wnt signalling, thereby increasing the cells' responsiveness to drugs targeting these pathways.

Moreover, as either ETS or EGFR overexpression are found in multiple cancers, the partial restoration of ciliogenesis observed in this study suggests that Erlotinib could be particularly effective in ETS-positive cancers, in general, where ciliogenesis may be disrupted, namely melanoma and pancreatic cancer (Heeg et al., 2016; Qu et al., 2020). By restoring ciliary functions, Erlotinib could potentially reduce the aggressive behaviour of these cancers and improve patient outcomes.

Nevertheless, the partial restoration of ciliogenesis suggests that Erlotinib might need to be combined with other therapeutic agents to achieve optimal results. Combining Erlotinib with drugs that target other aspects of ciliary function or cancer cell signalling could provide a synergistic effect, leading to more effective ciliogenesis restoration and improved cancer control.

CONCLUSION

Conclusion

This study allowed to reach our main objectives, unveiling that:

- Oncogenic transformation driven by ΔERG or ETV1 overexpression is sufficient to drive major loss of primary cilia in prostate cells;
- Ciliogenesis is differentially regulated in different ETS backgrounds, with ERG overexpression being associated with primary cilia characteristics of ciliogenesis instability;
- Treatment with 5-10μM Erlotinib partially restores primary cilia loss in prostate cells, with greater efficiency in cells with oncogenic ΔERG or ETV1 overexpression;

FUTURE PERSPECTIVES

Future perspectives

This study has provided valuable insights into the impact of ΔERG and ETV1 overexpression on ciliogenesis in prostate cells, while also highlighting a potential therapeutic approach to restore primary cilia in PCa cells. Nevertheless, complementary analyses would be valuable to deepen our understanding of ciliogenesis in PCa, namely:

- Evaluate how the restoration of primary cilia through Erlotinib treatment affects the oncogenic phenotype of ΔERG- or ETV1-overexpressing cell lines. Although we have shown that Erlotinib has the ability to restore primary cilia in ETS-overexpressing cells, its impact on the oncogenic behaviour of these cells remains unclear. To address this, we will investigate several oncogenic characteristics, including proliferation/apoptosis rates (dual staining with calcein-AM and Propidium Iodide) and migration and invasion abilities (using transwell migration/invasion assays and/or wound-healing assays) in Erlotinib-treated cells, where ciliogenesis has been partially restored.

- Clarify the fraction of primary cilia that are affected by specific EGFR activation. While we have demonstrated that Erlotinib can restore primary cilia in cells with *de novo* overexpression of ΔERG and ETV1, we have to keep in mind that Erlotinib is a non-specific inhibitor. Thus, we intend to activate EGFR using a specific activator (EGF), to confirm a direct association between EGFR inhibition/activation and primary cilia assembly/disassembly (Preliminary data – Appendix 6).

- Assess the reproducibility of our findings in advanced PCa cell models with ETS overexpression. To validate our results, we aim to treat LNCaP and VCaP cells, representing advanced prostate carcinomas with overexpression of ETV1 and ΔERG, respectively, with Erlotinib. This will help validate the effect of Erlotinib in the partial restoration of ciliogenesis in ETS-overexpressing advance cancer models, providing a more accurate representation of its potential implications in the treatment of ETS-overexpressing prostate tumours.

- Establish cell models for live cell analysis of primary cilia. By stablishing cell models expressing GFP-Arl13B, it will be possible to visualize fluorescently-labelled primary cilia without the need to perform immunofluorescence assays. This will allow us to assess ciliary dynamics in real-time and address the impact of Erlotinib (or other stimuli/drugs) on ciliogenesis assembly/disassembly over-time (Preliminary data – Appendix 7).

- Evaluate the effect of Erlotinib on primary cilia restoration in 3D cell models with fluorescently tagged nuclei and primary cilia. Given that 3D cell models more accurately mimic the tumours' architecture and environment, we aim to evaluate the effects of Erlotinib treatment on these models, allowing us to better understand how tumours respond to the restoration of primary cilia in a more physiologically relevant tumour structure (Preliminary data – Appendix 7).

REFERENCES

REFERENCES

Aarnio, M., Sankila, R., Pukkala, E., Salovaara, R., Aaltonen, L. A., de la Chapelle, A., Peltomäki, P., Mecklin, J. P., & Järvinen, H. J. (1999). Cancer risk in mutation carriers of DNA-mismatch-repair genes. *Int J Cancer*, *81*(2), 214-218. https://doi.org/10.1002/(sici)1097-0215(19990412)81:2<214::aid-ijc8>3.0.co;2-l

Ahdoot, M., Wilbur, A. R., Reese, S. E., Lebastchi, A. H., Mehralivand, S., Gomella, P. T., Bloom, J., Gurram, S., Siddiqui, M., Pinsky, P., Parnes, H., Linehan, W. M., Merino, M., Choyke, P. L., Shih, J. H., Turkbey, B., Wood, B. J., & Pinto, P. A. (2020). MRI-Targeted, Systematic, and Combined Biopsy for Prostate Cancer Diagnosis. *N Engl J Med*, *382*(10), 917-928. https://doi.org/10.1056/NEJMoa1910038

Albany, C., Alva, A. S., Aparicio, A. M., Singal, R., Yellapragada, S., Sonpavde, G., & Hahn, N. M. (2011). Epigenetics in prostate cancer. *Prostate Cancer*, *2011*, 580318. https://doi.org/10.1155/2011/580318

Allott, E. H., Masko, E. M., & Freedland, S. J. (2013). Obesity and Prostate Cancer: Weighing the Evidence. *European Urology*, *63*(5), 800-809. https://doi.org/https://doi.org/10.1016/j.eururo.2012.11.013

Antoniou, A. C., Sinilnikova, O. M., McGuffog, L., Healey, S., Nevanlinna, H., Heikkinen, T., Simard, J., Spurdle, A. B., Beesley, J., Chen, X., The Kathleen Cuningham Foundation Consortium for Research into Familial Breast, C., Neuhausen, S. L., Ding, Y. C., Couch, F. J., Wang, X., Fredericksen, Z., Peterlongo, P., Peissel, B., Bonanni, B., . . . on behalf of, C. (2009). Common variants in LSP1, 2q35 and 8q24 and breast cancer risk for BRCA1 and BRCA2 mutation carriers. *Human Molecular Genetics*, *18*(22), 4442-4456. https://doi.org/10.1093/hmg/ddp372

Aronson, W. J., & deKernion, J. B. (2007). Prostate. In J. E. Birren (Ed.), *Encyclopedia of Gerontology (Second Edition)* (pp. 391-399). Elsevier. https://doi.org/https://doi.org/10.1016/B0-12-370870-2/00028-7

Atkinson, K. F., Sherpa, R. T., & Nauli, S. M. (2019). The Role of the Primary Cilium in Sensing Extracellular pH. *Cells*, *8*(7). https://doi.org/10.3390/cells8070704

Attard, G., Clark, J., Ambroisine, L., Mills, I. G., Fisher, G., Flohr, P., Reid, A., Edwards, S., Kovacs, G., Berney, D., Foster, C., Massie, C. E., Fletcher, A., De Bono, J. S., Scardino, P., Cuzick, J., Cooper, C. S., & on behalf of the Transatlantic Prostate, G. (2008). Heterogeneity and clinical significance of ETV1 translocations in human prostate cancer. *British Journal of Cancer*, *99*(2), 314-320. https://doi.org/10.1038/sj.bjc.6604472

Baena, E., Shao, Z., Linn, D. E., Glass, K., Hamblen, M. J., Fujiwara, Y., Kim, J., Nguyen, M., Zhang, X., Godinho, F. J., Bronson, R. T., Mucci, L. A., Loda, M., Yuan, G. C.,

Orkin, S. H., & Li, Z. (2013). ETV1 directs androgen metabolism and confers aggressive prostate cancer in targeted mice and patients. *Genes Dev*, *27*(6), 683-698. https://doi.org/10.1101/gad.211011.112

Barry, M. J., & Simmons, L. H. (2017). Prevention of Prostate Cancer Morbidity and Mortality: Primary Prevention and Early Detection. *Medical Clinics of North America*, *101*(4), 787-806. https://doi.org/https://doi.org/10.1016/j.mcna.2017.03.009

Barsouk, A., Padala, S. A., Vakiti, A., Mohammed, A., Saginala, K., Thandra, K. C., Rawla, P., & Barsouk, A. (2020). Epidemiology, Staging and Management of Prostate Cancer. *Medical Sciences*, *8*(3).

Barwick, B. G., Abramovitz, M., Kodani, M., Moreno, C. S., Nam, R., Tang, W., Bouzyk, M., Seth, A., & Leyland-Jones, B. (2010). Prostate cancer genes associated with TMPRSS2–ERG gene fusion and prognostic of biochemical recurrence in multiple cohorts. *British Journal of Cancer*, *102*(3), 570-576. https://doi.org/10.1038/sj.bjc.6605519

Baselga, J. (2001). The EGFR as a target for anticancer therapy--focus on cetuximab. *Eur J Cancer*, *37 Suppl 4*, S16-22. https://doi.org/10.1016/s0959-8049(01)00233-7

Baumgart, S. J., & Haendler, B. (2017). Exploiting Epigenetic Alterations in Prostate Cancer. *International Journal of Molecular Sciences*, *18*(5).

Bax, C., Taverna, G., Eusebio, L., Sironi, S., Grizzi, F., Guazzoni, G., & Capelli, L. (2018). Innovative Diagnostic Methods for Early Prostate Cancer Detection through Urine Analysis: A Review. *Cancers*, *10*(4).

Berg, K. D. (2016). The prognostic and predictive value of TMPRSS2-ERG gene fusion and ERG protein expression in prostate cancer biopsies. *Dan Med J*, *63*(12).

Bergengren, O., Pekala, K. R., Matsoukas, K., Fainberg, J., Mungovan, S. F., Bratt, O., Bray, F., Brawley, O., Luckenbaugh, A. N., Mucci, L., Morgan, T. M., & Carlsson, S. V. (2023). 2022 Update on Prostate Cancer Epidemiology and Risk Factors-A Systematic Review. *Eur Urol*, *84*(2), 191-206. https://doi.org/10.1016/j.eururo.2023.04.021

Berthon, P., Cussenot, O., Hopwood, L., Leduc, A., & Maitland, N. (1995). Functional expression of sv40 in normal human prostatic epithelial and fibroblastic cells - differentiation pattern of nontumorigenic cell-lines. *Int J Oncol*, *6*(2), 333-343. https://doi.org/10.3892/ijo.6.2.333

Bostwick, D. G., Pacelli, A., & Lopez-Beltran, A. (1996). Molecular biology of prostatic intraepithelial neoplasia. *The Prostate*, *29*(2), 117-134. https://doi.org/https://doi.org/10.1002/(SICI)1097-0045(199608)29:2<117::AID-PROS7>3.0.CO;2-C

Bostwick, D. G., & Qian, J. (2004). High-grade prostatic intraepithelial neoplasia. *Modern Pathology*, *17*(3), 360-379. https://doi.org/https://doi.org/10.1038/modpathol.3800053

Boysen, G., Barbieri, C. E., Prandi, D., Blattner, M., Chae, S.-S., Dahija, A., Nataraj, S., Huang, D., Marotz, C., Xu, L., Huang, J., Lecca, P., Chhangawala, S., Liu, D., Zhou, P., Sboner, A., de Bono, J. S., Demichelis, F., Houvras, Y., & Rubin, M. A. (2015). SPOP mutation leads to genomic instability in prostate cancer. *eLife*, *4*, e09207. https://doi.org/10.7554/eLife.09207

Brandão, A., Paulo, P., & Teixeira, M. R. (2020). Hereditary Predisposition to Prostate Cancer: From Genetics to Clinical Implications. *International Journal of Molecular Sciences*, *21*(14).

Braun, D. A., & Hildebrandt, F. (2017). Ciliopathies. *Cold Spring Harb Perspect Biol*, *9*(3). https://doi.org/10.1101/cshperspect.a028191

Brawer, M. K. (2005). Prostatic intraepithelial neoplasia: an overview. *Rev Urol*, *7 Suppl 3*(Suppl 3), S11-18.

Bray, F., Ferlay, J., Soerjomataram, I., Siegel, R. L., Torre, L. A., & Jemal, A. (2018). Global cancer statistics 2018: GLOBOCAN estimates of incidence and mortality worldwide for 36 cancers in 185 countries. *CA Cancer J Clin*, *68*(6), 394-424. https://doi.org/10.3322/caac.21492

Brenner, J. C., Ateeq, B., Li, Y., Yocum, A. K., Cao, Q., Asangani, I. A., Patel, S., Wang, X., Liang, H., Yu, J., Palanisamy, N., Siddiqui, J., Yan, W., Cao, X., Mehra, R., Sabolch, A., Basrur, V., Lonigro, R. J., Yang, J., . . . Chinnaiyan, A. M. (2011). Mechanistic rationale for inhibition of poly(ADP-ribose) polymerase in ETS gene fusion-positive prostate cancer. *Cancer Cell*, *19*(5), 664-678. https://doi.org/10.1016/j.ccr.2011.04.010

Burgess, A. W. (2008). EGFR family: structure physiology signalling and therapeutic targets. *Growth Factors*, *26*(5), 263-274. https://doi.org/10.1080/08977190802312844

Cai, C., Chen, S., Ng, P., Bubley, G. J., Nelson, P. S., Mostaghel, E. A., Marck, B., Matsumoto, A. M., Simon, N. I., Wang, H., Chen, S., & Balk, S. P. (2011). Intratumoral De Novo Steroid Synthesis Activates Androgen Receptor in Castration-Resistant Prostate Cancer and Is Upregulated by Treatment with CYP17A1 Inhibitors. *Cancer Research*, *71*(20), 6503-6513. https://doi.org/10.1158/0008-5472.CAN-11-0532

Carotenuto, P., Gradilone, S. A., & Franco, B. (2023). Cilia and Cancer: From Molecular Genetics to Therapeutic Strategies. *Genes*, *14*(7).

Carvalho-Santos, Z., Azimzadeh, J., Pereira-Leal, J. B., & Bettencourt-Dias, M. (2011). Evolution: Tracing the origins of centrioles, cilia, and flagella. *J Cell Biol*, *194*(2), 165-175. https://doi.org/10.1083/jcb.201011152

Castro, E., Goh, C., Leongamornlert, D., Saunders, E., Tymrakiewicz, M., Dadaev, T., Govindasami, K., Guy, M., Ellis, S., Frost, D., Bancroft, E., Cole, T., Tischkowitz, M., Kennedy, M. J., Eason, J., Brewer, C., Evans, D. G., Davidson, R., Eccles, D., . . . Eeles, R. (2015). Effect of BRCA Mutations on Metastatic Relapse and Cause-specific Survival After Radical Treatment for Localised Prostate Cancer. *Eur Urol*, *68*(2), 186-193. https://doi.org/10.1016/j.eururo.2014.10.022

Catalona, W. J., Smith, D. S., Ratliff, T. L., Dodds, K. M., Coplen, D. E., Yuan, J. J., Petros, J. A., & Andriole, G. L. (1991). Measurement of prostate-specific antigen in serum as a screening test for prostate cancer. *N Engl J Med*, *324*(17), 1156-1161. https://doi.org/10.1056/nejm199104253241702

Center, M. M., Jemal, A., Lortet-Tieulent, J., Ward, E., Ferlay, J., Brawley, O., & Bray, F. (2012). International Variation in Prostate Cancer Incidence and Mortality Rates. *European Urology*, *61*(6), 1079-1092. https://doi.org/https://doi.org/10.1016/j.eururo.2012.02.054

Cerretelli, G., Ager, A., Arends, M. J., & Frayling, I. M. (2020). Molecular pathology of Lynch syndrome. *The Journal of Pathology*, *250*(5), 518-531. https://doi.org/https://doi.org/10.1002/path.5422

Chatrath, A., Ratan, A., & Dutta, A. (2021). Germline Variants That Affect Tumor Progression. *Trends in Genetics*, *37*(5), 433-443. https://doi.org/10.1016/j.tig.2020.10.005

Chen, Z., Greenwood, C., Isaacs, W. B., Foulkes, W. D., Sun, J., Zheng, S. L., Condreay, L. D., & Xu, J. (2013). The G84E mutation of HOXB13 is associated with increased risk for prostate cancer: results from the REDUCE trial. *Carcinogenesis*, *34*(6), 1260-1264. https://doi.org/10.1093/carcin/bgt055

Cheng, H. H., Sokolova, A. O., Schaeffer, E. M., Small, E. J., & Higano, C. S. (2019). Germline and Somatic Mutations in Prostate Cancer for the Clinician. *J Natl Compr Canc Netw*, *17*(5), 515-521. https://doi.org/10.6004/jnccn.2019.7307

Chervona, Y., & Costa, M. (2012). Histone modifications and cancer: biomarkers of prognosis? *Am J Cancer Res*, *2*(5), 589-597.

Chughtai, B., Forde, J. C., Thomas, D. D. M., Laor, L., Hossack, T., Woo, H. H., Te, A. E., & Kaplan, S. A. (2016). Benign prostatic hyperplasia. *Nature Reviews Disease Primers*, *2*(1), 16031. https://doi.org/10.1038/nrdp.2016.31

Cohen, M. H., Johnson, J. R., Chen, Y.-F., Sridhara, R., & Pazdur, R. (2005). FDA drug approval summary: erlotinib (Tarceva®) tablets. *The oncologist*, *10*(7), 461-466.

Cohen, M. H., Williams, G. A., Sridhara, R., Chen, G., & Pazdur, R. (2003). FDA drug approval summary: gefitinib (ZD1839) (Iressa) tablets. *Oncologist*, *8*(4), 303-306. https://doi.org/10.1634/theoncologist.8-4-303

Corbit, K. C., Shyer, A. E., Dowdle, W. E., Gaulden, J., Singla, V., Chen, M. H., Chuang, P. T., & Reiter, J. F. (2008). Kif3a constrains beta-catenin-dependent Wnt signalling through dual ciliary and non-ciliary mechanisms. *Nat Cell Biol*, *10*(1), 70-76. https://doi.org/10.1038/ncb1670

Creeden, J. F., Nanavaty, N. S., Einloth, K. R., Gillman, C. E., Stanbery, L., Hamouda, D. M., Dworkin, L., & Nemunaitis, J. (2021). Homologous recombination proficiency in ovarian and breast cancer patients. *BMC Cancer*, *21*(1), 1154. https://doi.org/10.1186/s12885-021-08863-9

Cui, J., Li, G., Yin, J., Li, L., Tan, Y., Wei, H., Liu, B., Deng, L., Tang, J., Chen, Y., & Yi, L. (2020). GSTP1 and cancer: Expression, methylation, polymorphisms and signaling (Review). *Int J Oncol*, *56*(4), 867-878. https://doi.org/10.3892/ijo.2020.4979

Culp, M. B., Soerjomataram, I., Efstathiou, J. A., Bray, F., & Jemal, A. (2020). Recent Global Patterns in Prostate Cancer Incidence and Mortality Rates. *Eur Urol*, *77*(1), 38-52. https://doi.org/10.1016/j.eururo.2019.08.005

Currie, S. L., Warner, S. L., Vankayalapati, H., Liu, X., Sharma, S., Bearss, D. J., & Graves, B. J. (2018). Development of High-Throughput Screening Assays for Inhibitors of ETS Transcription Factors. *SLAS DISCOVERY: Advancing the Science of Drug Discovery*, *24*(1), 77-85. https://doi.org/10.1177/2472555218798571

Das, H., & Rodriguez, R. (2020). Health Care Disparities in Urologic Oncology: A Systematic Review. *Urology*, *136*, 9-18. https://doi.org/https://doi.org/10.1016/j.urology.2019.09.058

Demichelis, F., Fall, K., Perner, S., Andrén, O., Schmidt, F., Setlur, S. R., Hoshida, Y., Mosquera, J. M., Pawitan, Y., Lee, C., Adami, H. O., Mucci, L. A., Kantoff, P. W., Andersson, S. O., Chinnaiyan, A. M., Johansson, J. E., & Rubin, M. A. (2007). TMPRSS2:ERG gene fusion associated with lethal prostate cancer in a watchful waiting cohort. *Oncogene*, *26*(31), 4596-4599. https://doi.org/10.1038/sj.onc.1210237

Denham, J. W., Steigler, A., Lamb, D. S., Joseph, D., Mameghan, H., Turner, S., Matthews, J., Franklin, I., Atkinson, C., North, J., Poulsen, M., Christie, D., Spry, N. A., Tai, K. H., Wynne, C., Duchesne, G., Kovacev, O., & D'Este, C. (2005). Short-term androgen deprivation and radiotherapy for locally advanced prostate cancer: results from the Trans-Tasman Radiation Oncology Group 96.01 randomised controlled trial. *Lancet Oncol*, *6*(11), 841-850. https://doi.org/10.1016/s1470-2045(05)70348-x

Dhara, A., Ghosh, S., & Sen, N. (2022). Regulation of ETS family of transcription factors in cancer. *J Cancer Biol*, *3*(1), 33-49.

Di Lorenzo, G., Tortora, G., D'Armiento, F. P., De Rosa, G., Staibano, S., Autorino, R., D'Armiento, M., De Laurentiis, M., De Placido, S., Catalano, G., Bianco, A. R., & Ciardiello, F. (2002). Expression of Epidermal Growth Factor Receptor Correlates with Disease Relapse and Progression to Androgen-independence in Human Prostate Cancer1. *Clinical Cancer Research*, *8*(11), 3438-3444.

Doghish, A. S., Ismail, A., El-Mahdy, H. A., Elkady, M. A., Elrebehy, M. A., & Sallam, A.-A. M. (2022). A review of the biological role of miRNAs in prostate cancer suppression and progression. *International Journal of Biological Macromolecules*, *197*, 141-156. https://doi.org/https://doi.org/10.1016/j.ijbiomac.2021.12.141

Duffy, M. J. (2020). Biomarkers for prostate cancer: prostate-specific antigen and beyond. *58*(3), 326-339. https://doi.org/doi:10.1515/cclm-2019-0693 (Clinical Chemistry and Laboratory Medicine (CCLM))

Dupont, W. D., Breyer, J. P., Johnson, S. H., Plummer, W. D., & Smith, J. R. (2021). Prostate cancer risk variants of the HOXB genetic locus. *Scientific Reports*, *11*(1), 11385. https://doi.org/10.1038/s41598-021-89399-7

Egeberg, D. L., Lethan, M., Manguso, R., Schneider, L., Awan, A., Jørgensen, T. S., Byskov, A. G., Pedersen, L. B., & Christensen, S. T. (2012). Primary cilia and aberrant cell signaling in epithelial ovarian cancer. *Cilia*, *1*(1), 15. https://doi.org/10.1186/2046-2530-1-15

Eguether, T., & Hahne, M. (2018). Mixed signals from the cell's antennae: primary cilia in cancer. *EMBO Rep*, *19*(11). https://doi.org/10.15252/embr.201846589

Emoto, K., Masugi, Y., Yamazaki, K., Effendi, K., Tsujikawa, H., Tanabe, M., Kitagawa, Y., & Sakamoto, M. (2014). Presence of primary cilia in cancer cells correlates with prognosis of pancreatic ductal adenocarcinoma. *Hum Pathol*, *45*(4), 817-825. https://doi.org/10.1016/j.humpath.2013.11.017

Epstein, J. I., Egevad, L., Amin, M. B., Delahunt, B., Srigley, J. R., Humphrey, P. A., & the Grading, C. (2016). The 2014 International Society of Urological Pathology (ISUP) Consensus Conference on Gleason Grading of Prostatic Carcinoma: Definition of Grading Patterns and Proposal for a New Grading System. *The American Journal of Surgical Pathology*, *40*(2). https://journals.lww.com/ajsp/fulltext/2016/02000/the_2014_international_society_of_urological.10.aspx

Epstein, J. I., Zelefsky, M. J., Sjoberg, D. D., Nelson, J. B., Egevad, L., Magi-Galluzzi, C., Vickers, A. J., Parwani, A. V., Reuter, V. E., Fine, S. W., Eastham, J. A., Wiklund, P., Han, M., Reddy, C. A., Ciezki, J. P., Nyberg, T., & Klein, E. A. (2016). A Contemporary

Prostate Cancer Grading System: A Validated Alternative to the Gleason Score. *European Urology*, *69*(3), 428-435. https://doi.org/https://doi.org/10.1016/j.eururo.2015.06.046

Esteban, M. A., Harten, S. K., Tran, M. G., & Maxwell, P. H. (2006). Formation of primary cilia in the renal epithelium is regulated by the von Hippel-Lindau tumor suppressor protein. *J Am Soc Nephrol*, *17*(7), 1801-1806. https://doi.org/10.1681/asn.2006020181

Ewing, C. M., Ray, A. M., Lange, E. M., Zuhlke, K. A., Robbins, C. M., Tembe, W. D., Wiley, K. E., Isaacs, S. D., Johng, D., Wang, Y., Bizon, C., Yan, G., Gielzak, M., Partin, A. W., Shanmugam, V., Izatt, T., Sinari, S., Craig, D. W., Zheng, S. L., . . . Cooney, K. A. (2012). Germline mutations in HOXB13 and prostate-cancer risk. *N Engl J Med*, *366*(2), 141-149. https://doi.org/10.1056/NEJMoa1110000

Fabbri, L., Bost, F., & Mazure, N. M. (2019). Primary Cilium in Cancer Hallmarks. *Int J Mol Sci*, *20*(6). https://doi.org/10.3390/ijms20061336

Ferlay J, E. M., Lam F, Laversanne M, Colombet M, Mery L, Piñeros M, Znaor A, Soerjomataram I, Bray F. (2024). *Global Cancer Observatory: Cancer Today*.

FitzGerald, L. M., Agalliu, I., Johnson, K., Miller, M. A., Kwon, E. M., Hurtado-Coll, A., Fazli, L., Rajput, A. B., Gleave, M. E., Cox, M. E., Ostrander, E. A., Stanford, J. L., & Huntsman, D. G. (2008). Association of TMPRSS2-ERG gene fusion with clinical characteristics and outcomes: results from a population-based study of prostate cancer. *BMC Cancer*, *8*, 230. https://doi.org/10.1186/1471-2407-8-230

Font-Tello, A., Juanpere, N., de Muga, S., Lorenzo, M., Lorente, J. A., Fumado, L., Serrano, L., Serrano, S., Lloreta, J., & Hernández, S. (2015). Association of ERG and TMPRSS2-ERG with grade, stage, and prognosis of prostate cancer is dependent on their expression levels. *The Prostate*, *75*(11), 1216-1226. https://doi.org/https://doi.org/10.1002/pros.23004

Fraser, M., & Rouette, A. (2019). Prostate Cancer Genomic Subtypes. *Adv Exp Med Biol*, *1210*, 87-110. https://doi.org/10.1007/978-3-030-32656-2_5

Freedland, S. J., Samjoo, I. A., Rosta, E., Lansing, A., Worthington, E., Niyazov, A., Nazari, J., & Arondekar, B. (2023). The impact of race on survival in metastatic prostate cancer: a systematic literature review. *Prostate Cancer and Prostatic Diseases*, *26*(3), 461-474. https://doi.org/10.1038/s41391-023-00710-1

Fujii, R., Hasegawa, S., Maekawa, H., Inoue, T., Yoshioka, K., Uni, R., Ikeda, Y., Nangaku, M., & Inagi, R. (2021). Decreased IFT88 expression with primary cilia shortening causes mitochondrial dysfunction in cisplatin-induced tubular injury. *Am J Physiol Renal Physiol*, *321*(3), F278-f292. https://doi.org/10.1152/ajprenal.00673.2020

García-Flores, M., Casanova-Salas, I., Rubio-Briones, J., Calatrava, A., Domínguez-Escrig, J., Rubio, L., Ramírez-Backhaus, M., Fernández-Serra, A., García-Casado, Z., & López-Guerrero, J. A. (2014). Clinico-pathological significance of the molecular alterations of the SPOP gene in prostate cancer. *European Journal of Cancer*, *50*(17), 2994-3002. https://doi.org/https://doi.org/10.1016/j.ejca.2014.08.009

Gate, D., Danielpour, M., Bannykh, S., & Town, T. (2015). Characterization of cancer stem cells and primary cilia in medulloblastoma. *CNS Neurol Disord Drug Targets*, *14*(5), 600-611. https://doi.org/10.2174/1871527314666150429113851

Gleason, D. F., & Mellinger, G. T. (1974). Prediction of prognosis for prostatic adenocarcinoma by combined histological grading and clinical staging. *J Urol*, *111*(1), 58-64. https://doi.org/10.1016/s0022-5347(17)59889-4

Gómez, A. E., Christman, A. K., Van De Weghe, J. C., Finn, M., & Doherty, D. (2022). Systematic analysis of cilia characteristics and Hedgehog signaling in five immortal cell lines. *PLoS One*, *17*(12), e0266433. https://doi.org/10.1371/journal.pone.0266433

Guardiola, S., Varese, M., Sánchez-Navarro, M., & Giralt, E. (2019). A Third Shot at EGFR: New Opportunities in Cancer Therapy. *Trends Pharmacol Sci*, *40*(12), 941-955. https://doi.org/10.1016/j.tips.2019.10.004

Guimaraes, C. T. S., Sauer, L. J., Romano, R. F. T., Pacheco, E. O., & Bittencourt, L. K. (2020). Prostate Benign Diseases. *Topics in Magnetic Resonance Imaging*, *29*(1). https://journals.lww.com/topicsinmri/fulltext/2020/02000/prostate_benign_diseases.1.aspx

Hanahan, D., & Weinberg, R. A. (2011). Hallmarks of cancer: the next generation. *Cell*, *144*(5), 646-674. https://doi.org/10.1016/j.cell.2011.02.013

Harfe, B. D., & Jinks-Robertson, S. (2000). DNA MISMATCH REPAIR AND GENETIC INSTABILITY. *Annual Review of Genetics*, *34*(Volume 34, 2000), 359-399. https://doi.org/https://doi.org/10.1146/annurev.genet.34.1.359

Hassounah, N. B., Nagle, R., Saboda, K., Roe, D. J., Dalkin, B. L., & McDermott, K. M. (2013). Primary cilia are lost in preinvasive and invasive prostate cancer. *PLoS One*, *8*(7), e68521. https://doi.org/10.1371/journal.pone.0068521

Heeg, S., Das, K. K., Reichert, M., Bakir, B., Takano, S., Caspers, J., Aiello, N. M., Wu, K., Neesse, A., Maitra, A., Iacobuzio-Donahue, C. A., Hicks, P., & Rustgi, A. K. (2016). ETS-Transcription Factor ETV1 Regulates Stromal Expansion and Metastasis in Pancreatic Cancer. *Gastroenterology*, *151*(3), 540-553.e514. https://doi.org/10.1053/j.gastro.2016.06.005

Heidegger, I., Tsaur, I., Borgmann, H., Surcel, C., Kretschmer, A., Mathieu, R., Visschere, P., Valerio, M., van den Bergh, R. C. N., Ost, P., Tilki, D., Gandaglia, G., & Ploussard,

G. (2019). Hereditary prostate cancer - Primetime for genetic testing? *Cancer Treat Rev*, *81*, 101927. https://doi.org/10.1016/j.ctrv.2019.101927

Henrique, R., & Jerónimo, C. (2004). Molecular Detection of Prostate Cancer: A Role for GSTP1 Hypermethylation. *European Urology*, *46*(5), 660-669. https://doi.org/https://doi.org/10.1016/j.eururo.2004.06.014

Higgins, M., Obaidi, I., & McMorrow, T. (2019). Primary cilia and their role in cancer. *Oncol Lett*, *17*(3), 3041-3047. https://doi.org/10.3892/ol.2019.9942

Hnasko, T. S., & Hnasko, R. M. (2015). The Western Blot. In R. Hnasko (Ed.), *ELISA: Methods and Protocols* (pp. 87-96). Springer New York. https://doi.org/10.1007/978-1-4939-2742-5_9

Holland, J. F., Frei, E., & Kufe, D. W. (2003). *Holland, Frei cancer medicine 6*. In BC Decker Inc. Hamilton, Ont.

Hong, Z., Cao, X., Li, N., Zhang, Y., Lan, L., Zhou, Y., Pan, X., Shen, L., Yin, Z., & Luo, L. (2014). Luteolin is effective in the non-small cell lung cancer model with L858R/T790M EGF receptor mutation and erlotinib resistance. *Br J Pharmacol*, *171*(11), 2842-2853. https://doi.org/10.1111/bph.12610

Hopkins, B. R., Sepil, I., & Wigby, S. (2017). Seminal fluid. *Curr Biol*, *27*(11), R404-r405. https://doi.org/10.1016/j.cub.2017.03.063

Hua, K., & Ferland, R. J. (2018). Primary cilia proteins: ciliary and extraciliary sites and functions. *Cellular and Molecular Life Sciences*, *75*(9), 1521-1540. https://doi.org/10.1007/s00018-017-2740-5

Huang, D., Matin, S. F., Lawrentschuk, N., & Roupret, M. (2018). Systematic Review: An Update on the Spectrum of Urological Malignancies in Lynch Syndrome. *Bladder Cancer*, *4*, 261-268. https://doi.org/10.3233/BLC-180180

Huang, L., & Fu, L. (2015). Mechanisms of resistance to EGFR tyrosine kinase inhibitors. *Acta Pharm Sin B*, *5*(5), 390-401. https://doi.org/10.1016/j.apsb.2015.07.001

Huang, Y., Ognjenovic, J., Karandur, D., Miller, K., Merk, A., Subramaniam, S., & Kuriyan, J. (2021). A molecular mechanism for the generation of ligand-dependent differential outputs by the epidermal growth factor receptor. *eLife*, *10*, e73218. https://doi.org/10.7554/eLife.73218

Incrocci, L., Wortel, R. C., Alemayehu, W. G., Aluwini, S., Schimmel, E., Krol, S., van der Toorn, P. P., Jager, H., Heemsbergen, W., Heijmen, B., & Pos, F. (2016). Hypofractionated versus conventionally fractionated radiotherapy for patients with localised prostate cancer (HYPRO): final efficacy results from a randomised, multicentre, open-label, phase 3 trial. *Lancet Oncol*, *17*(8), 1061-1069. https://doi.org/10.1016/s1470-2045(16)30070-5

Institute, N. C. (2021). *Dictionary of Cancer Terms*. Retrieved April 30th from https://www.cancer.gov/publications/dictionaries/cancer-terms/def/epigenetic-alteration

Ippoliti, S., Fletcher, P., Orecchia, L., Miano, R., Kastner, C., & Barrett, T. (2022). Optimal biopsy approach for detection of clinically significant prostate cancer. *Br J Radiol*, *95*(1131), 20210413. https://doi.org/10.1259/bjr.20210413

Ittmann, M. (2018). Anatomy and Histology of the Human and Murine Prostate. *Cold Spring Harb Perspect Med*, *8*(5). https://doi.org/10.1101/cshperspect.a030346

Jamal, M. H., Nunes, A. C. F., Vaziri, N. D., Ramchandran, R., Bacallao, R. L., Nauli, A. M., & Nauli, S. M. (2020). Rapamycin treatment correlates changes in primary cilia expression with cell cycle regulation in epithelial cells. *Biochemical Pharmacology*, *178*, 114056. https://doi.org/https://doi.org/10.1016/j.bcp.2020.114056

Jia, L., Strand, D. W., Goueli, R. S., Gahan, J. C., Roehrborn, C. G., & Mauck, R. J. (2022). PSA density is associated with BPH cellular composition. *The Prostate*, *82*(12), 1162-1169. https://doi.org/https://doi.org/10.1002/pros.24367

Joniau, S., Goeman, L., Pennings, J., & Van Poppel, H. (2005). Prostatic intraepithelial neoplasia (PIN): importance and clinical management. *Eur Urol*, *48*(3), 379-385. https://doi.org/10.1016/j.eururo.2005.03.015

Jorge, A. L., Pereira, E. R., Oliveira, C. S., Ferreira, E. D. S., Menon, E. T. N., Diniz, S. N., & Pezuk, J. A. (2021). MicroRNAs: understanding their role in gene expression and cancer. *Einstein (Sao Paulo)*, *19*, eRB5996. https://doi.org/10.31744/einstein_journal/2021RB5996

Kaffenberger, S. D., & Barbieri, C. E. (2016). Molecular subtyping of prostate cancer. *Curr Opin Urol*, *26*(3), 213-218. https://doi.org/10.1097/mou.0000000000000285

Karlsson, R., Aly, M., Clements, M., Zheng, L., Adolfsson, J., Xu, J., Grönberg, H., & Wiklund, F. (2014). A Population-based Assessment of Germline HOXB13 G84E Mutation and Prostate Cancer Risk. *European Urology*, *65*(1), 169-176. https://doi.org/https://doi.org/10.1016/j.eururo.2012.07.027

Kasahara, K., Aoki, H., Kiyono, T., Wang, S., Kagiwada, H., Yuge, M., Tanaka, T., Nishimura, Y., Mizoguchi, A., Goshima, N., & Inagaki, M. (2018). EGF receptor kinase suppresses ciliogenesis through activation of USP8 deubiquitinase. *Nat Commun*, *9*(1), 758. https://doi.org/10.1038/s41467-018-03117-y

Kasahara, K., & Inagaki, M. (2021). Primary ciliary signaling: links with the cell cycle. *Trends Cell Biol*, *31*(12), 954-964. https://doi.org/10.1016/j.tcb.2021.07.009

Kasivisvanathan, V., Rannikko, A. S., Borghi, M., Panebianco, V., Mynderse, L. A., Vaarala, M. H., Briganti, A., Budäus, L., Hellawell, G., Hindley, R. G., Roobol, M. J., Eggener, S., Ghei, M., Villers, A., Bladou, F., Villeirs, G. M., Virdi, J., Boxler, S., Robert, G., . .

. Moore, C. M. (2018). MRI-Targeted or Standard Biopsy for Prostate-Cancer Diagnosis. *New England Journal of Medicine*, *378*(19), 1767-1777. https://doi.org/10.1056/NEJMoa1801993

Kgatle, M. M., Kalla, A. A., Islam, M. M., Sathekge, M., & Moorad, R. (2016). Prostate Cancer: Epigenetic Alterations, Risk Factors, and Therapy. *Prostate Cancer*, *2016*, 5653862. https://doi.org/10.1155/2016/5653862

Khan, H. M., & Cheng, H. H. (2022). Germline genetics of prostate cancer. *The Prostate*, *82*(S1), S3-S12. https://doi.org/https://doi.org/10.1002/pros.24340

Khan, N. A., Willemarck, N., Talebi, A., Marchand, A., Binda, M. M., Dehairs, J., Rueda-Rincon, N., Daniels, V. W., Bagadi, M., Thimiri Govinda Raj, D. B., Vanderhoydonc, F., Munck, S., Chaltin, P., & Swinnen, J. V. (2016). Identification of drugs that restore primary cilium expression in cancer cells. *Oncotarget*, *7*(9), 9975-9992. https://doi.org/10.18632/oncotarget.7198

Kiseleva, A. A., Korobeynikov, V. A., Nikonova, A. S., Zhang, P., Makhov, P., Deneka, A. Y., Einarson, M. B., Serebriiskii, I. G., Liu, H., Peterson, J. R., & Golemis, E. A. (2019). Unexpected Activities in Regulating Ciliation Contribute to Off-target Effects of Targeted Drugs. *Clin Cancer Res*, *25*(13), 4179-4193. https://doi.org/10.1158/1078-0432.Ccr-18-3535

Kiseleva, A. A., Nikonova, A. S., & Golemis, E. A. (2023). Patterns of Ciliation and Ciliary Signaling in Cancer. *Rev Physiol Biochem Pharmacol*, *185*, 87-105. https://doi.org/10.1007/112_2020_36

Kulda, V., Topolcan, O., Kucera, R., Kripnerova, M., Srbecka, K., Hora, M., Hes, O., Klecka, J., Babuska, V., Rousarova, M., Benson, V., & Pesta, M. (2016). Prognostic Significance of TMPRSS2-ERG Fusion Gene in Prostate Cancer. *Anticancer Research*, *36*(9), 4787. http://ar.iiarjournals.org/content/36/9/4787.abstract

Lancaster, M. A., Schroth, J., & Gleeson, J. G. (2011). Subcellular spatial regulation of canonical Wnt signalling at the primary cilium. *Nat Cell Biol*, *13*(6), 700-707. https://doi.org/10.1038/ncb2259

Larkins, C. E., Aviles, G. D. G., East, M. P., Kahn, R. A., & Caspary, T. (2011). Arl13b regulates ciliogenesis and the dynamic localization of Shh signaling proteins. *Molecular Biology of the Cell*, *22*(23), 4694-4703. https://doi.org/10.1091/mbc.e10-12-0994

Lavagnino, M., Oslapas, A. N., Gardner, K. L., & Arnoczky, S. P. (2016). Hypoxia inhibits primary cilia formation and reduces cell-mediated contraction in stress-deprived rat tail tendon fascicles. *Muscles Ligaments Tendons J*, *6*(2), 193-197. https://doi.org/10.11138/mltj/2016.6.2.193

Lechtreck, K. F. (2015). IFT-Cargo Interactions and Protein Transport in Cilia. *Trends Biochem Sci*, *40*(12), 765-778. https://doi.org/10.1016/j.tibs.2015.09.003

Lee, C. H., Akin-Olugbade, O., & Kirschenbaum, A. (2011). Overview of prostate anatomy, histology, and pathology. *Endocrinol Metab Clin North Am*, *40*(3), 565-575, viii-ix. https://doi.org/10.1016/j.ecl.2011.05.012

Lee, K. H. (2023). Primary cilia: a novel research approach to overcome anticancer drug resistance [Review]. *Frontiers in Molecular Biosciences*, *10*. https://www.frontiersin.org/journals/molecular-biosciences/articles/10.3389/fmolb.2023.1270639

Leto, S. M., & Trusolino, L. (2014). Primary and acquired resistance to EGFR-targeted therapies in colorectal cancer: impact on future treatment strategies. *J Mol Med (Berl)*, *92*(7), 709-722. https://doi.org/10.1007/s00109-014-1161-2

Li, G.-M. (2008). Mechanisms and functions of DNA mismatch repair. *Cell Research*, *18*(1), 85-98. https://doi.org/10.1038/cr.2007.115

Li, X., Liu, G., & Wu, W. (2021). Recent advances in Lynch syndrome. *Experimental Hematology & Oncology*, *10*(1), 37. https://doi.org/10.1186/s40164-021-00231-4

Lim, Y. C., McGlashan, S. R., Cooling, M. T., & Long, D. S. (2015). Culture and detection of primary cilia in endothelial cell models. *Cilia*, *4*(1), 11. https://doi.org/10.1186/s13630-015-0020-2

Lin, C. J., Dang, A., Hernandez, E., & Hsieh, J. T. (2021). DAB2IP modulates primary cilia formation associated with renal tumorigenesis. *Neoplasia*, *23*(1), 169-180. https://doi.org/10.1016/j.neo.2020.12.002

Lin, T. C. (2021). Functional Roles of SPINK1 in Cancers. *Int J Mol Sci*, *22*(8). https://doi.org/10.3390/ijms22083814

Litwin, M. S., & Tan, H. J. (2017). The Diagnosis and Treatment of Prostate Cancer: A Review. *Jama*, *317*(24), 2532-2542. https://doi.org/10.1001/jama.2017.7248

Ma, Z., Qin, M., Liang, H., Chen, R., Cai, S., Huang, Z., & Tai, G. (2020). Primary cilia-dependent signaling is involved in regulating mesenchymal stem cell proliferation and pluripotency maintenance. *J Mol Histol*, *51*(3), 241-250. https://doi.org/10.1007/s10735-020-09876-7

Malins, D. C., Polissar, N. L., & Gunselman, S. J. (1997). Models of DNA structure achieve almost perfect discrimination between normal prostate, benign prostatic hyperplasia (BPH), and adenocarcinoma and have a high potential for predicting BPH and prostate cancer. *Proc Natl Acad Sci U S A*, *94*(1), 259-264. https://doi.org/10.1073/pnas.94.1.259

Martincorena, I., & Campbell, P. J. (2015). Somatic mutation in cancer and normal cells. *Science*, *349*(6255), 1483-1489. https://doi.org/10.1126/science.aab4082

McNeal, J. E. (1968). Regional morphology and pathology of the prostate. *Am J Clin Pathol*, *49*(3), 347-357. https://doi.org/10.1093/ajcp/49.3.347

McNeal, J. E. (1969). Origin and development of carcinoma in the prostate. *Cancer*, *23*(1), 24-34. https://doi.org/10.1002/1097-0142(196901)23:1<24::aid-cncr2820230103>3.0.co;2-1

McNeal, J. E. (1981). The zonal anatomy of the prostate. *Prostate*, *2*(1), 35-49. https://doi.org/10.1002/pros.2990020105

Meller, S., Meyer, H. A., Bethan, B., Dietrich, D., Maldonado, S. G., Lein, M., Montani, M., Reszka, R., Schatz, P., Peter, E., Stephan, C., Jung, K., Kamlage, B., & Kristiansen, G. (2016). Integration of tissue metabolomics, transcriptomics and immunohistochemistry reveals ERG- and gleason score-specific metabolomic alterations in prostate cancer. *Oncotarget*, *7*(2), 1421-1438. https://doi.org/10.18632/oncotarget.6370

Menzl, I., Lebeau, L., Pandey, R., Hassounah, N. B., Li, F. W., Nagle, R., Weihs, K., & McDermott, K. M. (2014). Loss of primary cilia occurs early in breast cancer development. *Cilia*, *3*(1), 7. https://doi.org/10.1186/2046-2530-3-7

Mesquita, D., Barros-Silva, J. D., Santos, J., Skotheim, R. I., Lothe, R. A., Paulo, P., & Teixeira, M. R. (2015). Specific and redundant activities of ETV1 and ETV4 in prostate cancer aggressiveness revealed by co-overexpression cellular contexts. *Oncotarget*, *6*(7), 5217-5236. https://doi.org/10.18632/oncotarget.2847

Mill, P., Christensen, S. T., & Pedersen, L. B. (2023). Primary cilia as dynamic and diverse signalling hubs in development and disease. *Nature Reviews Genetics*, *24*(7), 421-441. https://doi.org/10.1038/s41576-023-00587-9

Miller, D. B., Markt, S. C., Nguyen, C. T., & Coleman, O. C. (2022). Prostate Cancer Screening and Young Black Men: Can Early Communication Avoid Later Health Disparities? *Journal of Cancer Education*, *37*(5), 1460-1465. https://doi.org/10.1007/s13187-021-01984-6

Mitchell, P. S., Parkin, R. K., Kroh, E. M., Fritz, B. R., Wyman, S. K., Pogosova-Agadjanyan, E. L., Peterson, A., Noteboom, J., O'Briant, K. C., Allen, A., Lin, D. W., Urban, N., Drescher, C. W., Knudsen, B. S., Stirewalt, D. L., Gentleman, R., Vessella, R. L., Nelson, P. S., Martin, D. B., & Tewari, M. (2008). Circulating microRNAs as stable blood-based markers for cancer detection. *Proc Natl Acad Sci U S A*, *105*(30), 10513-10518. https://doi.org/10.1073/pnas.0804549105

The Molecular Taxonomy of Primary Prostate Cancer. (2015). *Cell*, *163*(4), 1011-1025. https://doi.org/10.1016/j.cell.2015.10.025

Moses, K. A., Sprenkle, P. C., Bahler, C., Box, G., Carlsson, S. V., Catalona, W. J., Dahl, D. M., Dall'Era, M., Davis, J. W., Drake, B. F., Epstein, J. I., Etzioni, R. B., Farrington,

T. A., Garraway, I. P., Jarrard, D., Kauffman, E., Kaye, D., Kibel, A. S., LaGrange, C. A., . . . Freedman-Cass, D. A. (2023). NCCN Guidelines® Insights: Prostate Cancer Early Detection, Version 1.2023: Featured Updates to the NCCN Guidelines. *Journal of the National Comprehensive Cancer Network*, *21*(3), 236-246. https://doi.org/10.6004/jnccn.2023.0014

Nair, S. S., Chakravarty, D., Dovey, Z. S., Zhang, X., & Tewari, A. K. (2022). Why do African-American men face higher risks for lethal prostate cancer? *Curr Opin Urol*, *32*(1), 96-101. https://doi.org/10.1097/mou.0000000000000951

Nakazawa, M., Fang, M., H. Marshall, C., Lotan, T. L., Isaacsson Velho, P., & Antonarakis, E. S. (2022). Clinical and genomic features of SPOP-mutant prostate cancer. *The Prostate*, *82*(2), 260-268. https://doi.org/https://doi.org/10.1002/pros.24269

Naldi, I., Taranta, M., Gherardini, L., Pelosi, G., Viglione, F., Grimaldi, S., Pani, L., & Cinti, C. (2014). Novel epigenetic target therapy for prostate cancer: a preclinical study. *PLoS One*, *9*(5), e98101. https://doi.org/10.1371/journal.pone.0098101

Nam, R. K., Sugar, L., Wang, Z., Yang, W., Kitching, R., Klotz, L. H., Venkateswaran, V., Narod, S. A., & Seth, A. (2007). Expression of TMPRSS2:ERG gene fusion in prostate cancer cells is an important prognostic factor for cancer progression. *Cancer Biology & Therapy*, *6*(1), 40-45. https://doi.org/10.4161/cbt.6.1.3489

National Comprehensive Cancer Network. (2024). *NCCN Clinical Practice Guidelines in Oncology - Prostate Cancer Early Detection, Version 1.2024*. https://www.nccn.org/professionals/physician_gls/pdf/prostate_detection.pdf

Nevalainen, J., Raitanen, J., Natunen, K., Kilpeläinen, T., Rannikko, A., Tammela, T., & Auvinen, A. (2024). Early detection of clinically significant prostate cancer: protocol summary and statistical analysis plan for the ProScreen randomised trial. *BMJ Open*, *14*(1), e075595. https://doi.org/10.1136/bmjopen-2023-075595

Ngollo, M., Dagdemir, A., Karsli-Ceppioglu, S., Judes, G., Pajon, A., Penault-Llorca, F., Boiteux, J. P., Bignon, Y. J., Guy, L., & Bernard-Gallon, D. J. (2014). Epigenetic modifications in prostate cancer. *Epigenomics*, *6*(4), 415-426. https://doi.org/10.2217/epi.14.34

Ni Raghallaigh, H., & Eeles, R. (2022). Genetic predisposition to prostate cancer: an update. *Fam Cancer*, *21*(1), 101-114. https://doi.org/10.1007/s10689-021-00227-3

Nicholas, T. R., Strittmatter, B. G., & Hollenhorst, P. C. (2019). Oncogenic ETS Factors in Prostate Cancer. *Adv Exp Med Biol*, *1210*, 409-436. https://doi.org/10.1007/978-3-030-32656-2_18

Ning, K., Luo, Z., Kowal, T. J., Tran, M., Majumder, R., Jarin, T. M., Wu, A. Y., Goldberg, J. L., & Sun, Y. (2023). Characterization of Primary Cilia Formation in Human ESC-

Derived Retinal Organoids. *Stem Cells Int*, *2023*, 6494486. https://doi.org/10.1155/2023/6494486

Normanno, N., De Luca, A., Bianco, C., Strizzi, L., Mancino, M., Maiello, M. R., Carotenuto, A., De Feo, G., Caponigro, F., & Salomon, D. S. (2006). Epidermal growth factor receptor (EGFR) signaling in cancer. *Gene*, *366*(1), 2-16. https://doi.org/https://doi.org/10.1016/j.gene.2005.10.018

Norris, J. D., Chang, C. Y., Wittmann, B. M., Kunder, R. S., Cui, H., Fan, D., Joseph, J. D., & McDonnell, D. P. (2009). The homeodomain protein HOXB13 regulates the cellular response to androgens. *Mol Cell*, *36*(3), 405-416. https://doi.org/10.1016/j.molcel.2009.10.020

Nowacka-Zawisza, M., & Wiśnik, E. (2017). DNA methylation and histone modifications as epigenetic regulation in prostate cancer (Review). *Oncol Rep*, *38*(5), 2587-2596. https://doi.org/10.3892/or.2017.5972

Ozah, E., & Imasogie, D. E. (2023). The Diagnostic Accuracy of Prostate-Specific Antigen and Digital Rectal Examination in the Diagnosis of Prostate Cancer at the University of Benin Teaching Hospital. *J West Afr Coll Surg*, *13*(3), 91-95. https://doi.org/10.4103/jwas.jwas_32_23

Pala, R., Alomari, N., & Nauli, S. M. (2017). Primary Cilium-Dependent Signaling Mechanisms. *Int J Mol Sci*, *18*(11). https://doi.org/10.3390/ijms18112272

Pande, M., Wei, C., Chen, J., Amos, C. I., Lynch, P. M., Lu, K. H., Lucio, L. A., Boyd-Rogers, S. G., Bannon, S. A., Mork, M. E., & Frazier, M. L. (2012). Cancer spectrum in DNA mismatch repair gene mutation carriers: results from a hospital based Lynch syndrome registry. *Fam Cancer*, *11*(3), 441-447. https://doi.org/10.1007/s10689-012-9534-6

Parker, C., Castro, E., Fizazi, K., Heidenreich, A., Ost, P., Procopio, G., Tombal, B., & Gillessen, S. (2020). Prostate cancer: ESMO Clinical Practice Guidelines for diagnosis, treatment and follow-up[†]. *Annals of Oncology*, *31*(9), 1119-1134. https://doi.org/10.1016/j.annonc.2020.06.011

Paulo, P., Maia, S., Pinto, C., Pinto, P., Monteiro, A., Peixoto, A., & Teixeira, M. R. (2018). Targeted next generation sequencing identifies functionally deleterious germline mutations in novel genes in early-onset/familial prostate cancer. *PLOS Genetics*, *14*(4), e1007355. https://doi.org/10.1371/journal.pgen.1007355

Paulo, P., Maia, S., Pinto, C., Pinto, P., Monteiro, A., Peixoto, A., & Teixeira, M. R. (2018). Targeted next generation sequencing identifies functionally deleterious germline mutations in novel genes in early-onset/familial prostate cancer. *PLoS Genet*, *14*(4), e1007355. https://doi.org/10.1371/journal.pgen.1007355

Paulo, P., Ribeiro, F. R., Santos, J., Mesquita, D., Almeida, M., Barros-Silva, J. D., Itkonen, H., Henrique, R., Jerónimo, C., Sveen, A., Mills, I. G., Skotheim, R. I., Lothe, R. A., & Teixeira, M. R. (2012). Molecular Subtyping of Primary Prostate Cancer Reveals Specific and Shared Target Genes of Different ETS Rearrangements. *Neoplasia*, *14*(7), 600-IN615. https://doi.org/https://doi.org/10.1593/neo.12600

Peixoto, E., Jin, S., Thelen, K., Biswas, A., Richard, S., Morleo, M., Mansini, A., Holtorf, S., Carbone, F., Pastore, N., Ballabio, A., Franco, B., & Gradilone, S. A. (2020). HDAC6-dependent ciliophagy is involved in ciliary loss and cholangiocarcinoma growth in human cells and murine models. *Am J Physiol Gastrointest Liver Physiol*, *318*(6), G1022-g1033. https://doi.org/10.1152/ajpgi.00033.2020

Pejčić, T., Tosti, T., Tešić, Ž., Milković, B., Dragičević, D., Kozomara, M., Čekerevac, M., & Džamić, Z. (2017). Testosterone and dihydrotestosterone levels in the transition zone correlate with prostate volume. *Prostate*, *77*(10), 1082-1092. https://doi.org/10.1002/pros.23365

Peraldo-Neia, C., Migliardi, G., Mello-Grand, M., Montemurro, F., Segir, R., Pignochino, Y., Cavalloni, G., Torchio, B., Mosso, L., Chiorino, G., & Aglietta, M. (2011). Epidermal Growth Factor Receptor (EGFR) mutation analysis, gene expression profiling and EGFR protein expression in primary prostate cancer. *BMC Cancer*, *11*(1), 31. https://doi.org/10.1186/1471-2407-11-31

Perdana, N. R., Mochtar, C. A., Umbas, R., & Hamid, A. R. (2016). The Risk Factors of Prostate Cancer and Its Prevention: A Literature Review. *Acta Med Indones*, *48*(3), 228-238.

Petrovics, G., Liu, A., Shaheduzzaman, S., Furusato, B., Sun, C., Chen, Y., Nau, M., Ravindranath, L., Chen, Y., Dobi, A., Srikantan, V., Sesterhenn, I. A., McLeod, D. G., Vahey, M., Moul, J. W., & Srivastava, S. (2005). Frequent overexpression of ETS-related gene-1 (ERG1) in prostate cancer transcriptome. *Oncogene*, *24*(23), 3847-3852. https://doi.org/10.1038/sj.onc.1208518

Phan, T., Crook, S. M., Bryce, A. H., Maley, C. C., Kostelich, E. J., & Kuang, Y. (2020). Review: Mathematical Modeling of Prostate Cancer and Clinical Application. *Applied Sciences*, *10*(8).

Pierorazio, P. M., Walsh, P. C., Partin, A. W., & Epstein, J. I. (2013). Prognostic Gleason grade grouping: data based on the modified Gleason scoring system. *BJU Int*, *111*(5), 753-760. https://doi.org/10.1111/j.1464-410X.2012.11611.x

Pilepich, M. V., Winter, K., John, M. J., Mesic, J. B., Sause, W., Rubin, P., Lawton, C., Machtay, M., & Grignon, D. (2001). Phase III radiation therapy oncology group (RTOG) trial 86-10 of androgen deprivation adjuvant to definitive radiotherapy in

locally advanced carcinoma of the prostate. *Int J Radiat Oncol Biol Phys*, *50*(5), 1243-1252. https://doi.org/10.1016/s0360-3016(01)01579-6

Plotnikova, O. V., Pugacheva, E. N., & Golemis, E. A. (2009). Chapter 7 - Primary Cilia and the Cell Cycle. In R. D. Sloboda (Ed.), *Methods in Cell Biology* (Vol. 94, pp. 137-160). Academic Press. https://doi.org/https://doi.org/10.1016/S0091-679X(08)94007-3

Pop, M. S., Stransky, N., Garvie, C. W., Theurillat, J. P., Hartman, E. C., Lewis, T. A., Zhong, C., Culyba, E. K., Lin, F., Daniels, D. S., Pagliarini, R., Ronco, L., Koehler, A. N., & Garraway, L. A. (2014). A small molecule that binds and inhibits the ETV1 transcription factor oncoprotein. *Mol Cancer Ther*, *13*(6), 1492-1502. https://doi.org/10.1158/1535-7163.Mct-13-0689

Porkka, K. P., Pfeiffer, M. J., Waltering, K. K., Vessella, R. L., Tammela, T. L. J., & Visakorpi, T. (2007). MicroRNA Expression Profiling in Prostate Cancer. *Cancer Research*, *67*(13), 6130-6135. https://doi.org/10.1158/0008-5472.CAN-07-0533

Prasad, R. M., Jin, X., & Nauli, S. M. (2014). Sensing a sensor: identifying the mechanosensory function of primary cilia. *Biosensors (Basel)*, *4*(1), 47-62. https://doi.org/10.3390/bios4010047

Pritchard, C. C., Mateo, J., Walsh, M. F., De Sarkar, N., Abida, W., Beltran, H., Garofalo, A., Gulati, R., Carreira, S., Eeles, R., Elemento, O., Rubin, M. A., Robinson, D., Lonigro, R., Hussain, M., Chinnaiyan, A., Vinson, J., Filipenko, J., Garraway, L., . . . Nelson, P. S. (2016). Inherited DNA-Repair Gene Mutations in Men with Metastatic Prostate Cancer. *N Engl J Med*, *375*(5), 443-453. https://doi.org/10.1056/NEJMoa1603144

Pugacheva, E. N., Jablonski, S. A., Hartman, T. R., Henske, E. P., & Golemis, E. A. (2007). HEF1-Dependent Aurora A Activation Induces Disassembly of the Primary Cilium. *Cell*, *129*(7), 1351-1363. https://doi.org/10.1016/j.cell.2007.04.035

Qi, M., Liu, Z., Shen, C., Wang, L., Zeng, J., Wang, C., Li, C., Fu, W., Sun, Y., & Han, B. (2015). Overexpression of ETV4 is associated with poor prognosis in prostate cancer: involvement of uPA/uPAR and MMPs. *Tumour Biol*, *36*(5), 3565-3572. https://doi.org/10.1007/s13277-014-2993-7

Qi, T., Qu, Q., Li, G., Wang, J., Zhu, H., Yang, Z., Sun, Y., Lu, Q., & Qu, J. (2020). Function and regulation of the PEA3 subfamily of ETS transcription factors in cancer. *Am J Cancer Res*, *10*(10), 3083-3105.

Qian, C., Li, D., & Chen, Y. (2022). ETS factors in prostate cancer. *Cancer Lett*, *530*, 181-189. https://doi.org/10.1016/j.canlet.2022.01.009

Qu, H., Zhao, H., Zhang, X., Liu, Y., Li, F., Sun, L., & Song, Z. (2020). Integrated Analysis of the ETS Family in Melanoma Reveals a Regulatory Role of ETV7 in the Immune

Microenvironment. *Front Immunol*, *11*, 612784. https://doi.org/10.3389/fimmu.2020.612784

Quesnelle, K. M., Boehm, A. L., & Grandis, J. R. (2007). STAT-mediated EGFR signaling in cancer. *J Cell Biochem*, *102*(2), 311-319. https://doi.org/10.1002/jcb.21475

Ragsdale, J. W., 3rd, Halstater, B., & Martinez-Bianchi, V. (2014). Prostate cancer screening. *Prim Care*, *41*(2), 355-370. https://doi.org/10.1016/j.pop.2014.02.009

Rahim, S., Beauchamp, E. M., Kong, Y., Brown, M. L., Toretsky, J. A., & Üren, A. (2011). YK-4-279 inhibits ERG and ETV1 mediated prostate cancer cell invasion. *PLoS One*, *6*(4), e19343. https://doi.org/10.1371/journal.pone.0019343

Rahim, S., Minas, T., Hong, S. H., Justvig, S., Çelik, H., Kont, Y. S., Han, J., Kallarakal, A. T., Kong, Y., Rudek, M. A., Brown, M. L., Kallakury, B., Toretsky, J. A., & Üren, A. (2014). A small molecule inhibitor of ETV1, YK-4-279, prevents prostate cancer growth and metastasis in a mouse xenograft model. *PLoS One*, *9*(12), e114260. https://doi.org/10.1371/journal.pone.0114260

Rahimi, A. M., Cai, M., Kılıç, I., Kazerouni, Z. B., Tapia Contreras, C., & Hoyer-Fender, S. (2021). Expression of α-Tubulin Acetyltransferase 1 and Tubulin Acetylation as Selective Forces in Cell Competition. *Cells*, *10*(2). https://doi.org/10.3390/cells10020390

Rana, S., Valbuena, G. N., Curry, E., Bevan, C. L., & Keun, H. C. (2022). MicroRNAs as biomarkers for prostate cancer prognosis: a systematic review and a systematic reanalysis of public data. *British Journal of Cancer*, *126*(3), 502-513. https://doi.org/10.1038/s41416-021-01677-3

Rebello, R. J., Oing, C., Knudsen, K. E., Loeb, S., Johnson, D. C., Reiter, R. E., Gillessen, S., Van der Kwast, T., & Bristow, R. G. (2021). Prostate cancer. *Nature Reviews Disease Primers*, *7*(1), 9. https://doi.org/10.1038/s41572-020-00243-0

Reynolds, N. A., & Wagstaff, A. J. (2004). Cetuximab. *Drugs*, *64*(1), 109-118. https://doi.org/10.2165/00003495-200464010-00007

Roach, M., 3rd, Bae, K., Speight, J., Wolkov, H. B., Rubin, P., Lee, R. J., Lawton, C., Valicenti, R., Grignon, D., & Pilepich, M. V. (2008). Short-term neoadjuvant androgen deprivation therapy and external-beam radiotherapy for locally advanced prostate cancer: long-term results of RTOG 8610. *J Clin Oncol*, *26*(4), 585-591. https://doi.org/10.1200/jco.2007.13.9881

Robinson, J. L., Holmes, K. A., & Carroll, J. S. (2013). FOXA1 mutations in hormone-dependent cancers [Mini Review]. *Frontiers in Oncology*, *3*. https://doi.org/10.3389/fonc.2013.00020

Roehrborn, C. G. (2005). Benign prostatic hyperplasia: an overview. *Rev Urol*, *7 Suppl 9*(Suppl 9), S3-s14.

Rubin, M. A. (2012). ETS rearrangements in prostate cancer. *Asian J Androl*, *14*(3), 393-399. https://doi.org/10.1038/aja.2011.145

Ryan, S., Jenkins, M. A., & Win, A. K. (2014). Risk of Prostate Cancer in Lynch Syndrome: A Systematic Review and Meta-analysis. *Cancer Epidemiology, Biomarkers & Prevention*, *23*(3), 437-449. https://doi.org/10.1158/1055-9965.EPI-13-1165

Sabbah, D. A., Hajjo, R., & Sweidan, K. (2020). Review on Epidermal Growth Factor Receptor (EGFR) Structure, Signaling Pathways, Interactions, and Recent Updates of EGFR Inhibitors. *Curr Top Med Chem*, *20*(10), 815-834. https://doi.org/10.2174/1568026620666200303123102

Sandhu, J. S., & Schlegel, P. N. (2004). Prostate Cancer. In L. Martini (Ed.), *Encyclopedia of Endocrine Diseases* (pp. 125-130). Elsevier. https://doi.org/https://doi.org/10.1016/B0-12-475570-4/01086-6

Saramäki, O. R., Harjula, A. E., Martikainen, P. M., Vessella, R. L., Tammela, T. L., & Visakorpi, T. (2008). TMPRSS2:ERG fusion identifies a subgroup of prostate cancers with a favorable prognosis. *Clin Cancer Res*, *14*(11), 3395-3400. https://doi.org/10.1158/1078-0432.Ccr-07-2051

Saternos, H., Ley, S., & AbouAlaiwi, W. (2020). Primary Cilia and Calcium Signaling Interactions. *Int J Mol Sci*, *21*(19). https://doi.org/10.3390/ijms21197109

Schaeffer, E. M., Srinivas, S., Adra, N., An, Y., Barocas, D., Bitting, R., Bryce, A., Chapin, B., Cheng, H. H., D'Amico, A. V., Desai, N., Dorff, T., Eastham, J. A., Farrington, T. A., Gao, X., Gupta, S., Guzzo, T., Ippolito, J. E., Kuettel, M. R., . . . Freedman-Cass, D. A. (2022). NCCN Guidelines® Insights: Prostate Cancer, Version 1.2023: Featured Updates to the NCCN Guidelines. *Journal of the National Comprehensive Cancer Network*, *20*(12), 1288-1298. https://doi.org/10.6004/jnccn.2022.0063

Schimmack, S., Kneller, S., Dadabaeva, N., Bergmann, F., Taylor, A., Hackert, T., Werner, J., & Strobel, O. (2016). Epithelial to Stromal Re-Distribution of Primary Cilia during Pancreatic Carcinogenesis. *PLoS One*, *11*(10), e0164231. https://doi.org/10.1371/journal.pone.0164231

Scholey, J. M. (2003). Intraflagellar Transport. *Annual Review of Cell and Developmental Biology*, *19*(Volume 19, 2003), 423-443. https://doi.org/https://doi.org/10.1146/annurev.cellbio.19.111401.091318

Schröder, F. H., Hugosson, J., Roobol, M. J., Tammela, T. L. J., Zappa, M., Nelen, V., Kwiatkowski, M., Lujan, M., Määttänen, L., Lilja, H., Denis, L. J., Recker, F., Paez, A., Bangma, C. H., Carlsson, S., Puliti, D., Villers, A., Rebillard, X., Hakama, M., . . . Auvinen, A. (2014). Screening and prostate cancer mortality: results of the European Randomised Study of Screening for Prostate Cancer (ERSPC) at 13

years of follow-up. *The Lancet*, *384*(9959), 2027-2035. https://doi.org/https://doi.org/10.1016/S0140-6736(14)60525-0

SEER Cancer Stat Facts: Prostate Cancer. National Cancer Institute.

Segalés, L., Juanpere, N., Lorenzo, M., Albero-González, R., Fumadó, L., Cecchini, L., Bellmunt, J., Lloreta-Trull, J., & Hernández-Llodrà, S. (2019). Strong cytoplasmic ETV1 expression has a negative impact on prostate cancer outcome. *Virchows Arch*, *475*(4), 457-466. https://doi.org/10.1007/s00428-019-02573-1

Sekhoacha, M., Riet, K., Motloung, P., Gumenku, L., Adegoke, A., & Mashele, S. (2022). Prostate Cancer Review: Genetics, Diagnosis, Treatment Options, and Alternative Approaches. *Molecules*, *27*(17). https://doi.org/10.3390/molecules27175730

Seligson, D. B., Horvath, S., McBrian, M. A., Mah, V., Yu, H., Tze, S., Wang, Q., Chia, D., Goodglick, L., & Kurdistani, S. K. (2009). Global levels of histone modifications predict prognosis in different cancers. *Am J Pathol*, *174*(5), 1619-1628. https://doi.org/10.2353/ajpath.2009.080874

Shah, R. B., Ghosh, D., & Elder, J. T. (2006). Epidermal growth factor receptor (ErbB1) expression in prostate cancer progression: correlation with androgen independence. *Prostate*, *66*(13), 1437-1444. https://doi.org/10.1002/pros.20460

Shamloo, K., Chen, J., Sardar, J., Sherpa, R. T., Pala, R., Atkinson, K. F., Pearce, W. J., Zhang, L., & Nauli, S. M. (2017). Chronic Hypobaric Hypoxia Modulates Primary Cilia Differently in Adult and Fetal Ovine Kidneys. *Front Physiol*, *8*, 677. https://doi.org/10.3389/fphys.2017.00677

Shariat, S. F., & Roehrborn, C. G. (2008). Using biopsy to detect prostate cancer. *Rev Urol*, *10*(4), 262-280.

Sharma, S. V., Bell, D. W., Settleman, J., & Haber, D. A. (2007). Epidermal growth factor receptor mutations in lung cancer. *Nature Reviews Cancer*, *7*(3), 169-181. https://doi.org/10.1038/nrc2088

Shlien, A., & Malkin, D. (2009). Copy number variations and cancer. *Genome Medicine*, *1*(6), 62. https://doi.org/10.1186/gm62

Shoag, J., Liu, D., Ma, X., Oromendia, C., Christos, P., Ballman, K., Angulo, C., Cai, P. Y., Gaffney, C., Klein, E., Karnes, J., Den, R. B., Liu, Y., Davicioni, E., & Barbieri, C. E. (2020). Prognostic value of the SPOP mutant genomic subclass in prostate cancer. *Urologic Oncology: Seminars and Original Investigations*, *38*(5), 418-422. https://doi.org/https://doi.org/10.1016/j.urolonc.2020.02.011

Siddiqui, M. M., Rais-Bahrami, S., Turkbey, B., George, A. K., Rothwax, J., Shakir, N., Okoro, C., Raskolnikov, D., Parnes, H. L., Linehan, W. M., Merino, M. J., Simon, R. M., Choyke, P. L., Wood, B. J., & Pinto, P. A. (2015). Comparison of MR/ultrasound

fusion-guided biopsy with ultrasound-guided biopsy for the diagnosis of prostate cancer. *Jama*, *313*(4), 390-397. https://doi.org/10.1001/jama.2014.17942

Siegel, R. L., Miller, K. D., Fuchs, H. E., & Jemal, A. (2022). Cancer statistics, 2022. *CA: A Cancer Journal for Clinicians*, *72*(1), 7-33. https://doi.org/https://doi.org/10.3322/caac.21708

Sigismund, S., Avanzato, D., & Lanzetti, L. (2018). Emerging functions of the EGFR in cancer. *Mol Oncol*, *12*(1), 3-20. https://doi.org/10.1002/1878-0261.12155

Sizemore, G. M., Pitarresi, J. R., Balakrishnan, S., & Ostrowski, M. C. (2017). The ETS family of oncogenic transcription factors in solid tumours. *Nat Rev Cancer*, *17*(6), 337-351. https://doi.org/10.1038/nrc.2017.20

Sizemore, G. M., Pitarresi, J. R., Balakrishnan, S., & Ostrowski, M. C. (2017). The ETS family of oncogenic transcription factors in solid tumours. *Nature Reviews Cancer*, *17*(6), 337-351. https://doi.org/10.1038/nrc.2017.20

Steidl, M. E., Nigro, E. A., Nielsen, A. K., Pagliarini, R., Cassina, L., Lampis, M., Podrini, C., Chiaravalli, M., Mannella, V., Distefano, G., Yang, M., Aslanyan, M., Musco, G., Roepman, R., Frezza, C., & Boletta, A. (2023). Primary cilia sense glutamine availability and respond via asparagine synthetase. *Nature Metabolism*, *5*(3), 385-397. https://doi.org/10.1038/s42255-023-00754-6

Stish, B. J., Davis, B. J., Mynderse, L. A., McLaren, R. H., Deufel, C. L., & Choo, R. (2018). Low dose rate prostate brachytherapy. *Translational Andrology and Urology*, *7*(3), 341-356. https://tau.amegroups.org/article/view/18019

Sugiura, M., Sato, H., Kanesaka, M., Imamura, Y., Sakamoto, S., Ichikawa, T., & Kaneda, A. (2021). Epigenetic modifications in prostate cancer. *International Journal of Urology*, *28*(2), 140-149. https://doi.org/https://doi.org/10.1111/iju.14406

Sung, H., Ferlay, J., Siegel, R. L., Laversanne, M., Soerjomataram, I., Jemal, A., & Bray, F. (2021). Global Cancer Statistics 2020: GLOBOCAN Estimates of Incidence and Mortality Worldwide for 36 Cancers in 185 Countries. *CA Cancer J Clin*, *71*(3), 209-249. https://doi.org/10.3322/caac.21660

Tomlins, S. A., Rhodes, D. R., Perner, S., Dhanasekaran, S. M., Mehra, R., Sun, X. W., Varambally, S., Cao, X., Tchinda, J., Kuefer, R., Lee, C., Montie, J. E., Shah, R. B., Pienta, K. J., Rubin, M. A., & Chinnaiyan, A. M. (2005). Recurrent fusion of TMPRSS2 and ETS transcription factor genes in prostate cancer. *Science*, *310*(5748), 644-648. https://doi.org/10.1126/science.1117679

Toss, A., Tenedini, E., Piombino, C., Venturelli, M., Marchi, I., Gasparini, E., Barbieri, E., Razzaboni, E., Domati, F., Caggia, F., Grandi, G., Combi, F., Tazzioli, G., Dominici, M., Tagliafico, E., & Cortesi, L. (2021). Clinicopathologic Profile of Breast Cancer in Germline ATM and CHEK2 Mutation Carriers. *Genes*, *12*(5).

Van Poppel, H., Hogenhout, R., Albers, P., van den Bergh, R. C. N., Barentsz, J. O., & Roobol, M. J. (2021). Early Detection of Prostate Cancer in 2020 and Beyond: Facts and Recommendations for the European Union and the European Commission. *Eur Urol*, *79*(3), 327-329. https://doi.org/10.1016/j.eururo.2020.12.010

Verze, P., Cai, T., & Lorenzetti, S. (2016). The role of the prostate in male fertility, health and disease. *Nat Rev Urol*, *13*(7), 379-386. https://doi.org/10.1038/nrurol.2016.89

Vietri, M. T., D'Elia, G., Caliendo, G., Resse, M., Casamassimi, A., Passariello, L., Albanese, L., Cioffi, M., & Molinari, A. M. (2021). Hereditary Prostate Cancer: Genes Related, Target Therapy and Prevention. *Int J Mol Sci*, *22*(7). https://doi.org/10.3390/ijms22073753

Vinothkumar, V., Arun, K., Arunkumar, G., Revathidevi, S., Ramani, R., Bhaskar, L., Murugan, A. K., & Munirajan, A. K. (2020). Association between functional TERT promoter polymorphism rs2853669 and cervical cancer risk in South Indian women. *Mol Clin Oncol*, *12*(5), 485-494. https://doi.org/10.3892/mco.2020.2003

Vogelstein, B., Papadopoulos, N., Velculescu, V. E., Zhou, S., Diaz, L. A., Jr., & Kinzler, K. W. (2013). Cancer genome landscapes. *Science*, *339*(6127), 1546-1558. https://doi.org/10.1126/science.1235122

Vonderfecht, T., Stemm-Wolf, A. J., Hendershott, M., Giddings, T. H., Jr., Meehl, J. B., & Winey, M. (2011). The two domains of centrin have distinct basal body functions in Tetrahymena. *Mol Biol Cell*, *22*(13), 2221-2234. https://doi.org/10.1091/mbc.E11-02-0151

Wang, G., Zhao, D., Spring, D. J., & DePinho, R. A. (2018). Genetics and biology of prostate cancer. *Genes Dev*, *32*(17-18), 1105-1140. https://doi.org/10.1101/gad.315739.118

Wang, J., Cai, Y., Ren, C., & Ittmann, M. (2006). Expression of variant TMPRSS2/ERG fusion messenger RNAs is associated with aggressive prostate cancer. *Cancer Res*, *66*(17), 8347-8351. https://doi.org/10.1158/0008-5472.Can-06-1966

Wang, L., Lu, B., He, M., Wang, Y., Wang, Z., & Du, L. (2022). Prostate Cancer Incidence and Mortality: Global Status and Temporal Trends in 89 Countries From 2000 to 2019. *Front Public Health*, *10*, 811044. https://doi.org/10.3389/fpubh.2022.811044

Wang, Y., Yao, X., Li, S. N., Suo, A. L., Tian, T., Ruan, Z. P., Guo, H., & Yao, Y. (2013). Detection of prostate cancer related copy number variations with SNP genotyping array. *Eur Rev Med Pharmacol Sci*, *17*(21), 2916-2922.

Wilson, K. M., & Mucci, L. A. (2019). Diet and Lifestyle in Prostate Cancer. *Adv Exp Med Biol*, *1210*, 1-27. https://doi.org/10.1007/978-3-030-32656-2_1

Wilt, T. J., Ullman, K. E., Linskens, E. J., MacDonald, R., Brasure, M., Ester, E., Nelson, V. A., Saha, J., Sultan, S., & Dahm, P. (2021). Therapies for Clinically Localized

Prostate Cancer: A Comparative Effectiveness Review. *J Urol*, *205*(4), 967-976. https://doi.org/10.1097/ju.0000000000001578

Winnes, M., Lissbrant, E., Damber, J. E., & Stenman, G. (2007). Molecular genetic analyses of the TMPRSS2-ERG and TMPRSS2-ETV1 gene fusions in 50 cases of prostate cancer. *Oncol Rep*, *17*(5), 1033-1036.

Wong, S. Y., Seol, A. D., So, P. L., Ermilov, A. N., Bichakjian, C. K., Epstein, E. H., Jr., Dlugosz, A. A., & Reiter, J. F. (2009). Primary cilia can both mediate and suppress Hedgehog pathway-dependent tumorigenesis. *Nat Med*, *15*(9), 1055-1061. https://doi.org/10.1038/nm.2011

Wu, Q., Qian, W., Sun, X., & Jiang, S. (2022). Small-molecule inhibitors, immune checkpoint inhibitors, and more: FDA-approved novel therapeutic drugs for solid tumors from 1991 to 2021. *Journal of Hematology & Oncology*, *15*(1), 143. https://doi.org/10.1186/s13045-022-01362-9

Xu, Q., Liu, W., Liu, X., Liu, W., Wang, H., Yao, G., Zang, L., Hayashi, T., Tashiro, S., Onodera, S., & Ikejima, T. (2016). Silibinin negatively contributes to primary cilia length via autophagy regulated by histone deacetylase 6 in confluent mouse embryo fibroblast 3T3-L1 cells. *Mol Cell Biochem*, *420*(1-2), 53-63. https://doi.org/10.1007/s11010-016-2766-2

Yoshida, R. (2021). Hereditary breast and ovarian cancer (HBOC): review of its molecular characteristics, screening, treatment, and prognosis. *Breast Cancer*, *28*(6), 1167-1180. https://doi.org/10.1007/s12282-020-01148-2

Yu, J., Yu, J., Mani, R. S., Cao, Q., Brenner, C. J., Cao, X., Wang, X., Wu, L., Li, J., Hu, M., Gong, Y., Cheng, H., Laxman, B., Vellaichamy, A., Shankar, S., Li, Y., Dhanasekaran, S. M., Morey, R., Barrette, T., . . . Chinnaiyan, A. M. (2010). An integrated network of androgen receptor, polycomb, and TMPRSS2-ERG gene fusions in prostate cancer progression. *Cancer Cell*, *17*(5), 443-454. https://doi.org/10.1016/j.ccr.2010.03.018

Yu, L., Wu, X., Chen, M., Huang, H., He, Y., Wang, H., Li, D., Du, Z., Zhang, K., Goodin, S., & Zheng, X. (2017). The Effects and Mechanism of YK-4-279 in Combination with Docetaxel on Prostate Cancer. *Int J Med Sci*, *14*(4), 356-366. https://doi.org/10.7150/ijms.18382

Zhang, J., Lipinski, R. J., Gipp, J. J., Shaw, A. K., & Bushman, W. (2009). Hedgehog pathway responsiveness correlates with the presence of primary cilia on prostate stromal cells. *BMC Developmental Biology*, *9*(1), 50. https://doi.org/10.1186/1471-213X-9-50

Zhang, P., Kiseleva, A. A., Korobeynikov, V., Liu, H., Einarson, M. B., & Golemis, E. A. (2019). Microscopy-Based Automated Live Cell Screening for Small Molecules That Affect Ciliation. *Front Genet*, *10*, 75. https://doi.org/10.3389/fgene.2019.00075

Zhou, E., Zhang, B., Zhu, K., Schaafsma, E., Kumar, R. D., & Cheng, C. (2020). A TMPRSS2-ERG gene signature predicts prognosis of patients with prostate adenocarcinoma. *Clin Transl Med*, *10*(8), e216. https://doi.org/10.1002/ctm2.216

Zhou, M. (2018). High-grade prostatic intraepithelial neoplasia, PIN-like carcinoma, ductal carcinoma, and intraductal carcinoma of the prostate. *Mod Pathol*, *31*(S1), S71-79. https://doi.org/10.1038/modpathol.2017.138

Zhu, D., Shi, S., Wang, H., & Liao, K. (2009). Growth arrest induces primary-cilium formation and sensitizes IGF-1-receptor signaling during differentiation induction of 3T3-L1 preadipocytes. *J Cell Sci*, *122*(Pt 15), 2760-2768. https://doi.org/10.1242/jcs.046276

APPENDIX

Appendix 1

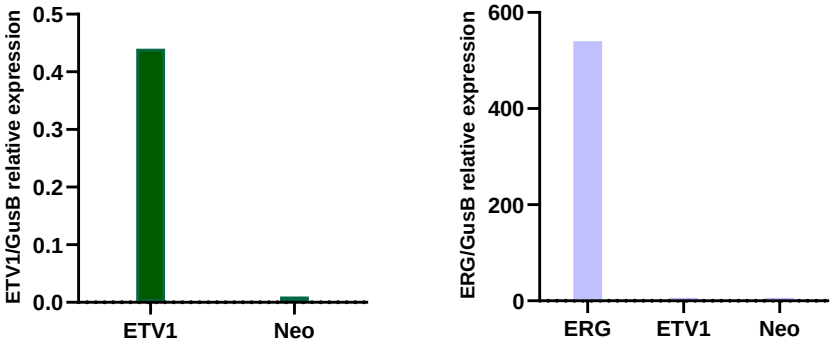

Figure A1. Validation of the expression levels of *ETV1* and *ERG* in the PNT2-derived cell models used in this study. Expression levels of *ETV1* are shown at *left* (green) and *ERG* at *right* (light purple). Data was obtained by qRT-PCR following the protocol previously described (Paulo et al., 2012).

Appendix 2

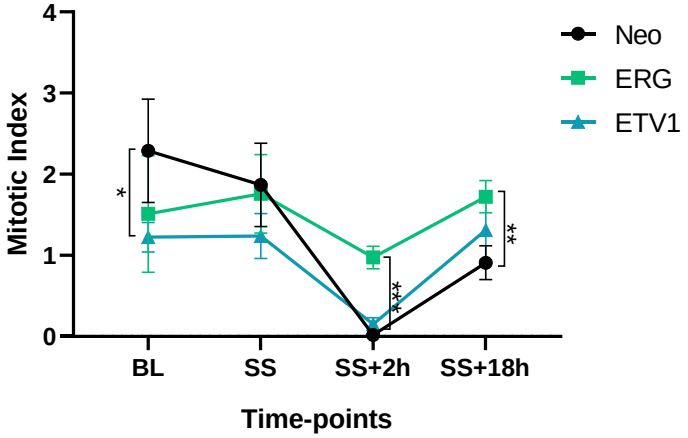

Figure A2. The mitotic index is affected by growth conditions and media changes in PNT2-derived cells. The mitotic index of PNT2-derived cells (PNT2-Neo, PNT2-ΔERG and PNT2-ETV1) was quantified under various conditions: Baseline (BL), Serum Starved (SS), Serum Starved plus 2 hours of complete growth medium (SS+2h of FBS), and Serum Starved plus 18 hours of complete growth medium (SS+18h of FBS). Data were obtained from three independent experiments. Unpaired two-tailed *t*-test was used for statistical analysis (*p<0.05; **p<0.01; ***p<0.001).

Appendix 3

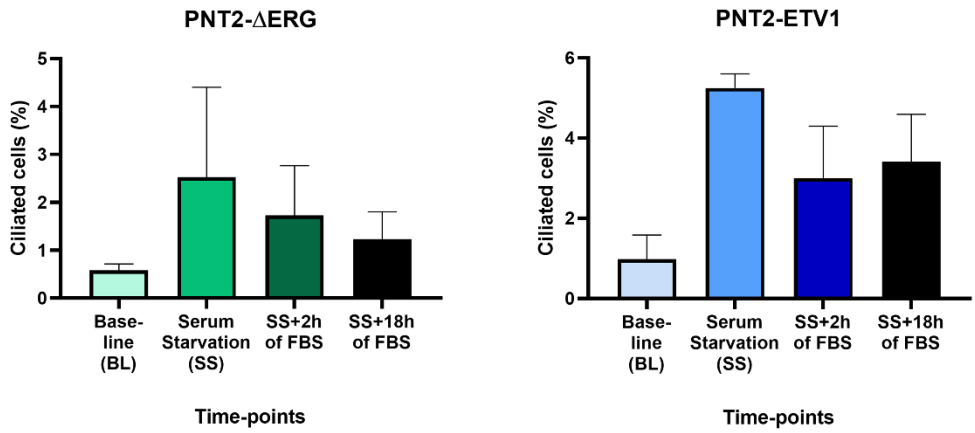

Figure A3. Primary cilia assembly/disassembly in PNT2-derived cells with de novo overexpression of ΔERG or ETV1 is affected by the presence of serum. The percentage of ciliated PNT2-ΔERG (left) and PNT2-ETV1 (right) cells was quantified under various conditions: Baseline (BL), Serum Starved (SS), Serum Starved plus 2 hours of complete growth medium (SS+2h of FBS), and Serum Starved plus 18 hours of complete growth medium (SS+18h of FBS). Data were obtained from two independent experiments. In each experiment, at least 1300 cells were analysed per condition. Unpaired two-tailed *t*-test was used for statistical analysis.

Appendix 4

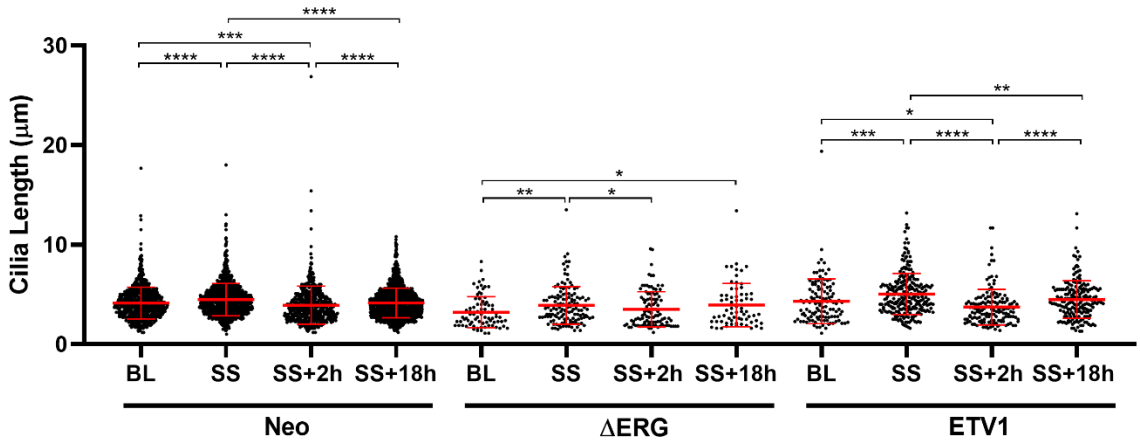

Figure A4. Cilia length is modulated by the defined growth conditions and time-points in culture in PNT2-derived cells. The quantification of the primary cilia length exhibited by PNT2-derived cells (PNT2-Neo, PNT2-ΔERG and PNT2-ETV1) was performed under the different growth conditions: Baseline (BL), Serum Starved (SS), Serum Starved plus 2 hours of complete growth medium (SS+2h of FBS), and Serum Starved plus 18 hours of complete growth medium

(SS+18h of FBS). Data were obtained from three independent experiments. For each condition, at least 70 cilia were measured. Mann-Whitney test was used for statistical analysis. Only statistically significant differences are shown (*p<0.05; **p<0.01; ***p<0.001; ****p<0.0001).

Appendix 5

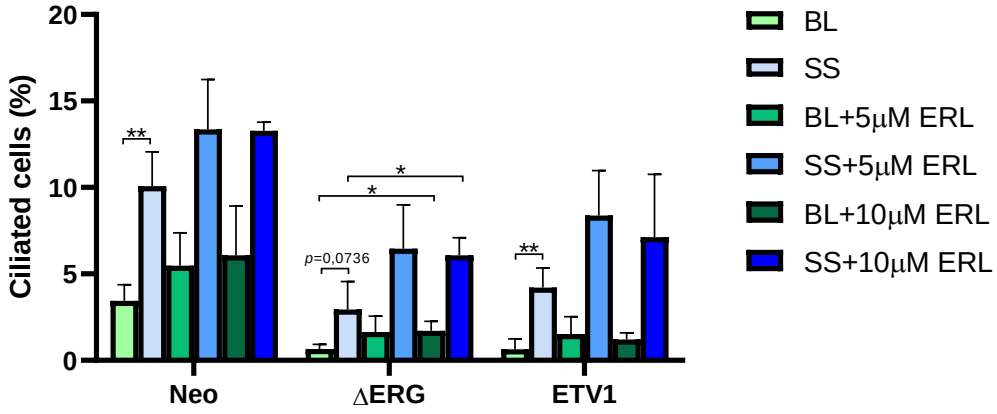

Figure A5. Erlotinib treatment has a cumulative effect with serum starvation in stimulating ciliogenesis in all PNT2-derived cells. Quantification of the percentage of ciliated cells in PNT2-derived cells upon treatment with different concentrations of Erlotinib (5 and 10μM) at different growth conditions: Baseline and Serum Starved. Data were obtained from three independent experiments. In each experiment, at least 500 total cells were analysed per condition. Unpaired two-tailed *t*-test was used for statistical analysis (*p<0.05; **p<0.01).

Appendix 6

EGF stimulation of PNT2-derived cells with *de novo* overexpression of ΔERG and ETV1

To evaluate the effect of EGFR activation in ciliogenesis, PNT2-derived cell lines were stimulated with EGF, and its effect was compared with that of FBS stimulation.

Briefly, PNT2-derived cell lines were seeded in glass bottom 96-well plates at a cell density of 200 000 cells/mL in complete growth medium (100μL/well), and incubated overnight in a humidified chamber, at 37°C with 5% CO_2. The following day, growth medium was replaced with FBS-free medium to stimulate primary cilia assembly. After 24 hours, cells were either fixed or exposed to EGF stimulation by adding 0.1μg/mL of EGF (Gibco) to growth medium without FBS. Cells were exposed to EGF for 18 hours, and either fixed or treated with Erlotinib (5μM or 10μM) for 24 hours. After treatment, cells were fixed and

subjected to immunofluorescence staining, where the number of ciliated cells and cilia length were quantified and the impact of EGF stimulation in EGFR treatment in the different ETS backgrounds was assessed.

The results revealed that treatment with EGF did not cause any alterations in the percentage of ciliated cells in PNT2-derived cells, comparing with “serum starved” cells (Figure A10). This lack of effect could be due to several reasons: 1. Although the EGF concentration used was already used in our research group and proved to activate EGFR, its effect had been studied after 20 minutes of administration to cells. Thus, it is possible that, after 18 hours, EGF had already been consumed by the cells and its effectiveness was no longer possible to evaluate; 2. The effect of EGFR activation in primary cilia disassembly was previously observed within 2-3 hours after administration, potentially diminishing over time; or 3. Erlotinib, while being an EGFR inhibitor, it is not EGFR-specific and may target other proteins that also affect ciliogenesis, thus, leading to a “no effect” upon treatment with EGF.

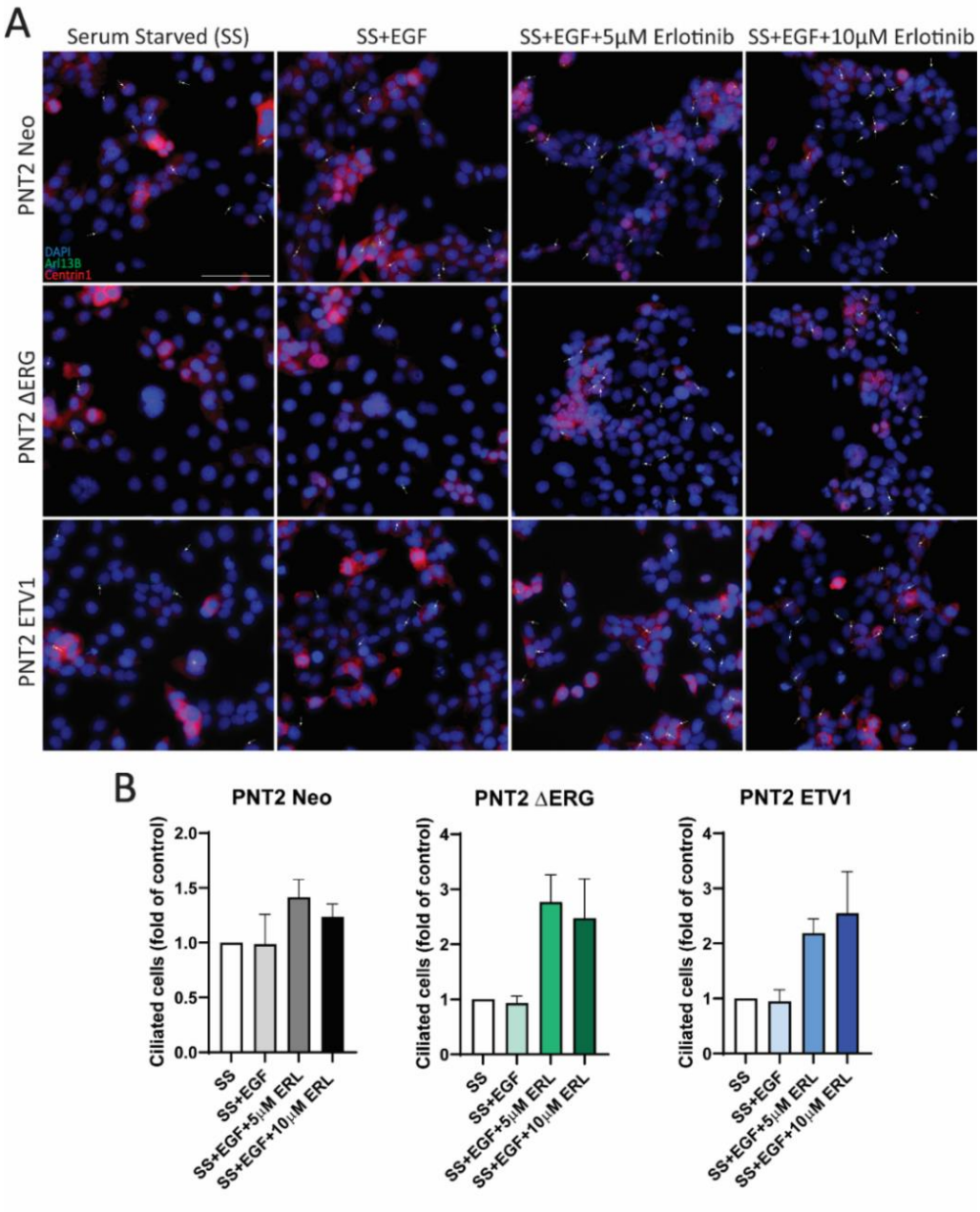

Figure A6. Erlotinib-mediated ciliary restoration is unaffected by EGF treatment after 18 hours of administration. **[A]** Representative immunofluorescence images of PNT2-derived cells (PNT2-Neo, PNT2-ΔERG and PNT2-ETV1) under different conditions: Serum Starved (SS), Serum Starved plus 18 hours of EGF stimulus (SS+EGF), Serum Starved plus 18 hours of EGF stimulus and 24 hours of treatment with 5μM Erlotinib (SS+EGF+5μM ERL) or with 10μM Erlotinib (SS+EGF+10μM ERL). Nuclei are stained with DAPI (blue), primary cilia are stained with Arl13B (green), and the basal body is stained with Centrin1 (red). White arrows indicate primary cilia. Cells were grown in 96-well plates and images were acquired with the Cytation C10 confocal microscope (40x magnification). Scale bar: 100μm. **[B]** Quantification of the percentage of ciliated cells in PNT2-derived cell populations upon exposure to EGF stimulus and treatment with different concentrations of Erlotinib (5 and 10μM). For each cell line and growth condition, levels in treated cells were

normalized to those of untreated (SS) cells. Data were obtained from three independent experiments. In each experiment, at least 1100 total cells were analysed per condition. Unpaired two-tailed *t*-test was used for statistical analysis.

Appendix 7

Establishment of 3D cell models of PNT2-derived cells with stable expression of mCherry-H2B and GFP-Arl13B

To enable the dynamic visualization of both cell nuclei and primary cilia *in vivo*, we transduced the PNT2-derived cells (PNT2 Neo, PNT2 ΔERG and PNT2 ETV1) with lentiviral particles carrying the mCherry-H2B and/or the GFP-Arl13B constructs. This approach allows stable expression of fluorescence-tagged histone 2B (H2B) and Arl13B, facilitating real-time monitoring of primary cilia assembly and disassembly without requiring endpoint immunofluorescence assays.

Lentiviral particle production and transduction

Lenti-X 293T cells ($4.8x10^6$) were seeded in a 100mm cell culture dish (Orange Scientific, Paris, France) with 10mL of DMEM supplemented with 10% FBS only (without antibiotics), and incubated overnight in a humidified chamber, at 37°C with 5% CO_2. In the following day, cells were transfected with lentiviral plasmids using lipofectamine 2000. Briefly, a DNA Transfection Mix containing 2.5µg of the packaging plasmid psPAX2 (Addgene, plasmid #12260), 5µg of the envelope plasmid pMD2.G (Addgene, plasmid #12259), and either 2.5ug of the plasmid pLenti6-H2B-mCherry (Addgene, plasmid #89766) or 2.5µg of the plasmid L13-Arl13bGFP (Addgene, plasmid #40879), was prepared in a final volume of 625µL in OptiMEM (Gibco, Thermo Fisher Scientific, Carlsbad, CA). In parallel, 50µL of lipofectamine 2000 were diluted in 575µL of OptiMEM and left incubating for 5 minutes at RT. Then, the DNA Transfection Mix previously prepared was added dropwise to the Lipofectamine dilution, and allowed to incubate 20 minutes at RT. After that, the full solution was added dropwise to the Lenti-X 293T cells.

After 24 and 48 hours, the conditioned medium from the Lenti-X 293T cells containing lentiviral particles was collected, centrifuged at 12,000 rpm for 5 minutes, and filtered through a 0.45µm syringe filter. Polybrene (Sigma-Aldrich) was added at 4ug/mL and viral particles-containing medium was used to infect PNT2-derived cell lines.

For transduction, PNT2-derived cells ($2.5x10^5$) were seeded in a 6-well plate and allowed to incubate overnight under standard growth conditions. The following day, the growth medium was removed and replaced with 1mL of viral particles-containing medium collected from Lenti-X 293T cells, as described above. Transduction was carried out under regular growth conditions for 24 hours, after which medium was replaced with complete growth medium to allow for cell recovery.

Cell sorting and validation by western-blot

To selectively obtain enriched PNT2-derived cell populations with medium-to-high levels of mCherry-H2B or GFP-Arl13B expression, cell sorting was performed using a Fluorescence-Activated Cell Sorting (FACS) system (Baker SterilGARD® e3 Necropsy Unit Class II, Type A2). Briefly, confluent cells grown in a monolayer in T75 flasks were washed with PBS and trypsinized with 1mL of TrypLE™ Express Enzyme (Gibco). Then, cell suspensions were collected and centrifuged at 12,000 rpm for 5 minutes. Cells' pellets were resuspended in PBS for subjected to FACS. Sorted PNT2-derived cell populations were expanded in regular growth conditions for subsequent studies.

To validate the efficacy of the transduction with GFP-Arl13B in the sorted PNT2-derived cell populations, a western blot assay was conducted to assess the expression of GFP and/or Arl13B.

Western Blot

Western blot is a widely used technique that employs antibodies to analyse the expression of proteins of interest in a protein extract, allowing for the relative quantification of specific proteins within a complex protein mixture (Hnasko & Hnasko, 2015).

To obtain protein extracts, PNT2-derived cells were cultured in T25 flasks under standard growth conditions. Once cells reached 70-90% confluence, the growth medium was discarded, and cells were washed twice with *ice-cold* PBS (4°C). After carefully removing all the PBS, 100µL of *ice-cold* lysis buffer (50mM Tris-HCl pH 7.4, 150mM NaCl, 1mM EDTA and 0.5% Triton) was added to the cells, and protein extracts were obtained by cell scraping. Protein lysates were collected after centrifugation at 13,000 rpm for 30 minutes at 4°C by discarding cell debris. Protein concentration was measured using the Qubit™ Protein Assay Kit (Thermo Fisher Scientific, Carlsbad, CA) and the Invitrogen Qubit 4 Fluorometer (by Thermo Fisher Scientific), following the manufacturers' instructions. For each sample, 30 or 60µg of total protein extract were combined with 1x loading buffer (0.1M

Tris-HCl – pH 6.8, 0.4% SDS, 2% glycerol, 0.01% bromophenol blue, and 5% β-Mercaptoethanol), and proteins were denatured at 95°C for 5 minutes.

Then, to separate proteins according to their size, gel electrophoresis was performed under denatured conditions. For that purpose, a running gel containing a 10% resolving gel and a 4% stacking gel was prepared. The composition of both gels is described in Table 3.

Table 3. Chemical composition of the resolving (10%) and the stacking (4%) gels

	Resolving gel (10%)	**Stacking gel (4%)**
Acrylamide (MARCA)	1.25mL	250µL
Tris-HCl 1.5M pH 8.8	1.25mL	---
Tris-HCl 0.5M pH 6.8	---	630µL
10% SDS	50µL	25µL
Glycerol	200µL	---
ddH_2O	2.25mL	1.59mL
TEMED	5µL	5µL
APS 20%	25µL	12.5µL
Final volume	5.00mL	2.50mL

Once the gels were fully polymerized, the denatured protein samples were loaded into the wells of the stacking gel, and electrophoresis took place in 1x Tris-Glycine-SDS buffer (Bio-Rad, Hercules, CA, USA) using a constant voltage of 12V/cm for 90 minutes.

Following gel electrophoresis, the separated proteins were transferred from the gel to a 0.22µm nitrocellulose membrane in 1x Tris-Glycine buffer (Bio-Rad) containing 20% methanol, using the Mini Trans-Blot® Cell system (Bio-Rad). The transfer process was carried out at 50V/cm for 60 minutes.

To avoid nonspecific antibody binding, the membrane was blocked with 5% non-fat-dry milk in TBS-0.1% Tween 20 (TBST) for 60 minutes, under gentle agitation. Then, immunodetection took place by incubating the membrane overnight at 4°C, under agitation, in a solution containing the primary antibody diluted in blocking solution, either a chicken anti-GFP polyclonal antibody (1:5000 dilution), kindly provided by Professor Claudio Sunkel, the mouse anti-Arl13B monoclonal antibody (1:500 dilution), or the mouse anti-β-actin monoclonal antibody (1:8000 dilution; Sigma-Aldrich, St. Louis, MO, USA).

In the following day, the membrane was washed three times with TBST, for 10 minutes each, under agitation, to remove any unbound primary antibody. The membrane was, then, incubated with HRP-bound secondary antibodies diluted in the same blocking solution, namely, the goat anti-chicken IgY H&L (1:2000 dilution; #ab6877, Abcam, Cambridge, MA, USA) or the rabbit anti-mouse (1:10.000 dilution; #1706516, Bio-Rad Laboratories, Hercules, California, USA), for 1 hour at RT, under agitation. After incubation, the membrane was again washed three times with TBST, and protein detection was carried out using an enhanced chemiluminescence (ECL) method. Bands were visualized using the ChemiDoc™ MP Imaging System (Bio-Rad).

Establishment of 3D cell models

PNT2-derived cell lines overexpressing mCherry-H2B were seeded into a black 384-well plate with Ultra-Low Attachment Surface (Corning®, #4516) at various cell densities: 250, 500, 750, 1000, 1500, 2000, 2500, 3000 and 3500 cells per well, in 70µL of complete growth medium. Following seeding, plates were centrifuged at 300 x g for 1 minute to promote spheroid formation. Spheroids were maintained under standard growth conditions for 6 days, with half-volume medium changes every 48 hours.

Lentiviral transfection on PNT2-derived cell lines using lentiviral particles carrying mCherry-H2B was successful, with most cells expressing mCherry in their nuclei. Following transfection, cell sorting was conducted to obtain a cell population enriched in cells displaying a medium-to-high mCherry-H2B signal. The effectiveness of this process is evidenced by the uniform mCherry-H2B signal observed in the sorted cell populations, both qualitatively and quantitatively (Figure A6). Unfortunately, the PNT2-ΔERG cells exhibited a bacterial contamination after the sorting procedure and had to be discarded.

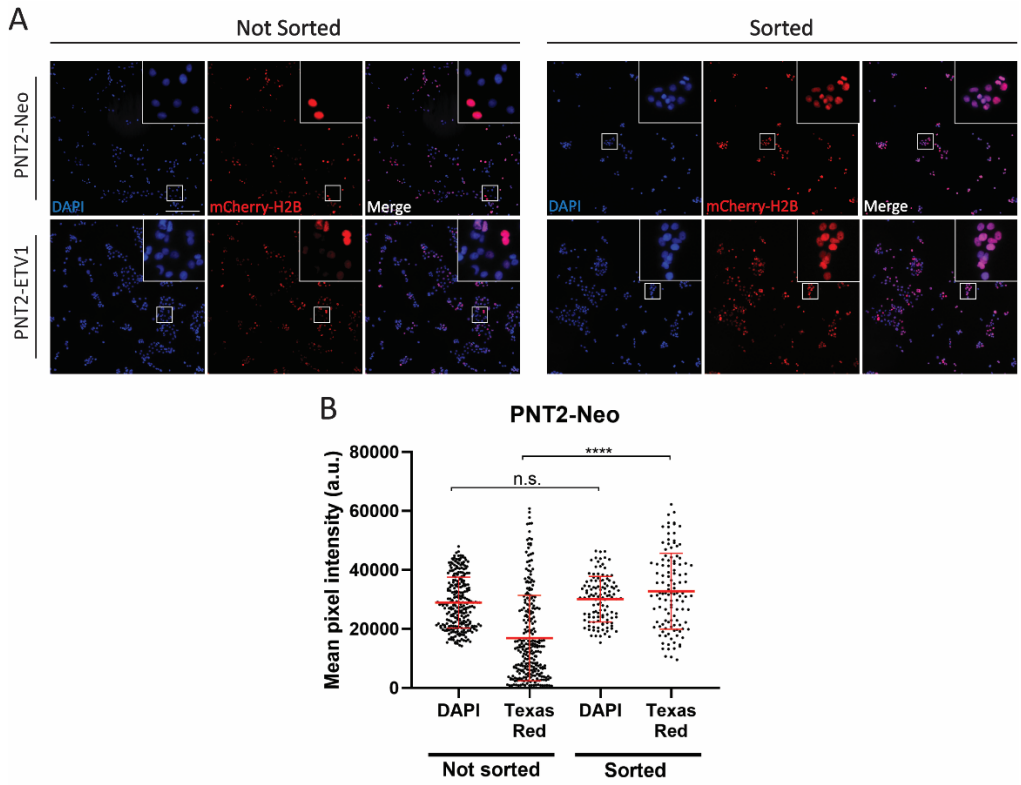

Figure A7. Comparison of mCherry-H2B expression in PNT2-derived cells before and after cell sorting. **[A]** Representative images of PNT2-Neo and PNT2-ETV1 cells expressing mCherry-H2B, either unsorted (*left*) or sorted (*right*). Nuclei are labelled with DAPI (blue) and mCherry-H2B (red). Cells were grown on coverslips and images were acquired with the Cytation C10 confocal microscope (10x magnification). Scale bar: 300µm. Insets show 4x magnifications of selected regions. **[B]** Quantification of DAPI and Texas Red signals in PNT2-Neo cells expressing mCherry-H2B by mean pixel intensity (arbitrary units, a.u.), comparing unsorted and sorted populations. The minimum number of cells analysed (n) for each condition was 100. Unpaired two-tailed *t*-test was used for statistical analysis (****p<0.0001). Ns – not significant (p>0.05).

Following the successful transduction, we established 3D cell models with the PNT2-derived cells expressing mCherry-H2B, using ultra-low attachment plates. For initial optimisation experiments, various cell concentrations were tested, and spheroid growth was monitored over 6 consecutive days (Figure A7). For simplification, only results obtained for PNT2-ETV1 were panelled in Figure A7A. Globally, we observed that PNT2-derived cell lines readily form spheroids, with spheroids visible at all cell concentrations as early as day 1 (24 hours after seeding). These spheroids maintained a consistent circularity over time, with little variation based on cell concentration. However, spheroid integrity began to decline around day 4 or 5, particularly at higher cell concentrations. Thus, lower cell concentrations, specifically 750 cells per well, and earlier time points (e.g., day 2) proved to be optimal for future studies using 3D cell models since it allows rapid spheroid formation, maintains a regular shape and minimizes waste around the spheroid.

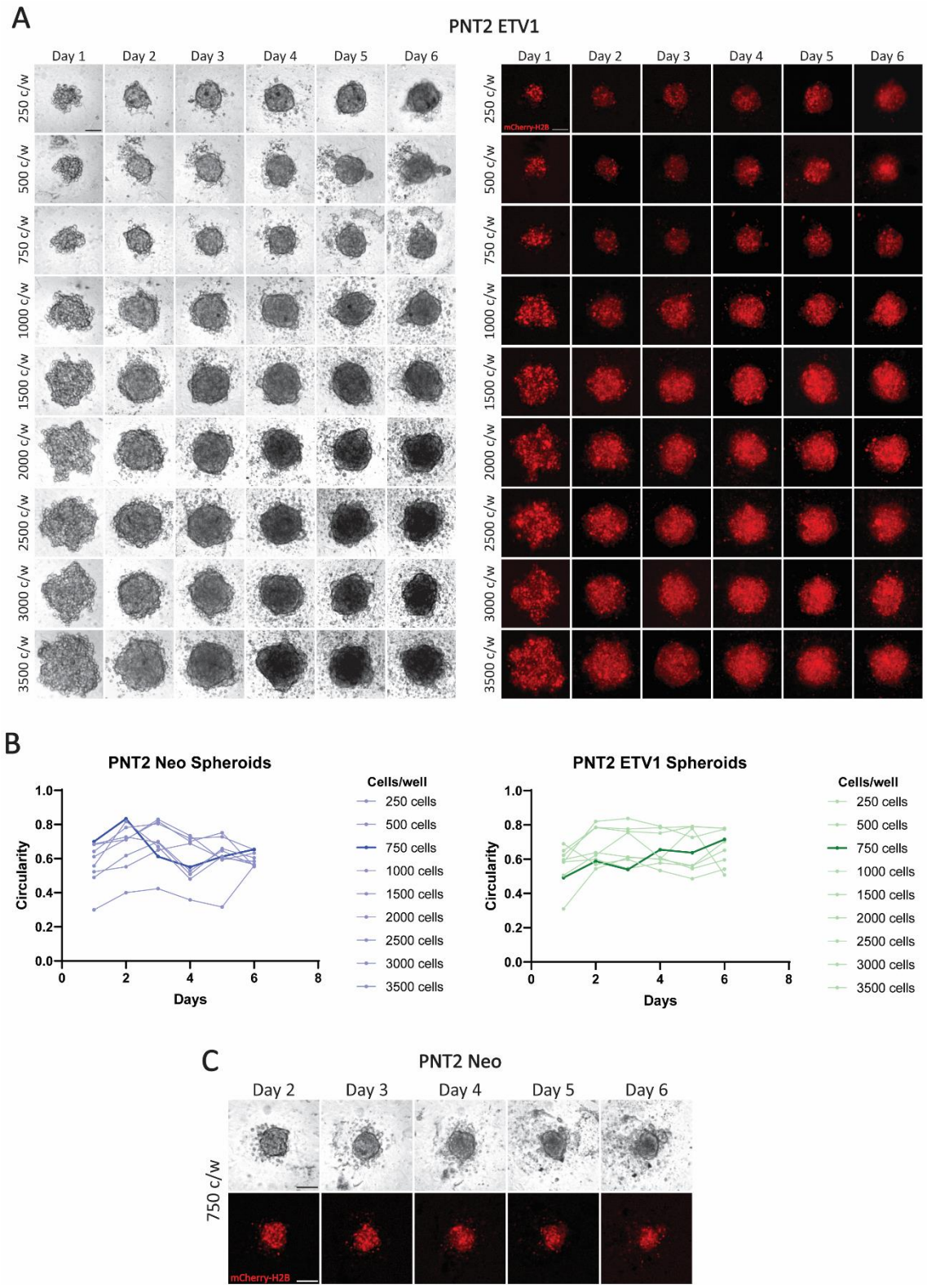

Figure A8. Assessment of PNT2-Neo and PNT2-ETV1 spheroid cultures over time. [A] Representative microscopy images of PNT2-ETV1 spheroids visualised with Brightfield (left panel) and Texas Red (right panel). Images were acquired with the Cytation C10 confocal microscope (4x magnification) every 24 hours for 6 days, after cell seeding at different cell densities in a 384-well ultra-low attachment plate. Scale bar: 100µm. **[B]** Analysis of spheroid circularity over time, starting from different cell densities. Lines in bold represent the optimized number of cells considered for

subsequent experiments (750 cells/well), considering it creates homogeneous stable spheroids. Circularity values were measured every 24 hours using the “Analysis” tool of Gen5 software. **[C]** Representative microscopy images of PNT2-Neo spheroids at a starting cell density of 750 cells per well, imaged daily (day 2 to day 6). Scale bar: 100µm

Moreover, cells overexpressing mCherry-H2B were subjected to another lentiviral transfection, this time with GFP-Arl13B. After the transfection, GFP expression was observed in the cells, but it was not specific to the primary cilia. In fact, the observed signal was diffuse throughout the cytoplasm rather than localized to Arl13B. Despite this, cell sorting was performed in these cells. In the end, the remaining cells displayed a high cytoplasmic GFP signal, and irregular, artifact-like structures started to appear (Figure A8).

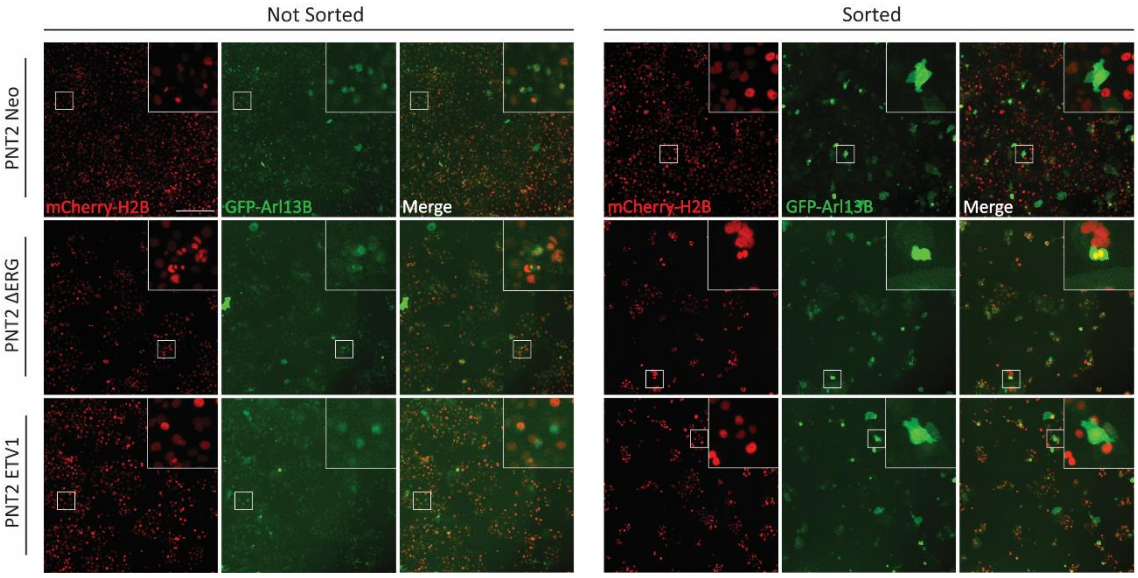

Figure A9. GFP-Arl13B expression in PNT2-derived cell lines before and after cell sorting for GFP signal. Representative images of PNT2-Neo, PNT2-ΔERG and PNT2-ETV1 cells transfected with mCherry-H2B (red) and GFP-Arl13B (green), either unsorted (left) or sorted (right) for mCherry or GFP, respectively. Images of mounted coverslips were acquired with the Cytation C10 confocal microscope (10x magnification). Scale bar: 300µm.

To investigate the specificity of the GFP signal, a western blot using an antibody targeting GFP was performed. Theoretically, if the lentiviral transfection was successful, we would expect to see only one band representing Arl13B-GFP, since cells should be overexpressing this fusion protein exclusively. Since Arl13B has a molecular weight of 50-60KDa and GFP has a molecular weight of ~27KDa, the band representing Arl13B-GFP fusion protein should appear around 80-90KDa on the blot. However, multiple bands were

observed (Figure A9), indicating that the GFP signal is also associated with non-specific proteins, justifying the diffuse signal previously seen throughout the cytoplasm. Despite this, a specific band with an approximate molecular weight of 90KDa (expected size for Arl13B-GFP) was detected in the transfected cell lines but not in the control cell line (PNT2 Neo), strongly suggesting that this band corresponds to the Arl13B-GFP fusion protein.

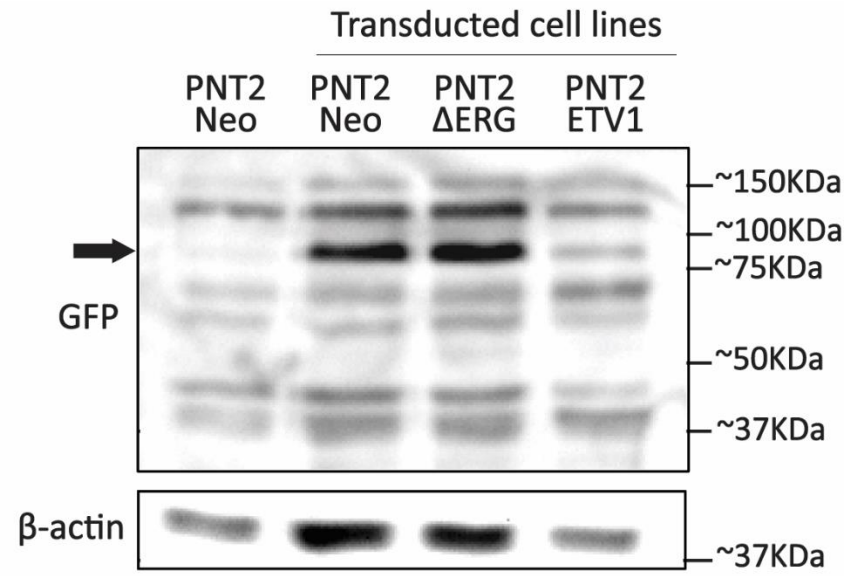

Figure A10. The PNT2-derived cell lines transduced with GFP-Alr13B exhibit non-specific GFP expression. Protein blots of GFP expression in control cells (PNT2-Neo) and in PNT2-derived cell lines (PNT2-Neo, PNT2-ΔERG and PNT2-ETV1) after transduction with lentiviral particles containing GFP-Arl13B. The arrow indicates the putative protein corresponding to the GFP-Arl13B fusion protein, according to the expected molecular weight. For each cell line, 55µg of total protein extract was analysed. β-actin was used as loading control.

This led us to conclude that the GFP-Arl13B transfection failed, possibly due to different reasons: 1. Issues with the plasmid or the transfection process could be causing an improper expression of the fusion protein; 2. High levels of GFP-Arl13B expression can be overwhelming for the cell, leading to an incorrect localization of the protein or 3. The GFP tag can be interfering with the normal function or localization of Arl13B, leading to GFP signal mislocalisation. To address this, we intend, in the near future, to transfect the PNT2-derived cells lines with a different vector, such as the pEGFP-mSmo plasmid, which expresses a fluorescently-tagged SMO protein, a ciliary membrane protein involved in Hedgehog signalling. This vector has already shown some potential in efficiently labelling the primary cilia with GFP (Zhang et al., 2019).